

**MODIFICATION OF ZEOLITE NaX AND CLAY MINERALS
WITH HEXADECYLTRIMETHYLAMMONIUM
CHLORIDE FOR REMOVAL OF AFLATOXIN B₁**

Thapanee Khumbudda

**A Thesis Submitted in Partial Fulfillment of the Requirements for the
Degree of Master of Science in Chemistry
Suranaree University of Technology
Academic Year 2008**

การดัดแปรซีไอไดต์ NaX และแร่ดินด้วยเฮกซะเดซิลไตรเมทิลแอมโมเนียม
คลอไรด์สำหรับการกำจัดอะฟลาทอกซินบี 1

นางสาวฐาปณี คำบุตตา

วิทยานิพนธ์นี้เป็นส่วนหนึ่งของการศึกษาตามหลักสูตรปริญญาวิทยาศาสตรมหาบัณฑิต
สาขาวิชาเคมี
มหาวิทยาลัยเทคโนโลยีสุรนารี
ปีการศึกษา 2551

**MODIFICATION OF ZEOLITE NaX AND CLAY MINERALS
WITH HEXADECYLTRIMETHYLAMMONIUM CHLORIDE
FOR REMOVAL OF AFLATOXIN B₁**

Suranaree University of Technology has approved this thesis submitted in partial fulfillment of the requirements for a Master's Degree.

Thesis Examining Committee

M. Tangsathitkulchai

(Assoc. Prof. Dr. Malee Tangsathitkulchai)

Chairperson

นางสาว กุญแจ รังศรีwatananon

(Asst. Prof. Dr. Kunwadee Rangriwatananon)

Member (Thesis Advisor)

ดร. จตุพร Wittayakun

(Assoc. Prof. Dr. Jatuporn Wittayakun)

Member

ดร. สันชัย Prayoonpokarach

(Dr. Sanchai Prayoonpokarach)

Member

P. Sattayatham

(Prof. Dr. Pairote Sattayatham)

Vice Rector for Academic Affairs

P. Manyum

(Assoc. Prof. Dr. Prapan Manyum)

Dean of Institute of Science

รูปนี้ คำพูดดา : การตัดแปรซีโอไลต์ NaX และแร่ดินด้วยเฮกซะเดซิลไตรเมทิลแอมโมเนียมคลอไรด์สำหรับการกำจัดอะฟลาทอกซินบี 1 (MODIFICATION OF ZEOLITE NaX AND CLAY MINERALS WITH HEXADECYLTRIMETHYL-AMMONIUM CHLORIDE FOR REMOVAL OF AFLATOXIN B₁) อาจารย์ที่ปรึกษา : ผู้ช่วยศาสตราจารย์ ดร.กุลวดี รั้งยี่วัฒนานนท์, 87 หน้า.

งานนี้มุ่งที่ตัดแปร เบนโทไนด์ เกลิน ฮาล์ลอายไซต์ และซีโอไลต์ NaX ด้วย เฮกซะเดซิลไตรเมทิลแอมโมเนียมคลอไรด์ (HDTMA) ด้วยความเข้มข้น 0.3 0.6 1.3 2.0 4.0 และ 6.0 mM วิธีที่ใช้เตรียมออร์แกโนเคลย์ และออร์แกโนซีโอไลต์ NaX คือ แบบทั่วไป และแบบไมโครเวฟ พบว่าเวลาในการเตรียม ออร์แกโนเคลย์ และออร์แกโนซีโอไลต์ NaX ลดลงจาก 24 ชั่วโมง โดยวิธีทั่วไป เป็น 10 นาที โดยวิธีไมโครเวฟ จึงเป็นการยืนยันว่าวิธีไมโครเวฟมีประสิทธิภาพในการเตรียมออร์แกโนเคลย์ และออร์แกโนซีโอไลต์ NaX ตามผลของ TGA พบว่า การเพิ่มความเข้มข้นของ HDTMA ทำให้จำนวน HDTMA ที่ถูกดูดซับบนออร์แกโนเบนโทไนด์เพิ่มขึ้นอย่างมาก ในขณะที่ออร์แกโนเกลิน ออร์แกโนฮาล์ลอายไซต์ และออร์แกโนซีโอไลต์ NaX ก่อนข้างคงที่ ในโครงสร้างระดับไมโครของชั้นการดูดซับถูกพิสูจน์ด้วย XRD พบว่า ในกรณีของเบนโทไนด์ ตัดแปรด้วย 6.0 mM ของ HDTMA ช่องว่างระหว่างชั้น (d_{001}) เพิ่มขึ้นอย่างมากจาก 14.68 Å ถึง 23.33 Å ในขณะที่ตัวอื่นเพิ่มขึ้นน้อยมาก ซึ่งสอดคล้องกับผลของ TGA และ DTA ยิ่งกว่านั้น จากข้อมูลทาง DTA เห็นได้ว่า มีการจัดเรียงตัวของ HDTMA ในเบนโทไนด์อย่างน้อยสามแบบ จากผลของการพิสูจน์เอกซ์กซ์ แสดงให้เห็นถึง HDTMA ถูกดูดซับไม่เพียงแค่นบนพื้นผิวด้านนอก แต่ถูกดูดซับข้างในระหว่างชั้นของเบนโทไนด์ด้วย HDTMA ส่วนใหญ่ถูกดูดซับบนพื้นผิวด้านนอกสำหรับ ออร์แกโนเกลิน ออร์แกโนฮาล์ลอายไซต์ และออร์แกโนซีโอไลต์ NaX

ในการศึกษาการดูดซับอะฟลาทอกซิน บี 1 ด้วยตัวอย่างที่ไม่ถูกตัดแปร และที่ถูกตัดแปร ได้พิจารณาอิทธิพลต่างๆ ต่อการดูดซับ พบว่า ในการศึกษาทุกกรณี ตัวอย่างที่ถูกตัดแปร สามารถดูดซับ AFB₁ สูงกว่าตัวอย่างที่ไม่ถูกตัดแปร และที่พีเอชต่ำ ความสามารถในการดูดซับของตัวดูดซับทั้งหมดต่ำกว่าที่สภาวะปกติ ออร์แกโนเบนโทไนด์ถูกพบว่าเป็นสารหนึ่งที่ดีที่สุดในการดูดซับอะฟลาทอกซิน บี 1

สาขาวิชาเคมี

ปีการศึกษา 2551

ลายมือชื่อนักศึกษา _____

ลายมือชื่ออาจารย์ที่ปรึกษา _____

THAPANEE KHUMBUDDA : MODIFICATION OF ZEOLITE NaX AND
CLAY MINERALS WITH HEXADECYLTRIMETHYLAMMONIUM
CHLORIDE FOR REMOVAL OF AFLATOXIN B₁. ASST. PROF.
KUNWADEE RANGSRIWATANANON, Ph.D. 87 PP.

HEXADECYLTRIMETHYLAMMONIUM CHLORIDE/ZEOLITE NaX/BENTONITE/
KAOLIN/HALLOYSITE/AFLATOXIN B₁

This work focused on modification of bentonite, kaolin, halloysite and zeolite NaX with hexadecyltrimethylammonium chloride (HDTMA) with concentration of 0.3, 0.6, 1.3, 2.0, 4.0 and 6.0 mM. The preparation of organoclays and organozeolite NaX were convention and microwave method. It was found that the preparation reaction time for organoclays and organozeolite NaX was decreased from 24 h by convention to only 10 min by microwave, which confirmed that microwave method was very effective for preparing organoclays organozeolite NaX. According to TGA it was found that with increasing concentration of HDTMA the amount of adsorbed HDTMA on organobentonite increased significantly, while it was rather constant on organokaolin, organohalloysite and organozeolite NaX. In the microstructure of adsorption layer by investigation with XRD it was found that in the case of bentonite modified with 6.0 mM HDTMA the interlayer spacing (d_{001}) increased significantly from 14.68 Å to 23.33 Å while it was very slightly increased in the case of the other. It corresponded to the result of TGA and DTA. Moreover, from DTA profile it implied that at least there were three different arrangements of adsorbed HDTMA on bentonite. Based on the investigation of characterizations, it revealed that HDTMA

was adsorbed not only on the external surface but also within the interlayer for bentonite, but it was mainly adsorbed on the external surface for organokaolin, organohalloysite and organozeolite NaX.

In the study of AFB₁ adsorption with unmodified and modified samples, various influences on the adsorption were considered. It was found that in all cases of the study the modified samples could adsorb AFB₁ higher than the unmodified samples and at low pH the adsorption capability of all the adsorbents was lower than that at normal condition. Organobentonite was found to be the best one for AFB₁ adsorption.

School of Chemistry

Academic Year 2008

Student's Signature_____

Advisor's Signature_____

ACKNOWLEDGEMENTS

The success of my work comes from the help of many people. I would like to express my gratitude to all those. First, I would like to thank my advisor, Assistant Professor Dr. Kunwadee Rangsiwatananon, for the encouragement in the M.Sc. program. She taught me how step of work and showed me different ways to solve problem. She has provided valuable review, comments, and suggestions during the finalization of the document. I also wish to thank all my thesis committee members Associate Professor Dr. Jatuporn Wittayakun and Dr. Sanchai Prayoonpokarach for their valuable and grateful direction, suggestion and criticism.

My thanks go to the Chairperson of School of Chemistry, Associate Professor Dr. Malee Tangsathitkulchai for serving as the chairperson of the committee and all lecturers at the School of Chemistry for their suggestions and encouragement. I would like to thanks all the staffs at the Center of Scientific and Technological Equipment for their service and helpful suggestions. I wish to thank Zeolite's group and all my friends at the Suranaree University of Technology for their kindness and help, all of the staffs at the Center for Scientific and Technological Equipment for their assistance and suggestion for the use of XRF, XRD, FT-IR, HPLC, DTA/TGA and SEM.

Last but not least, I would like to thank my family for their understanding, encouragement and support during the whole period of my education, thank you.

Thapanee Khumbudda

CONTENTS

| | Page |
|--|-------------|
| ABSTRACT IN THAI..... | I |
| ABSTRACT IN ENGLISH | II |
| ACKNOWLEDGEMENTS..... | IV |
| CONTENTS..... | V |
| LIST OF TABLES..... | IX |
| LIST OF FIGURES | X |
| LIST OF ABBREVIATIONS..... | XVI |
| CHAPTER | |
| I INTRODUCTION..... | 1 |
| 1.1 Modifications and Formulation..... | 3 |
| 1.1.1 Fundamental zeolite structure | 3 |
| 1.1.2 Clay minerals | 5 |
| 1.1.3 Ion exchange | 8 |
| 1.1.4 Surfactant | 9 |
| 1.2 Characterization techniques | 11 |
| 1.2.1 X-ray fluorescence | 11 |
| 1.2.2 Powder X-ray diffraction | 12 |
| 1.2.3 Fourier transform infrared spectroscopy..... | 13 |
| 1.2.4 Scanning electron microscopy | 14 |
| 1.2.5 Simultaneous thermogravimetry-differential thermal analysis | 15 |

CONTENTS (Continued)

| | Page |
|--|-------------|
| 1.2.6 High performance liquid chromatography..... | 15 |
| 1.3 Research objectives..... | 16 |
| II LITERATURE REVIEWS | 18 |
| 2.1 Modification of zeolite and clays..... | 18 |
| 2.2 Adsorption aflatoxin B ₁ | 21 |
| III MATERIALS, INSTRUMENTATION AND EXPERIMENTAL PROCEDURES | 23 |
| 3.1 Material lists..... | 23 |
| 3.1.1 Chemical and materials..... | 23 |
| 3.1.3 Apparatus | 24 |
| 3.2 Instrumentation | 25 |
| 3.2.1 X-ray fluorescence (XRF) | 25 |
| 3.2.2 X-ray powder diffraction (XRD) | 25 |
| 3.2.3 Fourier transform infrared spectroscopy (FT-IR) | 25 |
| 3.2.4 Scanning electron microscopy (SEM) | 26 |
| 3.2.5 Simultaneous thermogravimetry-differential thermal analyzer (TGA-DTA) | 26 |
| 3.2.6 High performance liquid chromatography (HPLC) | 26 |
| 3.3 Experimental methods | 27 |
| 3.3.1 Preparation of starting materials | 27 |
| 3.3.2 Synthesis of zeolite NaX..... | 27 |
| 3.3.3 Method of preparation of organosamples | 28 |

CONTENTS (Continued)

| | Page |
|--|-------------|
| 3.3.3.1 Preparation of organosamples by microwave method..... | 28 |
| 3.3.3.2 Preparation of organosamples by conventional method..... | 28 |
| 3.3.4 Chemical and physical characterization..... | 29 |
| 3.3.4.1 Cation exchange capacity (CEC) | 29 |
| 3.3.4.2 Characterization with different techniques | 29 |
| 3.3.5 Adsorption of aflatoxin B ₁ | 30 |
| 3.3.5.1 Normal condition | 30 |
| 3.3.5.2 Condition at pH 3..... | 31 |
| IV RESULTS AND DISCUSSIONS..... | 33 |
| 4.1 Chemical composition analysis of bentonite, kaolin and halloysite | 33 |
| 4.2 Characterization of zeolite NaX..... | 34 |
| 4.3 Cation exchange capacity | 37 |
| 4.4 Modification of clay minerals and zeolite NaX..... | 37 |
| 4.4.1 Characterization of clays by FT-IR..... | 38 |
| 4.4.2 Characterization of organoclays and organozeolite NaX by FT-IR | 40 |
| 4.4.3 Characterization of organoclays and organozeolite NaX by XRD..... | 46 |
| 4.4.4 Thermal analysis of organoclays and organozeolite NaX | 51 |

CONTENTS (Continued)

| | Page |
|---|-------------|
| 4.5 Study of adsorption of AFB ₁ | 59 |
| V CONCLUSION | 73 |
| REFERENCES | 75 |
| APPENDICES | 84 |
| CURRICULUM VITAE | 87 |

LIST OF TABLES

| Table | | Page |
|--------------|--|-------------|
| 4.1 | The chemical compositions of halloysite, kaolin and bentonite samples determined by XRF | 34 |
| 4.2 | Cation exchange capacity of clay minerals and zeolite NaX..... | 37 |
| 4.3 | Identification of IR bands of clay minerals..... | 40 |
| 4.4 | Summary of the percent mass loss of the clay minerals, zeolite NaX, organoclays and organozeolite NaX modified with various concentrations of HDTMA determined in different ranges of temperature..... | 58 |
| 4.5 | Summary of the peak area value of adsorption AFB ₁ with (a) kaolin/organokaolin, halloysite/organohalloysite and zeolite NaX/organozeolite NaX, (b) bentonite/organobentonite | 71 |

LIST OF FIGURES

| Figure | Page |
|---|-------------|
| 1.1 Chemical structure of aflatoxin B ₁ | 2 |
| 1.2 Chemical structure of hexadecyltrimethylammonium chloride (HDTMA)..... | 3 |
| 1.3 Representation of [SiO ₄] ⁴⁻ or [AlO ₄] ⁵⁻ tetrahedral | 4 |
| 1.4 Structure of zeolite NaX | 4 |
| 1.5 Single octahedron (shaded) and the sheet structure of octahedral Units..... | 5 |
| 1.6 Single silica tetrahedron (shaded) and the sheet structure of silica tetrahedrons arranged in a hexagonal network | 5 |
| 1.7 Structure of the kaolinite and halloysite layer | 6 |
| 1.8 Structure of the bentonite..... | 8 |
| 1.9 Schematic illustration of a surfactant..... | 10 |
| 1.10 The process of emission of characteristic X-ray: (a) an X-ray photon is absorbed by an inner shell electron (b) the electron is ejected from the atom creating a vacancy (c) an outer shell electron moves to the inner shell and emits the characteristic X-ray..... | 11 |
| 1.10 Geometrical illustration of the Bragg's equation..... | 13 |
| 4.1 The XRD pattern of synthesized zeolite NaX from kaolin..... | 35 |
| 4.2 The simulated XRD powder pattern of zeolite NaX..... | 35 |
| 4.3 IR spectrum of zeolite NaX | 36 |
| 4.4 SEM micrograph of the zeolite NaX | 36 |

LIST OF FIGURES (Continued)

| Figure | Page |
|--|-------------|
| 4.5 IR spectra of (a) bentonite, (b) kaolin and (c) halloysite | 38 |
| 4.6 IR spectra of bentonite (a) before and (b-d) after modification with 2.0 mM HDTMA by convention method at 12, 24 and 48 h, respectively | 41 |
| 4.7 IR spectra of kaolin (a) before and (b-d) after modification with 2.0 mM HDTMA by convention method at 12, 24 and 48 h, respectively | 41 |
| 4.8 IR spectra of halloysite (a) before and (b-d) after modification with 2.0 mM HDTMA by convention method at 12, 24 and 48 h, respectively | 42 |
| 4.9 IR spectra of zeolite X (a) before and (b-d) after modification with 2.0 mM HDTMA by convention method at 12, 24 and 48 h, respectively | 42 |
| 4.10 FTIR spectra of (a) COB and (b) MOB at concentration 0.3 (topmost), 0.6, 1.3, 2.0, 4.0 and 6.0 mM HDTM, respectively | 43 |
| 4.11 IR spectra of kaolin (a) before and (b-e) after modification with 0.6, 2.0, 4.0 and 6.0 mM HDTMA by convention method..... | 44 |
| 4.12 IR spectra of halloysite (a) before and (b-e) after modification with 0.6, 2.0, 4.0 and 6.0 mM HDTMA by convention method..... | 45 |
| 4.13 IR spectra of zeolite NaX (a) before and (b-e) after modification with 0.6, 2.0, 4.0 and 6.0 mM HDTMA by convention method..... | 45 |

LIST OF FIGURES (Continued)

| Figure | Page |
|---|-------------|
| 4.14 The XRD patterns of the organobentonite with various concentrations of HDTMA prepared by convention method | 46 |
| 4.15 The XRD patterns of the organobentonite with various concentrations of HDTMA prepared by microwave method | 47 |
| 4.16 2 theta plotted against d spacing of the organobentonite with various concentrations of HDTMA (a) prepared by convention method (b) prepared by microwave method | 48 |
| 4.17 The XRD patterns of the organokaolin with various concentrations of HDTMA prepared by convention method | 49 |
| 4.18 The XRD patterns of the organohalloysite with various concentrations of HDTMA prepared by convention method | 50 |
| 4.19 The XRD patterns of the organozeolite NaX with various concentrations of HDTMA prepared by convention method | 51 |
| 4.20 DTA profile of the organobentonite with various concentrations of HDTMA prepared by convention method..... | 52 |
| 4.21 DTA profile of the organokaolin with various concentrations of HDTMA prepared by convention method..... | 53 |
| 4.22 DTA profile of the organohalloysite with various concentrations of HDTMA prepared by convention method..... | 53 |
| 4.23 DTA profile of the organozeolite NaX with various concentrations of HDTMA prepared by convention method..... | 54 |

LIST OF FIGURES (Continued)

| Figure | Page |
|---|-------------|
| 4.24 DDTA profile of the organobentonite with various concentrations of HDTMA prepared by convention method..... | 54 |
| 4.25 DDTA profile of the organokaolin with various concentrations of HDTMA prepared by convention method..... | 55 |
| 4.26 DDTA profile of the organohalloysite with various concentrations of HDTMA prepared by convention method..... | 56 |
| 4.27 DDTA profile of the organozeolite NaX with various concentrations of HDTMA prepared by convention method..... | 57 |
| 4.28 The chromatogram of pure AFB ₁ solution at different Concentrations | 59 |
| 4.29 The chromatogram of adsorption AFB ₁ solution at 100 ppb with adsorbent..... | 60 |
| 4.30 Adsorption of AFB ₁ with different time | 61 |
| 4.31 Adsorption of 100 ppb AFB ₁ with 5, 10, 15, 20, 30, 50 and 80 mg of bentonite | 62 |
| 4.32 Adsorption of 100 ppb AFB ₁ on bentonite and modified bentonite with 0.3, 0.6, 1.3, 2.0, 4.0 and 6.0 mM HDTMA | 62 |
| 4.33 Adsorption of 200 ppb AFB ₁ on bentonite and organobentonite with 0.3, 0.6, 2.0 and 6.0 mM HDTMA | 63 |
| 4.34 Adsorption of 150 ppb AFB ₁ on kaolin and organokaolin with 0.6, 2.0 and 6.0 mM HDTMA | 64 |

LIST OF FIGURES (Continued)

| Figure | Page |
|--|------|
| 4.35 Adsorption of 150 ppb AFB ₁ on halloysite and organohalloysite with 0.6, 2.0 and 6.0 mM HDTMA..... | 64 |
| 4.36 Adsorption of 150 ppb AFB ₁ on zeolite NaX and modified zeolite NaX with 0.6, 2.0 and 6.0 mM HDTMA | 65 |
| 4.37 Adsorption of 100 ppb AFB ₁ on kaolin and modified kaolin with 0.6, 2.0 and 6.0 mM HDTMA | 65 |
| 4.38 Adsorption of 100 ppb AFB ₁ on halloysite and modifiedhalloysite with 0.6, 2.0 and 6.0 mM HDTMA | 66 |
| 4.39 Adsorption of 100 ppb AFB ₁ on zeolite NaX and modifiedzeolite NaX with 0.6, 2.0 and 6.0 mM HDTMA..... | 66 |
| 4.40 Peak area of 100 ppb AFB ₁ at pH 1.52, 1.80, 2.16 and 5.75 | 67 |
| 4.41 Peak area of (a) bentonite with 200 ppb AFB ₁ (b) kaolin, halloysite and zeolite NaX with 150 ppb..... | 68 |
| 4.42 Adsorption of 200 ppb AFB ₁ on bentonite and modified bentonite with concentration at 0.3, 0.6, 2.0 and 6.0 mM HDTMA at pH 3 | 68 |
| 4.43 Adsorption of 150 ppb AFB ₁ on kaolin and modified kaolin with concentration at 0.6, 2.0 and 6.0 mM HDTMA at pH 3..... | 69 |
| 4.44 Adsorption of 150 ppb AFB ₁ on halloysite and modified halloysite with concentration at 0.6, 2.0 and 6.0 mM HDTMA at pH 3..... | 69 |

LIST OF FIGURES (Continued)

| Figure | | Page |
|---------------|---|-------------|
| 4.45 | Adsorption of 150 ppb AFB ₁ on zeolite NaX and modified zeolite NaX with concentration at 0.6, 2.0 and 6.0 mM HDTMA at pH 3..... | 70 |
| 4.46 | Proposed β -dicarbonyl system (a) chelation of metal ion (b) reaction with H ⁺ | 70 |

LIST OF ABBREVIATIONS

| | | |
|------------------|---|---|
| XRD | = | X-ray diffractometer |
| DTA | = | Differential thermal analysis |
| TGA | = | Thermogravimetric analysis |
| FT-IR | = | Fourier transforms infrared spectrophotometer |
| XRF | = | X-ray fluorescence spectrometer |
| HPLC | = | High performance liquid chromatography |
| HDTMA | = | Hexadecyltrimethylammonium chloride |
| °C | = | Degree celcius |
| % T | = | Percent transmittance |
| cm ⁻¹ | = | Per centimeter |
| Å | = | Angstrom |
| nm | = | Nanometer |
| mM | = | Millimolar |
| M | = | Molar |
| kV | = | Kilovolt |
| mA | = | Milliampere |
| g | = | Gram |
| mg | = | Milligram |
| L | = | Liter |
| mL | = | Milliliter |

LIST OF ABBREVIATIONS (Continued)

| | | |
|--------------|---|----------------------|
| ppb | = | Part per billion |
| h | = | Hour |
| min | = | Minute |
| <i>et al</i> | = | et alia (and others) |

CHAPTER I

INTRODUCTIONS

Mycotoxins (aflatoxins, ochratoxin, fumonisines, trichotecenes, zearalenone, cyclopiasonic acid) are toxic metabolites produced by moulds under specific condition. Feed contaminated with mycotoxin is often a health and production dangerous for animals (Papp *et al.*, 2002 and Tavčar-Kalcher *et al.*, 2007). Moreover, mycotoxin residues in food of animal origin may pose a threat to human through their carcinogenic, teratogenic, immunosuppressive and other protagonist effects (Tomašević-Čanović and Dakovic, 2003). Aflatoxicosis in poultry is characterized by listlessness, anorexia with lowered growth rate, poor food utilization, decreased weight gain, decreased egg production, and increased susceptibility to environmental and microbial stresses, and increased mortality. Determination of biochemical and hematological toxic effects of aflatoxins is important for the diagnosis of toxicosis. Aflatoxins (AFB₁, AFB₂, AFG₁ and AFG₂) are a group of structurally diverse secondary fungal metabolites that occur as contaminants of grain worldwide (Otta *et al.*, 2000).

The most promising and economical approach for reducing aflatoxin is the utilization of adsorbents in animal feed to bind the mycotoxins efficiently in the gastro-intestinal tract and prevent their adsorption. AFB₁ is also known as being one of the most potent genotoxic agents and hepatocarcinogens identified (Otta *et al.*, 2002). The World Health Organization has set the maximum residue level for

aflatoxin in human food at 20 ppb. (Hell *et al.*, 2003; Grant and Philips, 1998). The aflatoxin B₁ is shown in the Figure 1.1.

It is complex organic compounds that contain a β -keto-lactone functional group with the molecular formula is C₁₇H₁₂O₆ (Tomašević-Čanović and Dakovic, 2003).

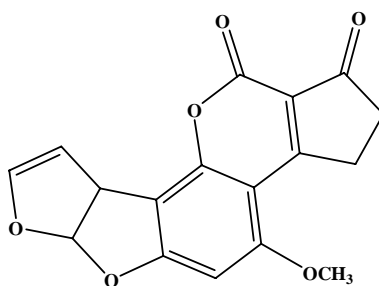


Figure 1.1 Chemical structure of aflatoxin B₁

Removing aflatoxin B₁ from contaminant food and foodstuffs remains a major problem and there is a great necessity for effective decontamination technology. Decontamination procedures have been concerned with degrading, destroying, inactivating or removing aflatoxin B₁ by physical, chemical or biological methods. Large-scale, practical, and cost-effective methods for detoxifying aflatoxin B₁ containing foodstuffs are currently not available although a variety of physical, chemical and biological method for detoxifying aflatoxin B₁ has been employed with limited success. Therefore, the use of aflatoxin B₁ contaminated food remains a significant problem, and one with serious economic implications.

Zeolites and clays modified by cationic surfactants have been applied wide variety of modern science and technology. The modification of surface properties of negatively charged zeolites/clays and the control of hydrophobicity are possible by

cation exchange of natural charge-balance cations (Na^+ , K^+ , Ca^{2+} or Mg^{2+}) with high molecular weight quaternary ammonium ions.

In this study zeolite NaX, bentonite, halloysite and kaoline have been used for modification with hexadecyltrimethylammonium chloride (HDTMA) with the molecular formula $\text{C}_{19}\text{H}_{42}\text{ClN}$ as well as the applications of modified clay (organoclays) and zeolite (organozeolite) for adsorption of aflatoxin B_1 have been investigated. The HDTMA is shown in the Figure 1.2.

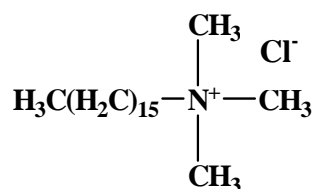


Figure 1.2 Chemical structure of hexadecyltrimethylammonium chloride (HDTMA)

1.1 Modifications and Formulation

1.1.1 Fundamental zeolite structure

The word “zeolite” has Greek roots and means “boiling stones” to demonstrate the loss of water when the naturals are heated. Zeolites are crystalline naturally occurring aluminosilicate minerals. Zeolite have framework (three-dimensional) structures constructed by joining together $[\text{SiO}_4]^{4-}$ and $[\text{AlO}_4]^{5-}$ coordination polyhedra. By definition are assembled together such that the oxygen at each tetrahedral corner is shared with that in an identical tetrahedron (Si or Al), as show in Figure 1.3. This corner (or vertex) sharing creates infinite lattices comprised of identical building blocks (unit cells) in a manner common to all crystalline materials (Wiley, 1988).

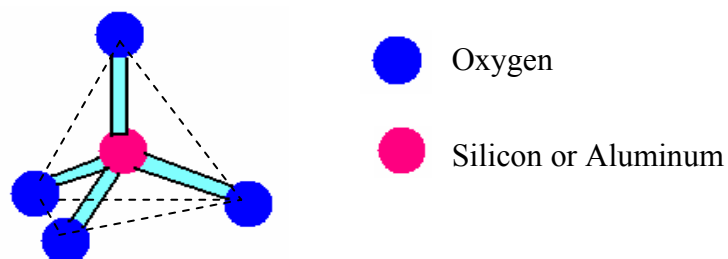


Figure 1.3 Representation of $[\text{SiO}_4]^{4-}$ or $[\text{AlO}_4]^{5-}$ tetrahedral

The structure formula of a zeolite is best expressed for the crystallographic unit cell as: $M_{x/n}[(\text{AlO}_2)_x (\text{SiO}_2)_y] \cdot w\text{H}_2\text{O}$ where n is the cation valence, M is the cation of valence n , w is the number of water molecules and the ratio y/x usually has values of 1-5 depending upon the structure. The sum $(x + y)$ is the total number of tetrahedral in the unit cell. The portion in bracket represents the framework composition (Breck, 1974).

Zeolite NaX is aluminosilicate compound with general formula $(\text{Na}_{86})(\text{Al}_{86}\text{Si}_{106}\text{O}_{384}) \cdot 264\text{H}_2\text{O}$. The structure of zeolite NaX consists of a diamond-like array of linked octahedral which are joined tetrahedral through the 6-rings. The linkage between adjoining truncated octahedral is a double 6-ring (D6R) or hexagonal prism, containing 12 $(\text{Si}, \text{Al})\text{O}_4$ tetrahedra. The framework structure can also be described in terms of the D6R units (see in Figure 1.4) (Breck, 1974).

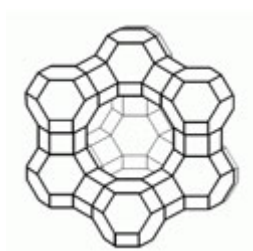


Figure 1.4 Structure of zeolite NaX

1.1.2 Clay mineral

The atomic structures of the common clay minerals have two structure units. One unit consists of two sheets of closely packed oxygens or hydroxyls in which aluminum, iron, or magnesium atoms are occupied in octahedral coordination (see in Figure 1.5). The second unit is built of silica tetrahedron. In tetrahedron a silicon atom is equidistant from four oxygens, or hydroxyls if needed to balance the structure, arranged in the form of a tetrahedron with a silicon atom at the center. The silica tetrahedral groups are arranged to form a hexagonal network (see in Figure 1.6) (Grim, 1968).

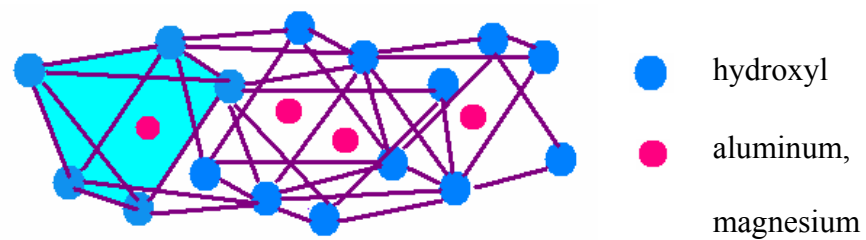


Figure 1.5 Single octahedron (shaded) and the sheet structure of octahedral Units

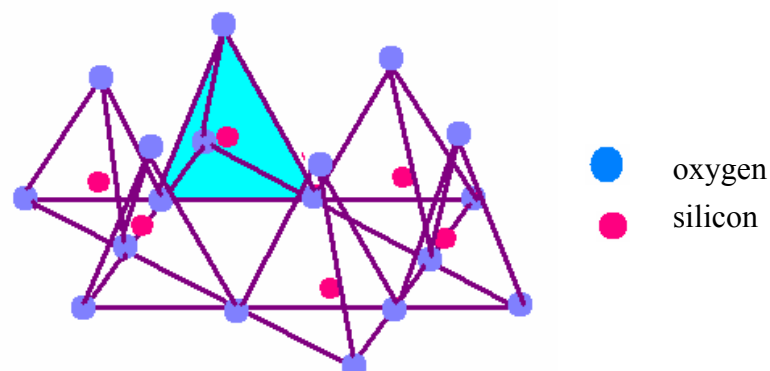


Figure 1.6 Single silica tetrahedron (shaded) and the sheet structure of silica tetrahedrons arranged in a hexagonal network

The crystal structure of all phyllosilicates is based on two types of layer. 1:1 layers in which one tetrahedral sheet is bonded to one octahedral sheet and 2:1 layers in which one octahedral sheet is sandwiched between two tetrahedral sheet (Meunier, 2005).

Kaolinite and halloysite are single-layer structures. Kaolin is a clay mineral consisted in the mineral kaolinite. The chemical formula of kaolinite is $(\text{OH})_8\text{Si}_4\text{Al}_4\text{O}_{10}$ and the theoretical composition expressed in oxides is SiO_2 , 46.54%; Al_2O_3 , 39.50%; H_2O , 13.96% . Halloysite are two forms, one with the composition $(\text{OH})_8\text{Si}_4\text{Al}_4\text{O}_{10}$ and the other with the composition $(\text{OH})_8\text{Si}_4\text{Al}_4\text{O}_{10}\cdot 4\text{H}_2\text{O}$. Both structure are composed of a single silica tetrahedral sheet and a single alumina octahedral sheet combined in a unit so that the tips of the silica tetrahedrons and one of the layers of the octahedral sheet form a common layer (see in Figure 1.7). All the tips of the silica tetrahedrons point in the same direction and toward the center of the unit made by the silica and octahedral sheets.

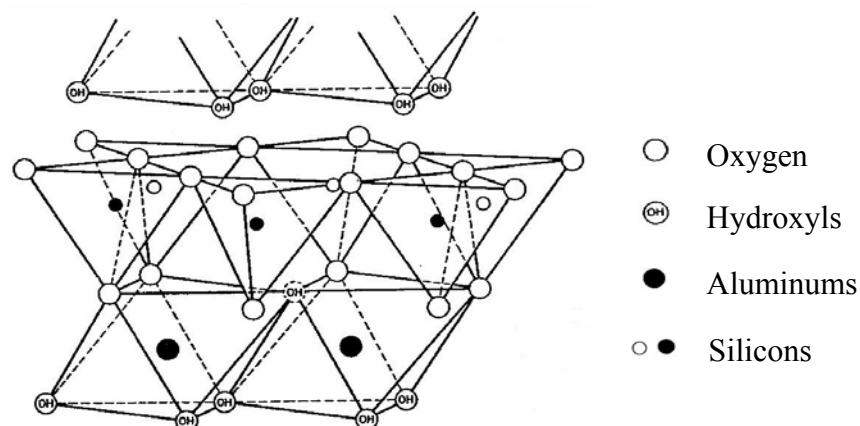


Figure 1.7 Structure of the kaolinite and halloysite layer

In the layer common to by the octahedral and tetrahedral groups, two-thirds of the atoms are shared by the silicon and aluminum, and then they become O instead of

OH. Only two-thirds of the possible positions for aluminum in the octahedral sheet are filled, and there are three possible plans of regular population of the octahedral layer with aluminums. The aluminum atoms are considered to be so placed that two aluminums are separated by an OH above and below, thus masking a hexagonal distribution in a single plane in the center of the octahedral sheet. The OH groups are placed so placed so that each OH is directly below the perforation of the hexagonal net of oxygens in the tetrahedral sheet (Grim, 1968). The difference of kaolinite and halloysite are compare that halloysite contain H₂O more than kaoline indicate that in some way the excess water causes the interlayer bonds to become too weak to overcome the misfit and that curved layers or tubes form are to be expected. In kaolinite, the interlayer bonds are presumably strong enough to stretch the gibbsite sheet of one layer to fit the Si-O sheet of the adjacent layer, thereby overcome the misfit and producing plate crystals.

Bentonite is a clay generated frequently from the alteration of volcanic ash, consisting predominantly of smectite minerals. It is an absorbent aluminium phyllosilicate generally impure clay consisting mostly of montmorillonite. They are three-layer clay minerals, which the chemical formula is $(\text{OH})_{12}\text{Si}_8\text{Al}_4\text{O}_{16}\cdot\text{H}_2\text{O}$. The structure is composed if units up of two silica tetrahedral sheet with a central aluminum octahedral sheet (see in Figure 1.8). The silicate layers have a slight negative charge that is compensated by exchangeable ions in the intercrystallite region. The charge is so weak that the cations (in natural form, predominantly Ca^{2+} , Mg^{2+} or Na^+ ions) can be adsorbed in this region with their hydrate shell. The extent of hydration produces intercrystalline swelling. Depending on the nature of their genesis, bentonites contain a variety of accessory minerals in addition to

montmorillonite. The chemical formula of bentonite is $(\text{OH})_{12}\text{Si}_8\text{Al}_4\text{O}_{16}\cdot\text{H}_2\text{O}$.

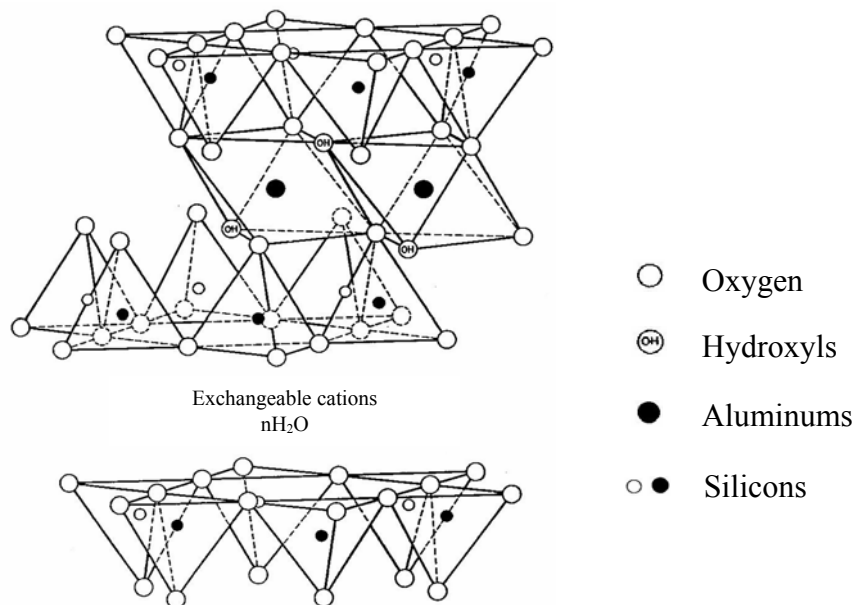


Figure 1.8 Structure of the bentonite

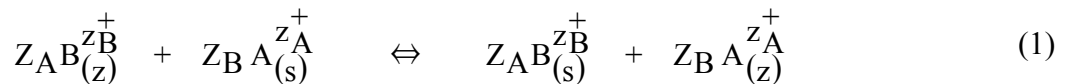
1.1.3 Ion exchange

The ion exchange behavior of various inorganic exchangers and other types of crystalline silicates such as clay minerals and feldspathoids has been extensively reviewed. Because of their three-dimensional framework structure, most zeolites and feldspathoids do not undergo any appreciable dimensional change with ion exchange; clay minerals, because of their two-dimensional structure, may undergo swelling or shrinking with cation exchange. One application for commonly occurring zeolite mineral minerals (such as clinoptilolite) is in the selective removal of radioactive ions from radioactive waste materials.

The cation exchange behavior of zeolites depends upon the nature of the cation species, the cation size, both anhydrous and hydrated, and cation exchange; the

temperature; the concentration of the cation species in solution; the solvent (most exchange has been carried out in aqueous solution, although some work has been done in organic solvents) and the structural characteristics of the particular zeolite. Cation selectivities in zeolites do not follow the typical rules that are evidenced by other inorganic and organic exchangers. Zeolite structures have unique features that lead to unusual types of cation selectivity and sieving. The recent structural analyses of zeolites form a basis for interpreting the variable cation exchange behavior of zeolites (1).

The ion exchange process zeolites are defined by:



Where Z_A , Z_B are the changes of the exchange cations A and B and the subscripts z and s refer to the zeolite and solution, respectively (Breck, D.W., 1974).

The position of the equilibrium is a measure of the ion-exchange selectivity. The selectivity for given cations is determined by the electric fields of the coordinating anionic locations in the zeolite framework. Thus, for each zeolite type there is a specific selectivity series with the cations arranged in order of increasing exchangeability (Dyer, 1998).

1.1.4 Surfactant

Surfactants are usually organic compounds that are amphiphilic, meaning they contain both hydrophobic groups (their “tails”) and hydrophilic groups (their “heads”) (Figure 1.9)

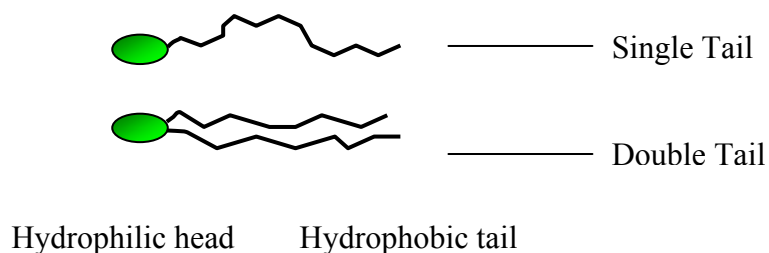


Figure 1.9 Schematic illustration of a surfactant

A surfactant can be classified by the presence of formally charged groups in its head. A nonionic surfactant has no charge groups in its head. The head of an ionic surfactant carries a net charge. If the charge is negative, the surfactant is more specifically called anionic; if the charge is positive, it is called cationic. If a surfactant contains a head with two oppositely charged groups, it is termed zwitterionic. The cationic surfactants are important as disinfectant soaps, as germicides, and in the textile industry. The central atom is nearly always nitrogen. As well as the amines and their salts, quaternary ammonium compounds and quaternary heterocyclic compounds are manufactured (Hummel, 2000).

Surfactants reduce the surface tension of water by adsorbing at the liquid-gas interface. They also reduce the interfacial tension between oil and water by adsorbing at the liquid-liquid interface. Many surfactants can also assemble in the bulk solution into aggregates. Some of these aggregates are known as micelles. The concentration at which surfactants begin to form micelles is known as the critical micelle concentration or CMC. When micelles form in water, their tails form a core that can encapsulate an oil droplet, and their (ionic/polar) heads form an outer shell that maintains favorable contact with water. When surfactants assemble in oil, the aggregate is referred to as a reverse micelle. In a reverse micelle, the heads are in the

core and the tails maintain favorable contact with oil.

In this study, various characterization techniques were used to analyze the properties of kaolin, halloysite, bentonite, zeolite NaX and the organosamples. In this section, a brief overview of the characterization techniques were described.

1.2 Characterization techniques

1.2.1 X-ray fluorescence

XRF is an elemental analysis technique with unique capabilities including highly accurate determinations for major elements and a broad elemental survey of the sample composition without standards. High energy photons (X-rays) displace inner shell electrons. Outer shell electrons then fall into the vacancy left by the displaced electron and normally emit light (fluoresce) equivalent to the energy difference between the two states (Figure 1.10). Since each element has electrons with more or less unique energy levels, the wavelength of light emitted is characteristic of the element. And the intensity of light emitted is proportional to the elements concentration (Whiston, 1987).

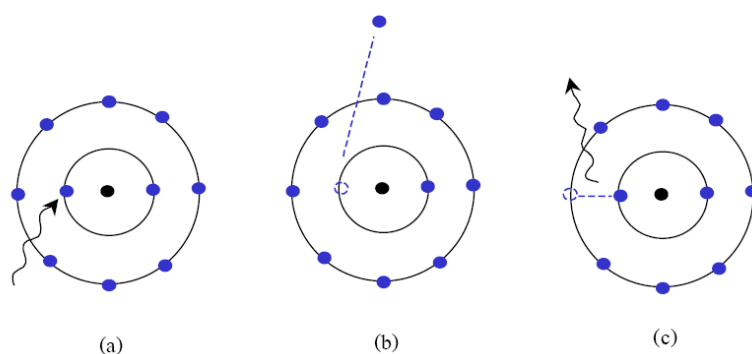


Figure 1.10 The process of emission of characteristic X-ray: (a) an X-ray photon is absorbed by an inner shell electron (b) the electron is ejected from the atom creating a vacancy (c) an outer shell electron moves to the inner shell and emits the characteristic X-ray

1.2.2 Powder X-ray diffraction

Power diffraction is mainly used for the identification of compounds by their diffraction patterns. X-ray are put to use to study the internal structure of objects that are opaque to visible light but transparent to X-rays. The wavelength, most commonly used in crystallography, range between ~ 0.5 and ~ 2.5 Å since they are of the same order of magnitude as the shortest interatomic distances observed in both organic and inorganic material. An X-ray diffraction has been used in two main areas; the fingerprint characterization of crystalline materials for its identification and the determination of their structures, i.e. how the atoms packed together in the crystalline state and what the inter-atomic distance and angle are. These unique properties make X-ray diffraction one of the most important characterization tools used in solid state chemistry and material science.

An important equation for X-ray diffraction is Bragg's equation, which is derived geometrically in Figure 1.11. From Bragg's equation is shows a relationship between X-ray wavelength (λ) with lattice point distance (d) and the incident diffraction angle (θ) (2).

$$n\lambda = 2d_{hkl}\sin\theta_{hkl} \quad (2)$$

The different crystal plane (hkl) in the crystal will diffract X-ray at different angle according to the Bragg's equation. Therefore, by rotate the sample plane with respect to the incident X-ray, the diffracted angles can be recorded by a detector and the diffraction pattern is obtained. The identification of the sample structure can be done by comparing the spectrum with the pattern stored in the database (Pecharsky and Zavalij, 2003).

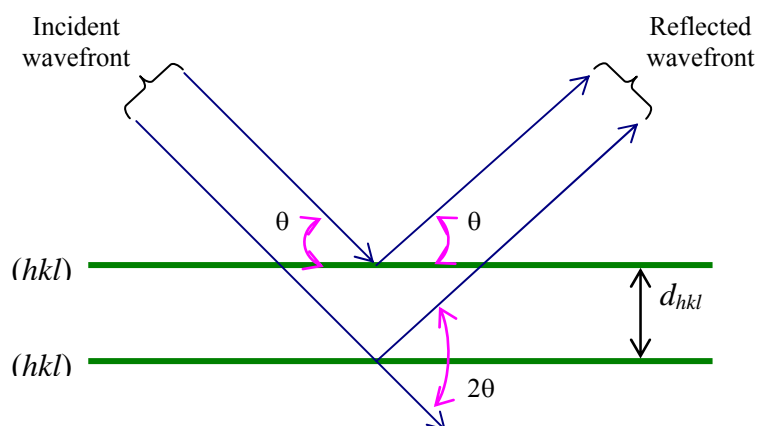


Figure 1.11 Geometrical illustration of the Bragg's equation

1.2.3 Fourier transform infrared spectroscopy

Infrared spectroscopy is the study of the interaction infrared light with matter. Light is composed of electric and magnetic waves. The radiation in the vibration infrared region of the electromagnetic spectrum in terms of a unit called a wavenumber (W), rather than wavelength (λ). Wavenumbers are expressed as reciprocal centimeters (cm^{-1}). The wavenumber of a light is defined as the reciprocal of the wavelength (3).

$$W = 1/\lambda \quad (3)$$

Fourier transform infrared (FTIR) spectroscopy measures dominantly vibrations of functional groups and highly polar bonds. Thus these chemical fingerprints are made up of the vibrational features of all the samples components.

The majority of FTIRs operate in mid infrared radiation will be defined as light between 4000 and 400 cm^{-1} . FTIR experiments generally can be classified into the following two categories: (a) qualitative analysis, where the aim is to identify the

sample and (b) quantitative analysis, where the intensity of absorptions are related to the concentration of the component.

Potassium bromide (KBr) pellets are used to obtain the infrared spectra of solid, and are particularly to powdered sample. KBr is an inert, infrared transparent material and acts as a support and a diluent for the sample (Smith, 1996).

1.2.4 Scanning electron microscopy

Scanning electron microscope (SEM) is a type of microscope that uses electrons rather than light to form an image. The SEM does not produce a true image of the specimen. Instead, SEM produces a point by point reconstruction of the specimen, basically the same way a television set reconstructs an image from signals sent by the television station transmitter. SEM reconstructs image of the specimen from a signal emitted from the specimen when it is illuminated by the high-energy electron beam, instead of a signal from the television transmitter. The preparation of samples is relatively easy since most SEM instruments only require the sample to be conductive. The combination of higher magnification, larger depth of focus, greater resolution and ease of sample observation make SEM one of the most heavily used instruments in present-day research. The samples must be a conductive material in order to be able to interact with an electron; SEM samples are coated with a very thin layer of gold by a machine called a sputter coater. The SEM shows very detailed 3-dimensional images at a much higher magnification than is possible with a light microscope.

The image in the scanning electron microscope is produced in basically the same way, except that, instead of the signal coming from the television station

transmitter, the signal now comes from the interaction of an electron beam with the specimen in the column of the SEM.

A detector counts these electrons and sends the signals to an amplifier. The final image is built up from the number of electrons emitted from each spot on the sample. By this way, the morphology of the sample can be seen directly from the micrograph (Lee, 1993).

1.2.5 Simultaneous thermogravimetry-differential thermal analysis

Differential thermal analysis has application in the study of minerals such as clay minerals, carbonates, sulphates and zeolites. Thermal analysis instruments predominantly use thermocouples platinum resistance thermometers and thermistors. When the sample undergoes a transformation, it will either absorb (endothermic) or release (exothermic) heat. In differential thermal analysis between a reactive sample and a non-reactive reference is determined as a function of time, providing useful information about the temperatures.

Thermogravimetric analysis determines the weight gain or loss of a condensed phase due to gas release or absorption as a function of temperature. Simultaneous Differential Techniques module is an analysis module that is capable of performing both thermogravimetric (TGA) and differential thermal analysis (DTA) at the same time. The simultaneous module measures the amount and rate of weight change in a material with a function of increasing temperature or isothermally as a function of time in a controlled atmosphere (TGA functions) (Haines, 2002).

1.2.6 High performance liquid chromatography

HPLC is used to separate components of a mixture by using a variety of

chemical interactions between the substance being analyzed and the chromatography column. A liquid sample or a solid sample dissolved in suitable solvent is carried through a chromatographic column by a liquid mobile phase. Separation is determined by solute/stationary-phase interactions, including liquid-solid adsorption, liquid-liquid partitioning, ion exchange and size exclusion and by solute/mobile-phase interaction.

In liquid-liquid chromatography the stationary phase is a liquid film coated on a packing material consisting of 3-10 μm porous silica particles. Bonded stationary phases are attached by react the silica particles with an organochlorosilane. The combination of a polar stationary phase and a nonpolar mobile phase is called normal-phase chromatography. In reverse-phase chromatography the stationary phase is nonpolar and the mobile phase is polar.

In a normal-phase separation the least polar solute spends proportionally less time in the polar stationary phase and is the first solute to elute from column. Retention times are controlled by selecting the mobile phase, with a less polar mobile phase leading to longer retention times. In a reverse-phase separation the order of elution is reversed with the most polar solute being the first to elute. Increasing the polarity of the mobile phase leads to longer retention times, whereas shorter retention times require a mobile phase of lower polarity. The most popular HPLC detectors are based on spectroscopic measurements including UV/Vis absorption and fluorescence (Harvey, 2000).

1.3 Research objectives

1.3.1 To improve the properties of zeolite NaX, halloysite, kaoline and bentonite by modification with surfactant (hexadecyltrimethylammonium chloride;

HDTMA).

1.3.2 To prepare the organozeolite NaX and organoclay with microwave and conventional method.

1.3.3 To characterize the physical and chemical properties of the organozeolite NaX and organoclays.

1.3.4 To compare some results from the microwave and convention methods. bentonite

1.3.5 To study the adsorption of aflatoxin B₁ by the organoclays and Organozeolite NaX.

CHAPTER II

LITERATURE REVIEWS

2.1 Modification of zeolites and clays

There are many studies on the modification of zeolites and clay minerals with surfactants in order to increase their hydrophobic properties for removing organic contaminants effectively as well as their physical and chemical properties have been characterized by thermal analysis, XRD, SEM, surface area and FT-IR method.

Modifications of bentonite with surfactants were widely used (Yapar *et al.*, 2005; Upson and Burns, 2006; Richards and Bouazza, 2006). Organobentonites (ODTMA-B, HDTMA-B) containing different organic cations (octadecyltrimethylammonium bromide; ODTMA and hexadecyltrimethylammonium bromide; HDTMA) were synthesized and used to adsorb benzoic acid and hydroquinone at different pH and temperatures. The results showed that the sorption capacities increased with decreasing pH value and increasing temperature. The adsorption capacity for benzoic acid was higher comparing to that of HDTMA-B at various pH and temperatures. Synthesized organobentonites were characterized by XRD, particle size and surface area. Particle size analysis showed that the organobentonite contained a greater number of coarse particle than that of the original bentonite. XRD results exhibited that the basal spacings of the organobentonites were increased, but surface area decreased (Yıldız *et al.*, 2005). Moreover, Organobentonite prepared with HDTMA-Br had been characterized by FT-IR and scanning electron microscopy

(Majdan *et al.*, 2005). FT-IR spectra showed the change from gauche to trans conformation in the surfactant arrangement in the clay interlayer. In addition, the formation of alkylammonium chromates of the HDTMA-modified bentonite was also examined by SEM (Yunfei *et al.*, 2008). They attempted to modify montmorillonite with octadecyl-trimethyl ammonium bromide at various concentrations and analyzed with thermogravimetric technique in order to determine the changes in the surfactant concentration on organomontmorillonite.

Li *et al.* (2006) found that the modifications of bentonite with cetylpyridium chloride (CPC) by conventional method took a lot of time, whereas that by microwave took a few minute. The results from XRD and atomic force microscopy (AFM) showed that the CPC moles have entered into interlayer spacing of bentonite and DTA/TG curves of modified bentonite by convention and microwave compared with natural bentonite the endothermic peak of desorbed water drifted to low temperature zone.

The characteristics of montmorillonites modified with HDTMA were evaluated by investigating adsorption isotherms and microstructures (Lee *et al.*, 2005). Determination of adsorption isotherms, XRD and TEM indicated that the interlayer structure of montmorillonites varies with the amount of HDTMA adsorbed in different ways for different sources of montmorillonites. However, He and coworker (He *et al.*, 2006) used the technique of X-ray photoelectron spectroscopy (XPS) in combination with X-ray diffraction (XRD) and high-resolution thermogravimetric analysis (HRTG) to investigate the HDTMA distribution within the organomontmorillonites. It was found that in the organoclays prepared at relatively low surfactant concentration, the surfactant cations mainly occupy the clay interlayer with lateral arrangement. However,

when the surfactant concentration are higher, the surfactants occupy both the clay interlayer space and the interparticle pores, and paraffin type arrangements of surfactant are adopted in the clay interlayer spaces. Montmorillonites modified with HDTMA to adsorb hydrophobic organic compound were linearly increased with the amount of HDTMA added to the clay (Lee *et al.*, 2004). Two different sources of montmorillonites which were reacted with amounts of different alkylammonium cations, octadecyl (C₁₈)-, hexadecyltrimethyl (HDT) and dioctadecyldimethyl (DOD)ammonium, in order to vary in their surface properties for adsorption-desorption of the herbicide, dicamba were studied (Carrizosa *et al.*, 2001). According to the swelling property of montmorillonite and surfactant intercalation, it is difficult to differentiate amount of surfactant sorbed on mineral surfaces from that in interlayer spaces.

Kaolinite has been used for modification because it is a 1:1 layered clay mineral showing no swelling in the presence of quaternary ammonium compounds, thus, making it ideal for the studied of HDTMA sorption on external mineral surfaces (Li and Gallus, 2005). In addition, the research (Li and Bowman, 2001) reported that kaolin modified with HDTMA can remove target anions from industrial wastewaters.

HDTMA was used to modify zeolite as in the report (Majdan *et al.*, 2006). Chabazite was modified with HDTMA to check its usefulness in the elimination of chromates from aqueous solutions. It is established that HDTMA⁺ cations are incorporated into the chabazite structure via ion-exchange and van der Waals forces. HDTMA-chabazite is evaluated as efficient adsorbent for chromates.

Sullivan *et al.* (1998) interested in the sorption enthalpies of HDTMA and

tetraethylammonium bromide used as monomers and micelles on natural clinoptilolite. The conformation, sorption mechanism and relative stability of the sorbed surfactants on natural clinoptilolite were discussed. In addition, the utilization of modified zeolites with HDTMA were interested for adsorbing antimonite (Wingenfelder *et al.*, 2006).

2.2 Adsorption aflatoxin B₁

Aflatoxins have many types such as AFB₁, AFB₂, AFG₁ and AFG₂ but AFB₁ is the most prevalent and toxic of the aflatoxins, with acute toxicity demonstrated in all species of animal. Council for Agricultural Science and Technology has fixed maximum level for aflatoxin in human foods contaminant at 20 ppb (Grant and Phillips., 1998; Hell *et al.*, 2003). Moreover, AFB₁ is also known as being one of most potent genotoxic agents and hepatocarcinogens identified. Aflatoxin B₁ was the most dangerous of these secondary metabolites. Because there was no definitive way in which complete detoxification of food and feed contaminants with aflatoxin B₁. New methods to eliminate aflatoxin B₁ will be sought. Huwig *et al.* (2001) reported adsorption mycotoxins with the different adsorbents. Aluminosilicates were the preferred adsorbents, followed by activated charcoal and polymers.

Ramos and Hernández (1997) interested in using natural zeolite as sorbent to sorb aflatoxins. The protective effect against the development of aflatoxicosis in farm animals with add of natural zeolite to feedstuffs. Adsorption of AFB₁ was investigated by natural montmorillonite (MONT) and montmorillonite modified with copper ions (Cu-MONT) at different pH. It found that montmorillonite and Cu-MONT are able to adsorb AFB₁ more over 93% and no difference in AFB₁ adsorption by both MONTs,

at pH 3, 7 and 9 were observed (Daković *et al.*, 2008).

The natural zeolites were used for adsorption of aflatoxin B₁, zearalenone and ochratoxin A. Tomašević-Ćanović and others (2003) have been interested in the study of adsorption of mycotoxin on natural clinoptilolite-heulandite rich tuff and the modified samples with octadecyldimethylbenzyl ammonium chloride (Do) and dioctadecyl-dimethylammonium chloride (Pr). The modification of natural clinoptilolite-heulandite rich tuff was prepared by wet and dry process. Adsorption studies of mycotoxin showed that all the organozeolites effectively adsorbed aflatoxin B₁, zearalenone, ochratoxin A and ergopeptine alkaloids. In addition, the clinoptilolite-heulandite-rich tuff modified with different amounts of octadecyldimethylbenzyl ammonium (ODMBA) ion applied for adsorbing zearalenone (ZEN), ochratoxin A (OCHRA) and aflatoxin B₁ (AFB₁) was also investigated (Daković *et al.*, 2005).

The most commonly used determined aflatoxin B₁ with high performance liquid chromatography (HPLC) is a reversed phase C₁₈ column and detected with fluorescence spectroscopy. The most frequently used compounds for pre-column derivatization are trifluoroacetic or its anhydride, while iodine was reported as a post-column derivatizing agent (Papp *et al.*, 2002; Hajian and Ensafi., 2009; Daković *et al.*, 2005).

Many researchers have conducted the researches on modification of zeolites and clay minerals with different surfactants for adsorbing organic compounds. In our study HDTMA has been selected to be used as a surfactant because it is cationic surfactant having a long chain. Moreover, there are no reports on study of modification of zeolite NaX, bentonite, kaolin and halloysite with HDTMA for removing of aflatoxin B₁ and a huge amount of bentonite, kaolin and halloysite have been found in many provinces of Thailand.

CHAPTER III

MATERIALS, INSTRUMENTATIONS AND EXPERIMENTAL METHODS

This chapter is divided in three parts. In the first part, it refers to materials lists, instrumentations and experimental methods. The material lists are presented chemicals, material, glassware and apparatus. The second part mentions the analytical instruments using to characterize the samples, such as X-ray fluorescence (XRF), X-ray powder diffraction (XRD), fourier transform infrared spectroscopy (FTIR), simultaneous thermogravimetry-differential thermal analyzer (TGA-DTA), scanning electron microscopy (SEM) and high performance liquid chromatography (HPLC). The third part of the chapter describes about the experimental methods.

3.1 Material lists

3.1.1 Chemicals and materials

- (a) Bentonite, Thai Nippon Chemical Industry Co., Ltd.
- (b) Halloysite Thai Nippon Chemical Industry Co., Ltd.
- (c) Kaolin, Sibelco minerals (Thailand) Co., Ltd.
- (d) Ammonium acetate, $\text{CH}_3\text{COONH}_4$, BDH
- (e) Hexadecyltrimethylammonium chloride, $\text{C}_{19}\text{H}_{42}\text{NCl}$, Fluka
- (f) Isopropyl alcohol, $(\text{C}_3\text{H}_8\text{O})$, BDH
- (g) Ammonium chloride, NH_4Cl , Fluk

- (h) Ammonium oxalate, $(\text{NH}_4)_2\text{C}_2\text{O}_4\text{H}_2\text{O}$, BDH
- (i) Silver nitrate, AgNO_3 , Carloerba
- (j) Sodium hydroxide, NaOH , Merck
- (k) Boric acid, H_3BO_3 , Carloerba
- (l) Hydrochloric, HCl , Merck
- (m) Methyl alcohol, CH_3OH , Carloerba
- (n) Methyl red, $\text{C}_{15}\text{H}_{15}\text{N}_3\text{O}_2$, Merck
- (o) Bromocresol green, $\text{C}_{21}\text{H}_{14}\text{Br}_4\text{O}_5\text{S}$, Fluka
- (p) Aflatoxin B₁, $\text{C}_{17}\text{H}_{12}\text{O}_6$, Aldrich
- (q) Glass microfiber filters, whatman GF/C diameter 47 mm
- (r) Nylon Membrane filters, vertical diameter 13 mm

3.1.2 Apparatuses

- (a) Vacuum filtration apparatus (Gast)
- (b) Hot air oven
- (c) Furnace
- (d) Thermostatic shaker bath (SBD 50)
- (e) Kjeldahl
- (f) Microwave with 600 W (Mar 5)
- (g) pH meter (Schott)
- (h) Analytical balance (Mettler Toledo)
- (i) Oven for drying sample (Binder, ED)
- (j) Freeze dry
- (k) Desiccators

(l) Standard sieve 230 mesh (63 μm) (Analysensieb, Retsch, USA)

(m) Glass microfiber filters, Whatman GF/C diameter 47 mm

(n) Sieve Shaker (Octagon digital, Endecotts, England)

3.2 Instrumentation

3.2.1 X-ray fluorescence (XRF)

XRF is one of the techniques, widely used to determine elemental compositions of solid samples especially in soil or powder samples, such as aluminium, silicon, iron, calcium, potassium and titanium. X-ray fluorescence spectrometer, Phillip MagiX Pro, was used. The samples were prepared by pressing into pellets. The measurement time was about 5 min per sample. The results were reported in the form of oxide percentage.

3.2.2 X-ray powder diffraction (XRD)

XRD was used for the analysis of the structural properties and the identifications of mineral in solid state and material science. This technique was obtained using a Bruker D5005 Powder X-ray diffractometer with Ni-filtered Cu $K\alpha$ radiation source and operated at 35 kV/35 mA for record all of the diffraction spectra. All XRD data were collected under the same experimental conditions, in the angular range $3^\circ \leq 2\theta \leq 50^\circ$ and scan speed of 0.5 degree/0.02 angle. Typically, the data was expressed in the plot between intensity of diffraction peaks and 2θ angle. The positions of diffraction peaks were compared with a reference data base and the identifications of compounds.

3.2.3 Fourier transform infrared spectroscopy (FT-IR)

Infrared spectra were obtained using a Perkin-Elmer spectrum GX FTIR Spectrophotometer and infrared spectra were taken in the range of mid infrared (4000-400 cm^{-1}). The samples were recorded with 13 of number scan and with 4 cm^{-1} resolution. The samples were prepared by KBr pellet technique. The solid sample and KBr were dried at 110°C for at least 1 h before obtaining the spectra. The sample and KBr were mixed with a mortar and pestle. The ground powder was pressed into a transparent disk using a hydraulic pressing machine with an equivalent weight of about 10 tons for 1 minute.

3.2.4 Scanning electron microscopy (SEM)

All samples were sieved with mesh number 63 micron and spatter onto the specimen stub. Then, the sample was dried by using UV light for ten minutes. After that, the sample was coated with a layer of gold approximately 20-25 Å thick with a Balzer sputtering coater to make them conductive. The micrographs were recorded with an accelerating voltage of 20 kV.

3.2.5 Simultaneous thermogravimetry-differential thermal analyzer (TGA-DTA)

Simultaneous DTA/TGA is a powerful thermoanalytical technique that combines a DTA and a TGA into one instrument that performs both DTA and TGA on the same sample at the same time. Thermal analysis was performed simultaneously on a Model SDT 2960 under static air atmosphere with rate 120 ml min^{-1} at a heating rate of 10°C min^{-1} from room temperature to 1000°C. Alumina was taken as a reference.

3.2.6 High performance liquid chromatography (HPLC)

Analysis of aflatoxin B₁ was carried out on a high performance liquid chromatography Model HP1100 which was cooperated with post column on PCX 5200 by reverse phase chromatography. The separation was done on C18 column with specifications of 250×4 mm (dimension) and 5 μm (particle size). The mobile phase was the mixture of water: methanol (30:70, v/v). The operation with flow rate of 0.5 mL/min and post column with iodine aqueous solution with flow rate of 0.3 mL/min were applied. The injected sample volume was 10 μL and the column temperature was controlled at 30°C. The fluorescence spectrometer was used as a detector and the excitation and emission wavelengths were set at 365 nm and 450 nm, respectively.

3.3 Experimental methods

3.3.1 Preparation of starting materials

Natural kaolin, bentonite and halloysite were ground in agate mortar and sieved with mesh number 63 micron aperture and dried at 110°C before using in the following step (2.3.2-2.3.5).

3.3.2 Synthesis of zeolite NaX

Zeolite NaX was synthesized with the method of Thammavong (2003). The kaolin samples was calcined in the furnace at 900°C for 1.5 h to transform into metakaolin. The metakaolin was reacted with Na₂SiO₃ 1.5 g and 7.5% NaOH 20 ml and was shaken at room temperature for 72 h, then the mixture was crystallized at 90°C for 24 h. The obtained solid was washed with deionized water until the pH of

filtrate became 7. Zeolite NaX was dried overnight in the oven at 110°C to remove moisture.

3.3.3 Method of preparation of organosamples

Two methods were used to modify the samples to obtain organozeolite NaX and organoclays (organobentonite, organokaolin and organohalloysite) described as follows:

3.3.3.1 Preparation of organosamples by microwave method

To examine the equilibrium time for ion exchange between cation in the starting samples and HDTMA, 0.2 g of zeolite NaX or clays was mixed with HDTMA 50 mL at concentration of 2.0 mM. The mixture was mixed throughout then put into microwave oven with power 600 W and different irradiation times (5, 10 and 15 min). After that the solid phase was separated by centrifugation. The treated zeolite NaX or clays was washed with deionized water at least three times until it was chloride free and dried by freeze dry for 24 h. Then the modified samples known as organosamples were analyzed by FT-IR to indicate what the time reached to equilibrium. Then equilibrium time was used for preparing organosamples at different concentrations of HDTMA (0.3, 0.6, 1.3, 2.0, 4.0 and 6.0 mM).

3.3.3.2 Preparation of organosamples by conventional method

In order to determine the equilibrium time of ion exchange process, 1 g of zeolite NaX or clays was mixed with HDTMA 250 mL at concentration of 2.0 mM. The mixture was subjected to stirring at different times (12, 24 and 48 h). Then the solid phase was separated by centrifugation. The treated zeolite NaX or clays was washed with deionized water at least three times until it was chloride free and dried by freeze dry for 24 h. The modified samples were analyzed by FT-IR to find out the

equilibrium time. Then, the time reached to equilibrium was fixed for preparing organosamples at different concentrations of HDTMA (0.3, 0.6, 1.3, 2.0, 4.0 and 6.0 mM).

3.3.4 Chemical and physical characterization

3.3.4.1 Cation exchange capacity (CEC)

The CEC of clay and zeolite was determined by the ammonium acetate method according to Maria (1997). The procedures for CEC were described as follows:

10 g of sieved halloysite, bentonite and kaolin were weighed into 500 mL Erlenmeyer flask mixed with 200 mL 1 M $\text{CH}_3\text{COONH}_4$ and shaken for 24 h. Then, the samples were washed again with 200 mL 1 M $\text{CH}_3\text{COONH}_4$ and shaken for 24 h. The samples were filtered and kept wet. The samples were rinsed for 4 times with 25 mL aliquots of neutral 1 M NH_4Cl .

Then, the samples were rinsed again with 0.25 M NH_4Cl for 1 times and followed with isopropyl alcohol until it was Cl^- free. NH_4^+ adsorbed on surface clay were removed by 10% acidified NaCl solution until 425 mL passed through the sample. Then, the 10% acidified NaCl was added in small portions allowing each portion to pass through sample before adding the next portion. The solution samples were transferred to a 500 mL volumetric flask and filled to mark with 10% acidified NaCl. The ammonia exchanged was determined by taking an aliquot of about 20 mL of the solution and was titrated directly with a solution 0.05 M HCl.

Finally, the ammonia was determined by Kjeldahl method. The result was calculated as milliequivalents per gram sample.

3.3.4.2 Characterization with different techniques

Chemical compositions of the starting materials were determined by XRF. FT-IR and XRD were used to determine alkyl chain molecules containing in the organosamples and d-spacing, respectively. DTA/TGA were applied to thermal analyze of the starting materials and also the prepared organosamples.

3.3.5 Adsorption of aflatoxin B₁

Adsorptions of aflatoxin B₁ (AFB₁) by organoclays and organozeolite NaX were determined at 30°C with the condition at pH 3 and at pH of the solutions without adjusting acid or alkali described as follows.

3.3.5.1 Normal condition

Normal condition in this study was defined as the condition that the mixture was made up with only the solution of AFB₁ and adsorbents without any adjustment of acid or alkali.

1. To determine the correlation between the concentration of AFB₁ and its peak area, the concentrations of AFB₁ with 30, 60, 100, 150 and 200 ppb were set up and amounts of AFB₁ were determined by HPLC.

2. To determine the equilibrium time, 10 mg of bentonite was mixed with 25 ml of AFB₁ at only concentration of 60 ppb. The mixtures were subjected to shaken at different times (12, 24 and 48 h) at 30°C. Then the solid phase was firstly separated by centrifugation. After that the supernatant was filtered and kept in vial and amount of AFB₁ was determined by HPLC.

3. To examine the suitable amount of bentonite for adsorption study, about 5, 10, 15, 20, 30, 50 and 80 mg bentonite were set up. Then each weight of bentonite was mixed with 25 ml of AFB₁ at only concentration of 100 ppb and was

done further as described above. The amount of 30 mg was selected for the next experiment.

4. To determine the amount of adsorbed AFB₁ with bentonite and organobentonite which were modified with 0.3, 0.6, 1.3, 2.0, 4.0 and 6.0 mM HDTMA by convention method. Bentonite or organobentonite 30 mg was mixed with 25 mL of AFB₁ solution with concentration of 100 and 200 ppb. In the case of AFB₁ solution 200 ppb, only organobentonite with 0.3, 0.6, 2.0 and 6.0 mM HDTMA were applied. The experiment was carried on as mentioned above.

5. To determine the amount of adsorbed AFB₁ with kaolin, halloysite, zeolite NaX organokaolin, organohalloysite and organozeolite NaX were performed under the same condition as done on bentonite and organobentonite, but the weight of the samples used 50 mg and 150 ppb AFB₁ instead of 200 ppb.

3.3.5.2 Condition at pH 3

1. To determine the effect of acid on the transformation of aflatoxin B₁, the concentration of 60 ppb AFB₁ was used and mixed with different pH of HCl solution. The amount of AFB₁ and the other form was determined by HPLC.

2. To determine the amount of adsorbed AFB₁ at pH 3, bentonite 30 mg or organobentonite which was modified with 0.3, 0.6, 2.0 and 6.0 mM HDTMA by convention method were used. The samples were mixed with 25 mL of solution containing 200 ppb AFB₁ and HCl and the mixture was shaken for 48 h. Then some portion of the mixture was taken to measure the pH and the left portion was done as mentioned in 2.3.5.1.

3. To determine the amount of adsorbed AFB₁ at pH 3, 50 mg of

kaolin, halloysite, zeolite NaX, organokaolin, organohalloysite and organozeolite NaX were applied. The organosamples with 0.6, 2.0 and 6.0 mM HDTMA by convention method were mixed with 25 mL of solution containing 150 ppb AFB₁ and HCl. Then some portion of the mixture was taken to measure the pH and the left portion was done as mentioned in 2.3.5.1.

CHAPTER IV

RESULTS AND DISCUSSIONS

This chapter described and discussed the experimental results. The results are divided into five parts namely, halloysite, kaolin and bentonite composition analysis, characterization of synthesized zeolite NaX, cation exchange capacity (CEC), modification with HDTMA and adsorption of the aflatoxin B₁.

4.1 Chemical composition analysis of bentonite, kaolin and halloysite

The chemical compositions of bentonite, kaolin and halloysite samples were determined by XRF as given in the Table 4.1. The main compositions of clay minerals are oxides of Si and Al. The Si/Al ratio of all the samples were seemingly high compared to the theoretical composition. It might contain some silica in the samples. The value of Si/Al ratio for kaolin (1.43) and for halloysite (1.63) was nearly the same, that agreed with their formulas. A seemingly high Si/Al ratio of bentonite (6.32) caused by its layer structure and some content of silica. In halloysite sample it showed high content of ferric oxide (6.85%), which might affect the adsorption of AFB₁, while in kaolin sample it showed very low amount of Fe₂O₃ which indicates that kaolin is appropriate for preparation of zeolite NaX.

Table 4.1 The chemical compositions of halloysite, kaolin and bentonite samples determined by XRF

| Chemical content (% weight) | halloysite | kaolin | bentonite |
|--|-------------------|---------------|------------------|
| Al ₂ O ₃ | 29.58 | 29.33 | 10.59 |
| SiO ₂ | 47.84 | 53.98 | 75.79 |
| K ₂ O | - | 1.44 | 0.81 |
| TiO ₂ | 0.63 | 1.10 | 0.38 |
| Fe ₂ O ₃ | 6.85 | 0.94 | 2.15 |
| MgO | - | - | 0.45 |
| CaO | - | - | 1.35 |
| S (ppm) | 129 | 88 | - |
| Cr (ppm) | 355 | - | - |
| Mn (ppm) | 516 | - | 233 |
| Si/Al ratio | 1.43 | 1.63 | 6.32 |

4.2 Characterization of zeolite NaX

The X-ray diffraction pattern of synthesized zeolite NaX was shown in Figure 4.1. The diffractogram of synthesized zeolite NaX matched with the diffractogram from collection of simulated XRD powder patterns for zeolites in Figure 4.2 (Treacy, M. M. J., Higgins, J. B., and Ballmoos, R., 1996). The XRD pattern of synthesized solid showed only single phase of zeolite NaX. The major reflection peak at $2\theta = 6.15^\circ$ which corresponds to a basal spacing of $d_{111} = 14.36 \text{ \AA}$.

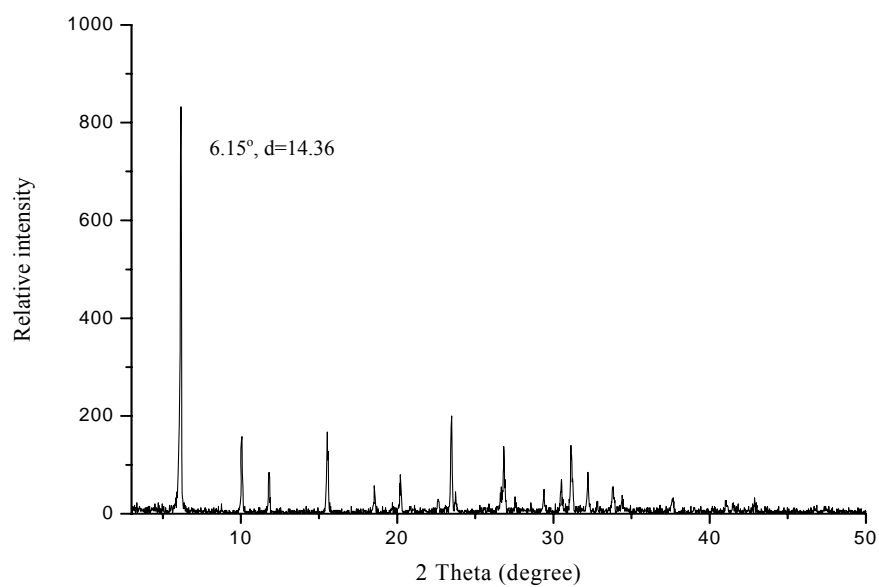


Figure 4.1 The XRD pattern of synthesized zeolite NaX from kaolin

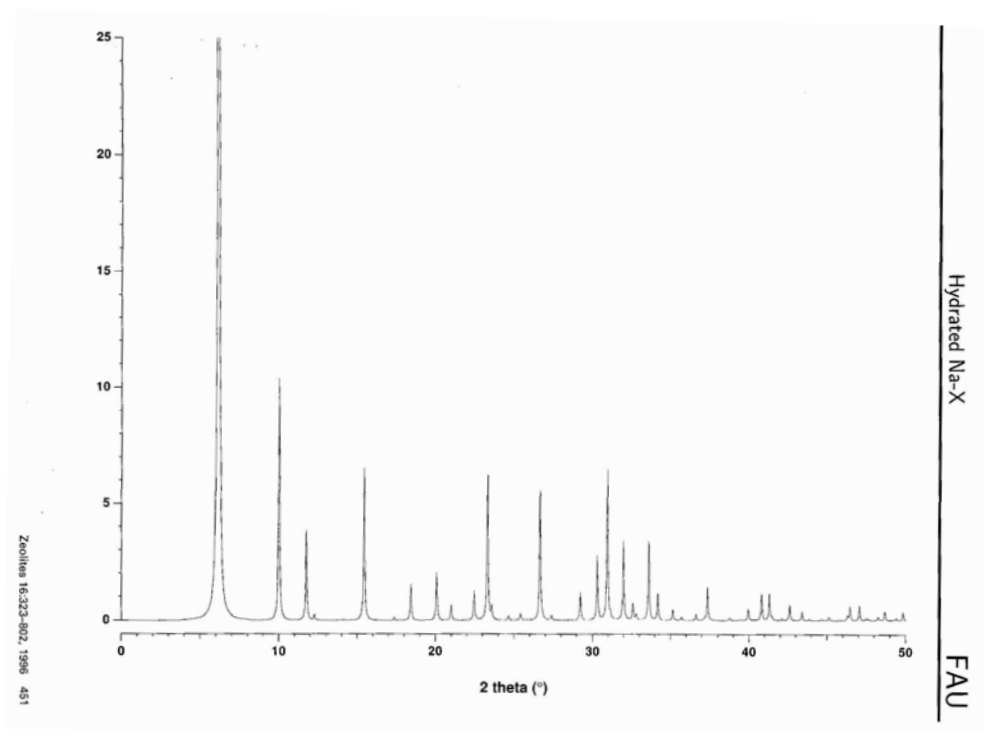


Figure 4.2 The simulated XRD powder pattern of zeolite NaX

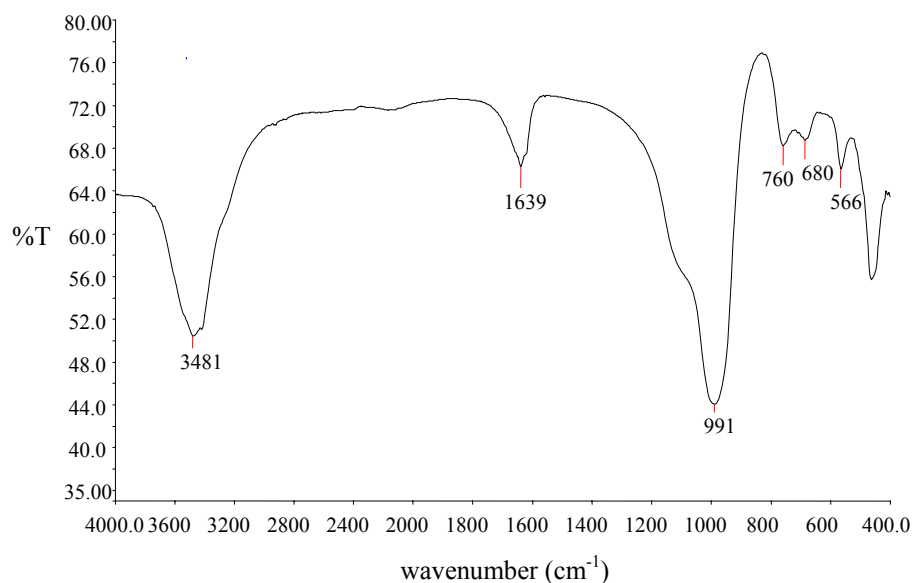


Figure 4.3 IR spectrum of zeolite NaX

IR spectrum of zeolite NaX was recorded in the MIR (4000-400 cm^{-1}) (Figure 4.3). The IR band at 566 cm^{-1} is attributed to double six rings (D6R) which is related to a Faujasite structure (Breck, 1974 and Barrer, 1982). The strongest vibration at 991 cm^{-1} is assigned to a T-O-T (T = Si or Al) stretch and the stretching modes involving mainly the tetrahedral atoms are assigned in the region of 760 cm^{-1} and 680 cm^{-1} .

The morphology of zeolite NaX was determined by SEM which shown in Figure 4.4. The SEM showed the octahedral shape of synthesized zeolite NaX.

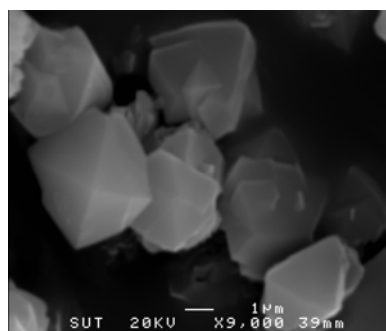


Figure 4.4 SEM micrograph of the zeolite NaX

4.3 Cation exchange capacity

The CEC values were determined using a modified ammonium acetate method. The results were shown in the Table 4.2. The value of cation exchange capacity of zeolite NaX is very high compared to that of clay minerals. Because its characteristic of silicon-aluminum-oxygen framework, forming a system of communicating cavities and channels in which cations balancing the negative charge associated with the framework are easily exchangeable with another cation (Grim, R. E., 1968). In the case of clay minerals, CEC value of bentonite is the highest, while CEC values of kaolin and halloysite are similar. In bentonite the ion exchange may occur mainly between the sheets of the layered minerals and less around their edges, whereas in kaolin and halloysite the exchangeable cations may occur only on particle surface.

Table 4.2 Cation exchange capacity of clay minerals and zeolite NaX

| Clay minerals and zeolite NaX | Cation exchange capacity (mmol/g) |
|-------------------------------|-----------------------------------|
| Halloysite | 0.130 |
| Kaolin | 0.138 |
| Bentonite | 0.650 |
| Zeolite NaX | 2.800 |

4.4 Modification of clay minerals and zeolite NaX

Cations in zeolite NaX and clays can be replaced by quaternary ammonium cations (hexadecyltrimethyl-ammonium chloride; HDTMA). The structure of zeolite and clays are possibly changed after modification. Therefore, the structure determinations by various techniques are quite important.

4.4.1 Characterization of clays by FT-IR

The FT-IR spectra of bentonite, kaolin and halloysite were recorded in the region of 4000-400 cm^{-1} (Figure 4.5).

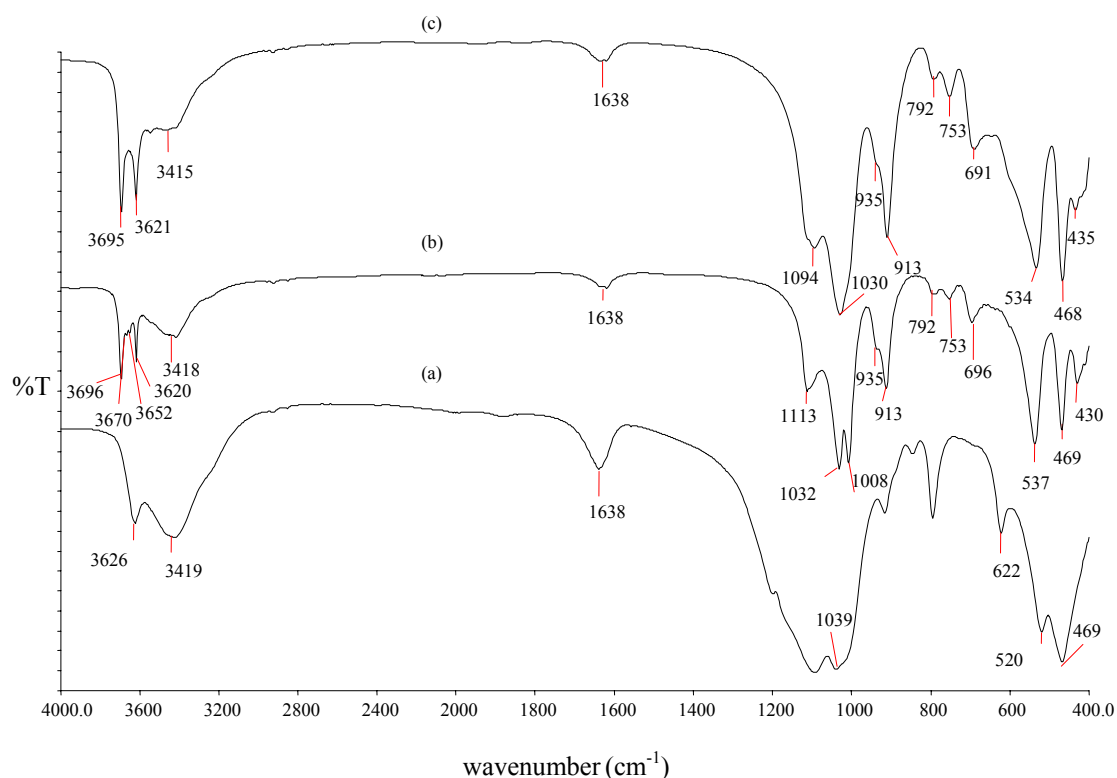


Figure 4.5 IR spectra of (a) bentonite, (b) kaolin and (c) halloysite

Bentonite showed its characteristic band at 3626 cm^{-1} which is attributed to the stretching vibrations of structure OH groups of dioctahedral smectite (Andrejikovičová, Janotka and Komadel, 2008). A band at 1039 cm^{-1} is assigned to the stretching vibration of Si-O groups and the bands at 520 and 469 cm^{-1} correspond to bending vibrations of Al-O-Si and Si-O-Si, respectively. The band at 622 cm^{-1} is assigned to coupled Al-O and Si-O out-of-plan vibration. O-H vibrations of water produce characteristic bands near 3419 and 1638 cm^{-1} (Eren and Afsin, 2008).

The vibrational spectra of kaolin are observed in the infrared spectrum at 3696, 3670, 3652 and 3620 cm^{-1} (Frost, Makó, Kristóf and Kloprogge, 2002; Breen, Illés, Yarwood and Skuse, 2007). The three higher frequency bands are assigned to OH stretching modes of the three inner surface hydroxyl groups. The band at 3620 cm^{-1} is strong and sharp with assigned to the stretching mode of an inner hydroxyl group. The 3670 and 3652 cm^{-1} bands are weak and are described as the out-of-phase vibrational modes (Makó, Senkár, Kristóf and Vágvölgyi, 2006; Farmer, 2000; Stuart and Thomas, 2008). The intensity of the OH stretching bands depends on the defect structure of the kaolinite. The band at 1032 cm^{-1} are attributed to the Si-O stretching vibrations of the siloxane layer of the kaolinite. Additional bands at around 792, 753 and 537 cm^{-1} should be associated to Al-O-Si vibrations of micas. Vibration of Al-OH appeared at around 913, 935 cm^{-1} and Si-O at around 430, 469, 696, 1008 and 1113 cm^{-1} (Makó *et al.*, 2006). Again the stretching vibration of adsorbed water forming H-bond in kaolin appeared at 3418 cm^{-1} and bending vibration at 1638 cm^{-1} .

The spectrum of raw halloysite displayed two intense characteristic bands at 3695 and 3621 cm^{-1} , which correspond to the O-H group vibration and to the surface hydroxyl group, respectively. The band at 1030 cm^{-1} is attributed to Si-O group and the band relative to the vibration of Al-OH group appeared at 911 cm^{-1} (Machado, Castro, Wypych and Nakagaki, 2008). The stretching and bending vibrations of water in halloysite were found at 3421 cm^{-1} and 1638 cm^{-1} , respectively. The assigned IR bands of the clay minerals were summarized in Table 4.3.

Table 4.3 Identification of IR bands of clay minerals

| IR absorption band (cm⁻¹) | | |
|---|--|--------------------------------|
| bentonite | kaolin | halloysite |
| 3626 O-H (dioctahedral smectite) | 3696, 3670, 3652, 3620 (O-H stretching) | 3695, 3621 (O-H stretching) |
| 1039 (Si-O stretching) | 1032 (Si-O stretching) | 1032 (Si-O stretching) |
| 622 (Al-O, Si-O out of plan) | 935, 913 (Al-O) | 935, 913 (Al-O) |
| 520 (Al-O-Si bending) | 792, 753, 537 (Al-O-Si) | 792, 753, 534 (Al-O-Si) |
| 469 (Si-O-Si bending) | 1113, 1008, 696, 469, 430 (Si-O) | 1094, 691, 468, 435 (Si-O) |

4.4.2 Characterization of organoclays and organozeolite NaX by FT-IR

The spectra of organoclays and organozeolite NaX prepared at different reaction time and different concentrations of HDTMA were recorded in the region of 4000-400 cm⁻¹. After modification with HDTMA, the obtained organoclays and organozeolite NaX showed the three new bands at 3000, 2800 and 1450 cm⁻¹ which resulting from HDTMA (see in Figure 4.6). The band at 3000 and 2800 cm⁻¹ are assigned to asymmetric and symmetric stretching vibration of C-CH₂ of alkyl chain, respectively, and the band at 1450 cm⁻¹ is assigned to vibration of trimethyl ammonium quaternary group C-N(CH₃)₃⁺. The intensity of these bands increased from reaction time of 12 to 24 hours and quite constant until 48 hour for bentonite but it was not different in the case of

halloysite, kaolin and zeolite NaX (see in Figure 4.7-4.9). In the case of bentonite it is clearly that the band at 3626 cm^{-1} was reduced after modification. It might result from that the O-H groups of dioctahedral smectite were decreased due to more dissociation when HDTMA existed.

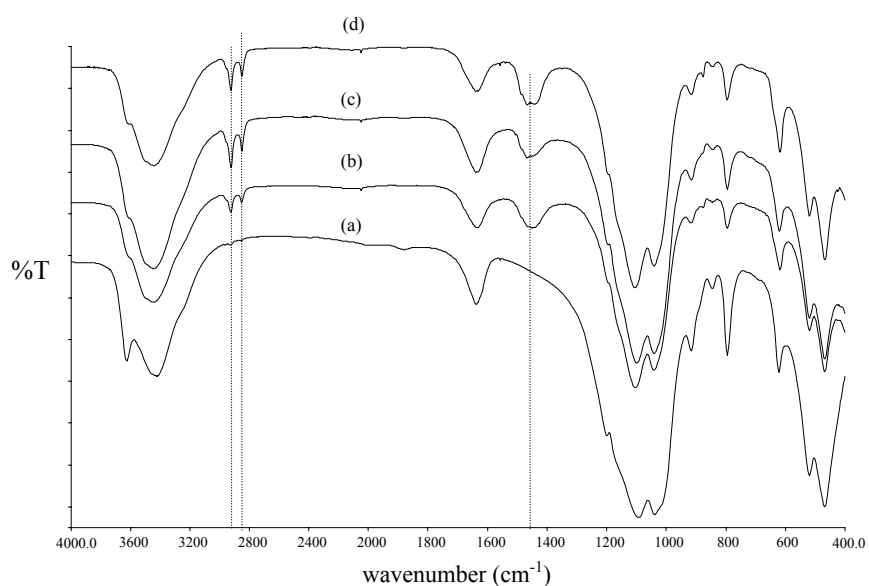


Figure 4.6 IR spectra of bentonite (a) before and (b-d) after modification with 2.0 mM HDTMA by convention method at 12, 24 and 48 h, respectively

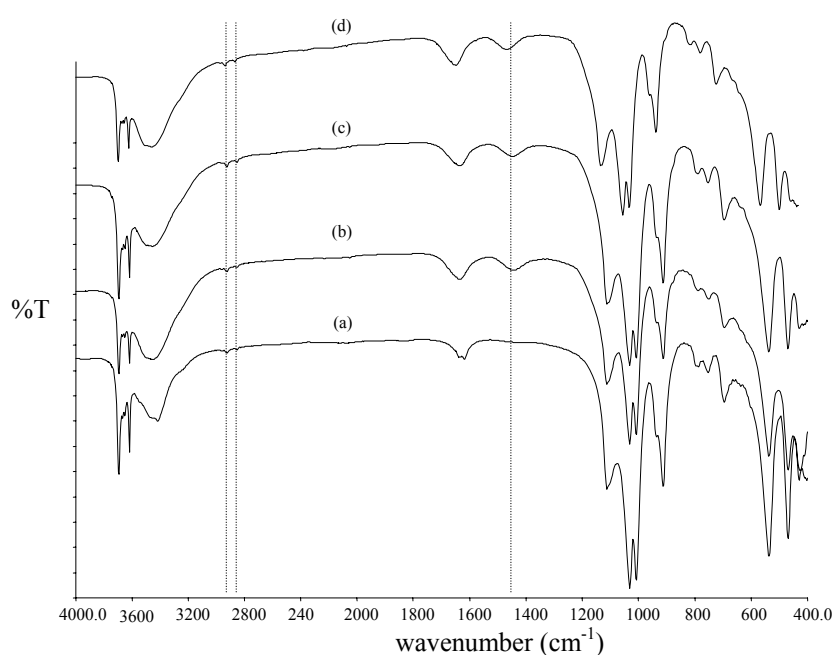


Figure 4.7 IR spectra of kaolin (a) before and (b-d) after modification with 2.0 mM HDTMA by convention method at 12, 24 and 48 h, respectively

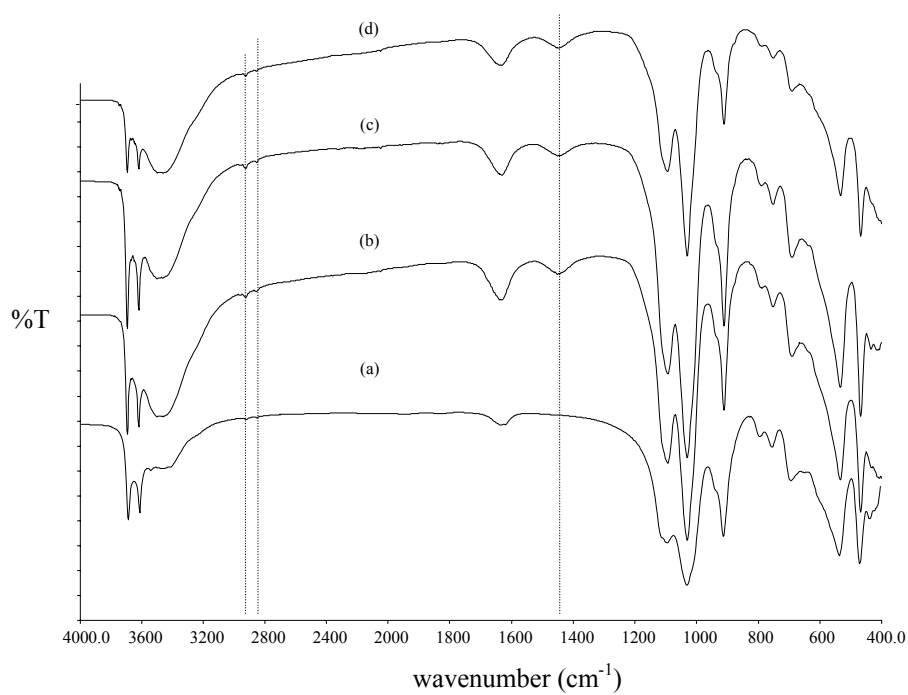


Figure 4.8 IR spectra of halloysite (a) before and (b-d) after modification with 2.0 mM HDTMA by convention method at 12, 24 and 48 h, respectively

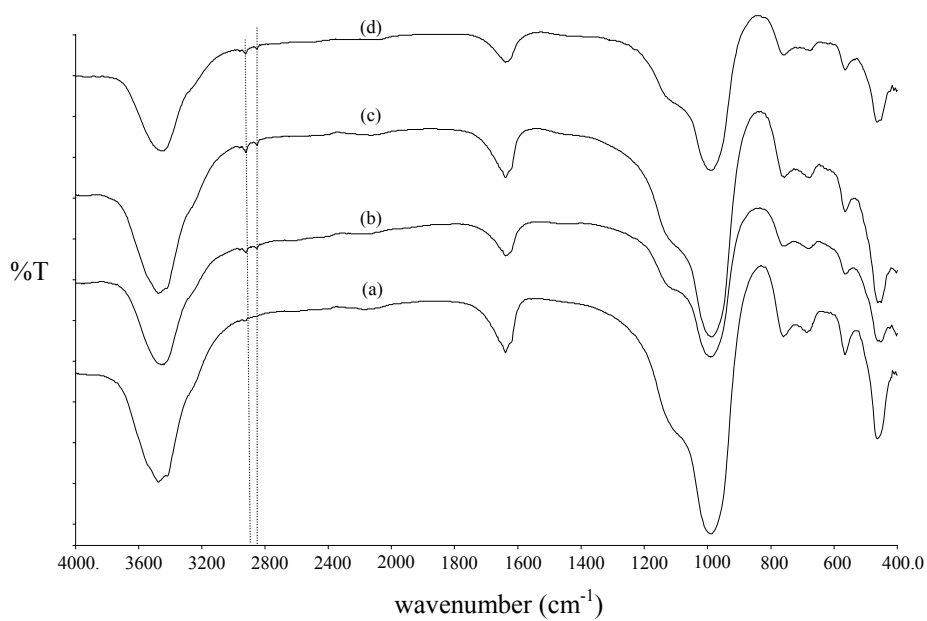


Figure 4.9 IR spectra of zeolite NaX (a) before and (b-d) after modification with 2.0 mM HDTMA by convention method at 12, 24 and 48 h, respectively

In the case modification by microwave method it found that the intensity of the band at 3000 and 2800 and 1450 cm^{-1} of organoclays and organozeolite NaX for reaction time 10 and 15 min was constant (see in appendices, Figure 1-4). It indicated that the reaction time for preparing organosamples by microwave method at least was 10 min, while that by convention method at least 24 hours. This is an advantage of microwave method.

In Figure 4.10 organobentonites obtained by convention (COB) and microwave (MOB) method at different concentrations of HDTMA were shown. In the vibration range of 3000-2800 cm^{-1} , their intensities increased with increasing HDTMA concentration. It indicated that its packing form is more dense in the solid phase. These bands shifted to lower wave number probably the consequence of the change in the arrangement of surfactant in the clay interlayer from disorder to ordered form (Majdan *et al.*, 2005). It causes the increased Van der Waals interchain interaction and consequently in the increased number of ordered conformers.

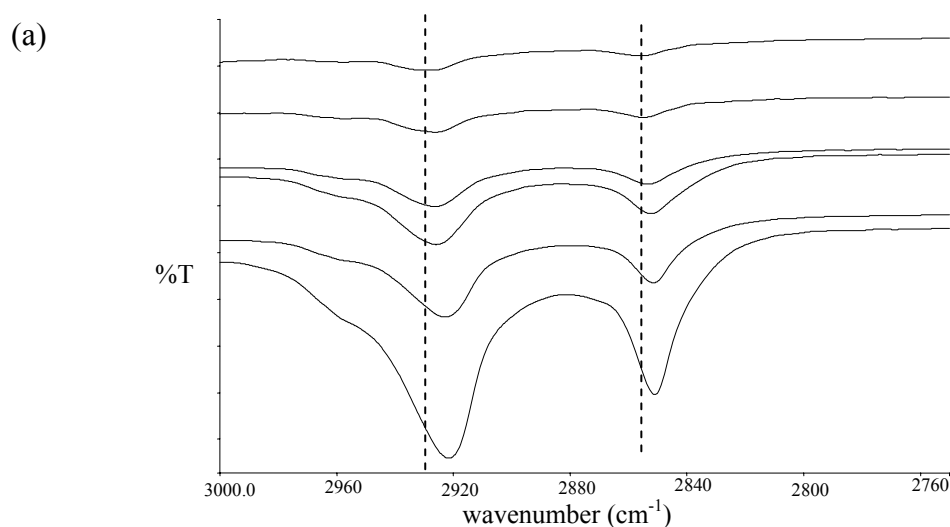


Figure 4.10 FTIR spectra of (a) COB and (b) MOB at concentration 0.3 (topmost), 0.6, 1.3, 2.0, 4.0 and 6.0 mM HDTMA, respectively

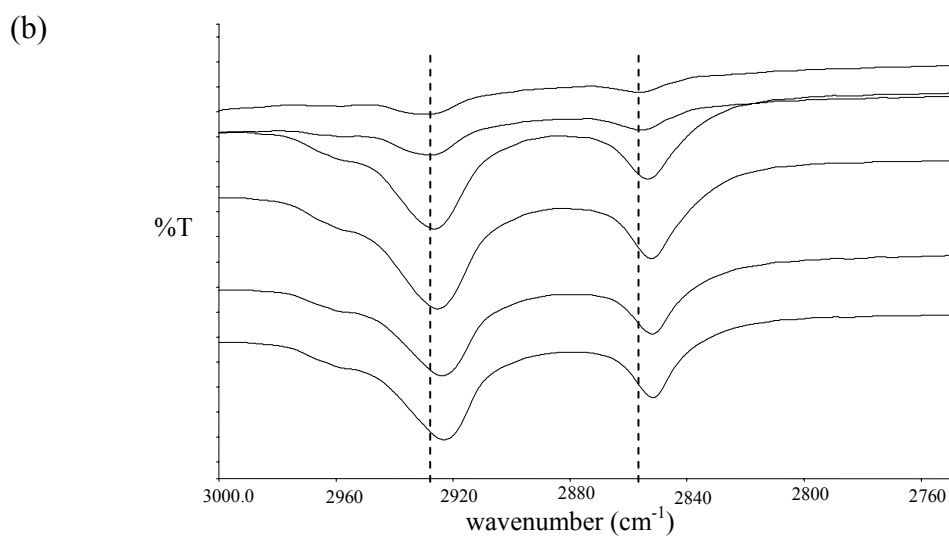


Figure 4.10 FTIR spectra of (a) COB and (b) MOB at concentration 0.3 (topmost), 0.6, 1.3, 2.0, 4.0 and 6.0 mM HDTMA, respectively (continued)

However, for organokaolin, organohalloysite and organozeolite NaX even in increase of concentration of HDTMA, the vibrational intensity of alkyl chain are not significantly different (see in Figure 4.11-4.13). It was found that the results from preparation with both convention and microwave were similar.

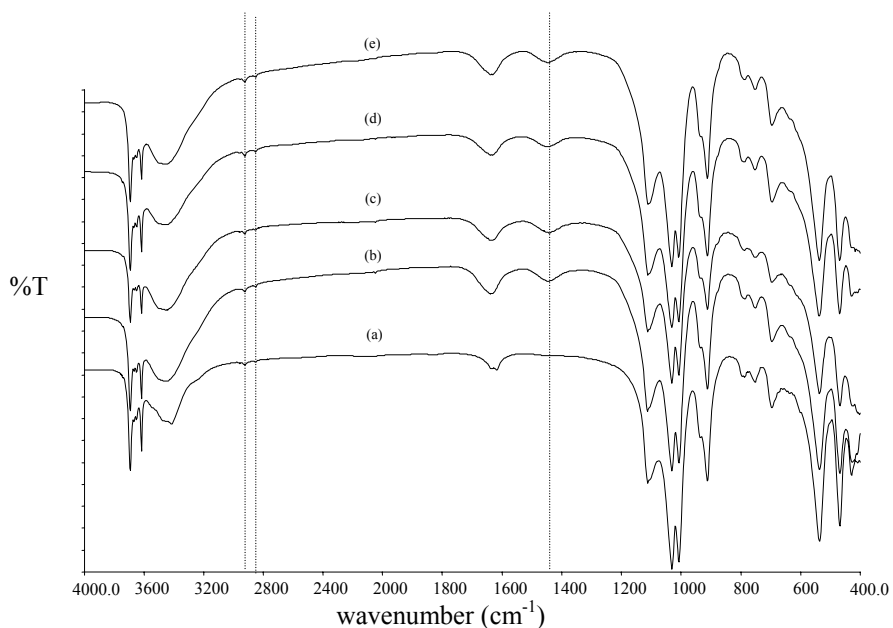


Figure 4.11 IR spectra of kaolin (a) before and (b-e) after modification with 0.6, 2.0, 4.0 and 6.0 mM HDTMA by convention method

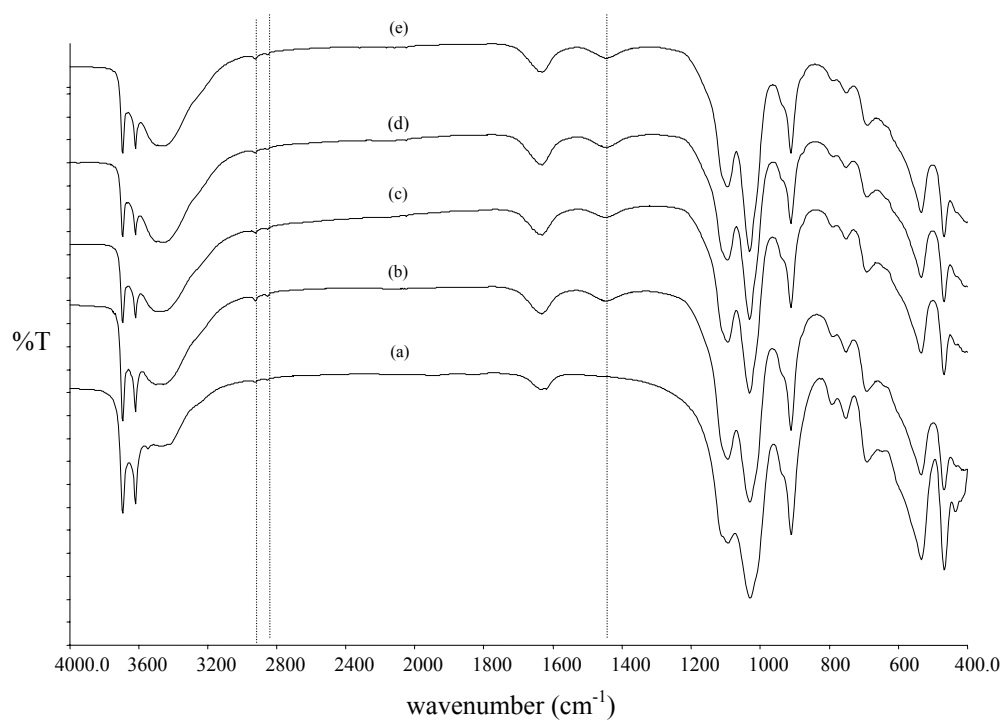


Figure 4.12 IR spectra of halloysite (a) before and (b-e) after modification with 0.6, 2.0, 4.0 and 6.0 mM HDTMA by convention method

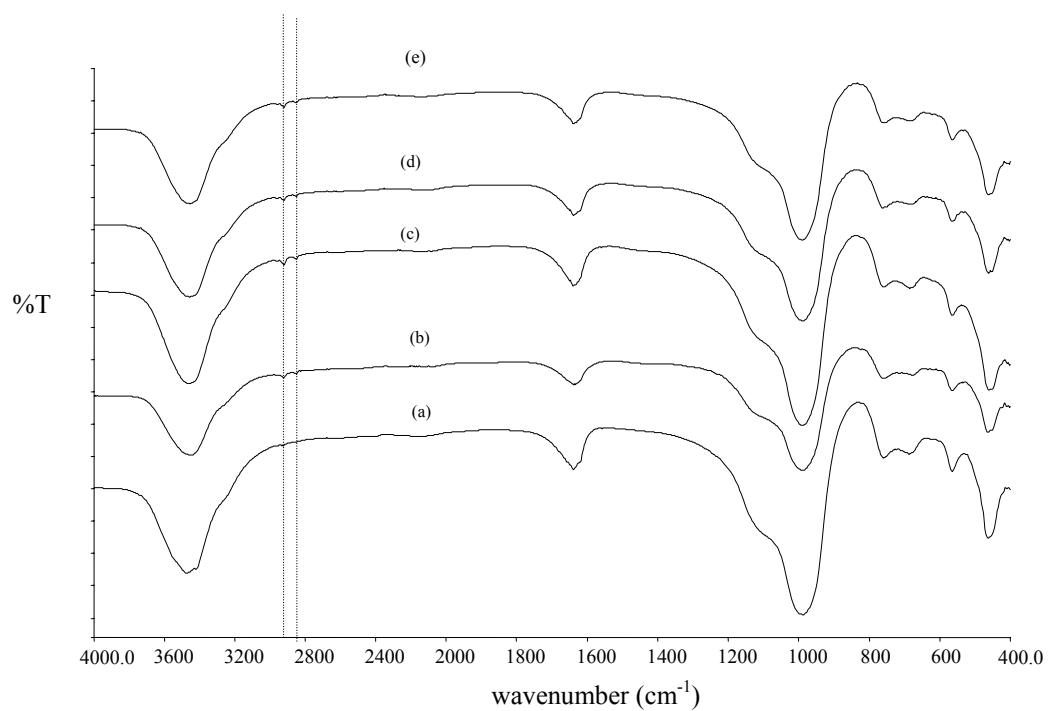


Figure 4.13 IR spectra of zeolite NaX (a) before and (b-e) after modification with 0.6, 2.0, 4.0 and 6.0 mM HDTMA by convention method

4.4.3 Characterization of organoclays and organozeolite NaX by XRD

Diffraction characteristics of the natural bentonite showed a reflection peak at about $2\theta = 6.02^\circ$ which corresponds to a basal spacing of d_{001} 14.68 Å. After modification the reflection peaks shifted to lower than that of $2\theta = 6.02^\circ$. In the case of organobentonites prepared by convention method (COB) the 2θ slightly shifted to lower angle at about 5.97° and 5.87° with concentration of 0.3 and 0.6 mM HDTMA, respectively, whereas it dramatically shifted with concentration of 1.3 mM (4.17°) and again slightly shifted with higher concentration at 2.0, 4.0 and 6.0 mM HDTMA at about $2\theta = 3.94^\circ$, 3.89° and 3.85° , respectively. For organobentonites prepared by microwave method (MOB) the great shift of 2θ started with 2.0 mM HDTMA at about $2\theta = 4.20^\circ$. The XRD patterns of the organobentonite prepared by both method were shown in Figure 4.14-4.15.

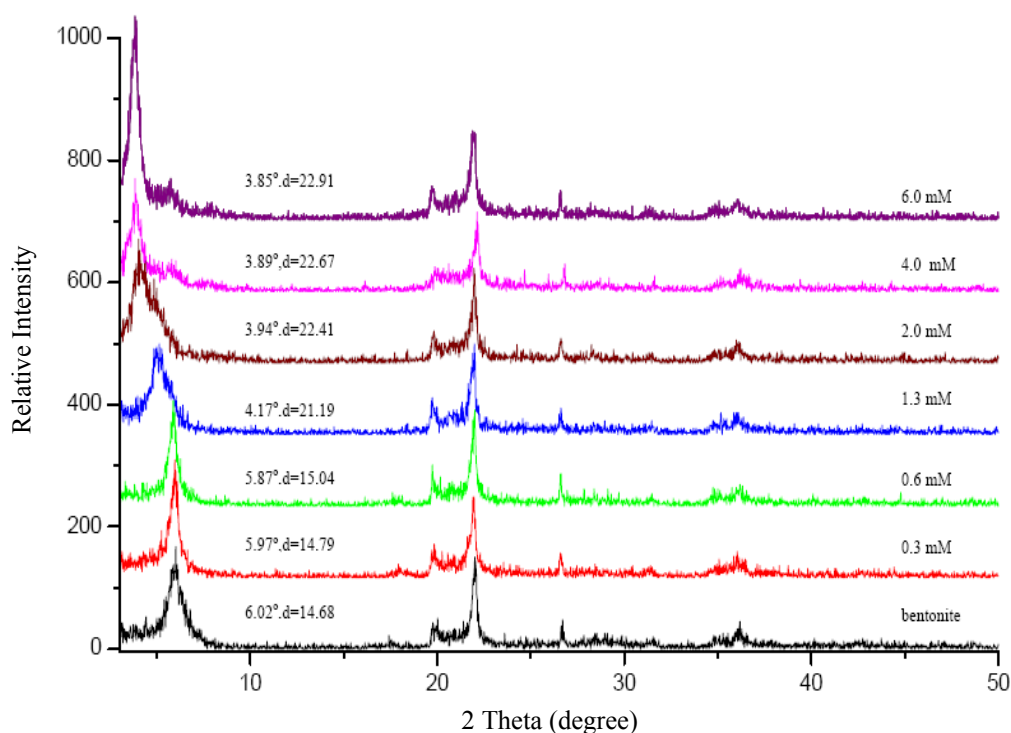


Figure 4.14 The XRD patterns of the organobentonite with various concentrations of HDTMA prepared by convention method

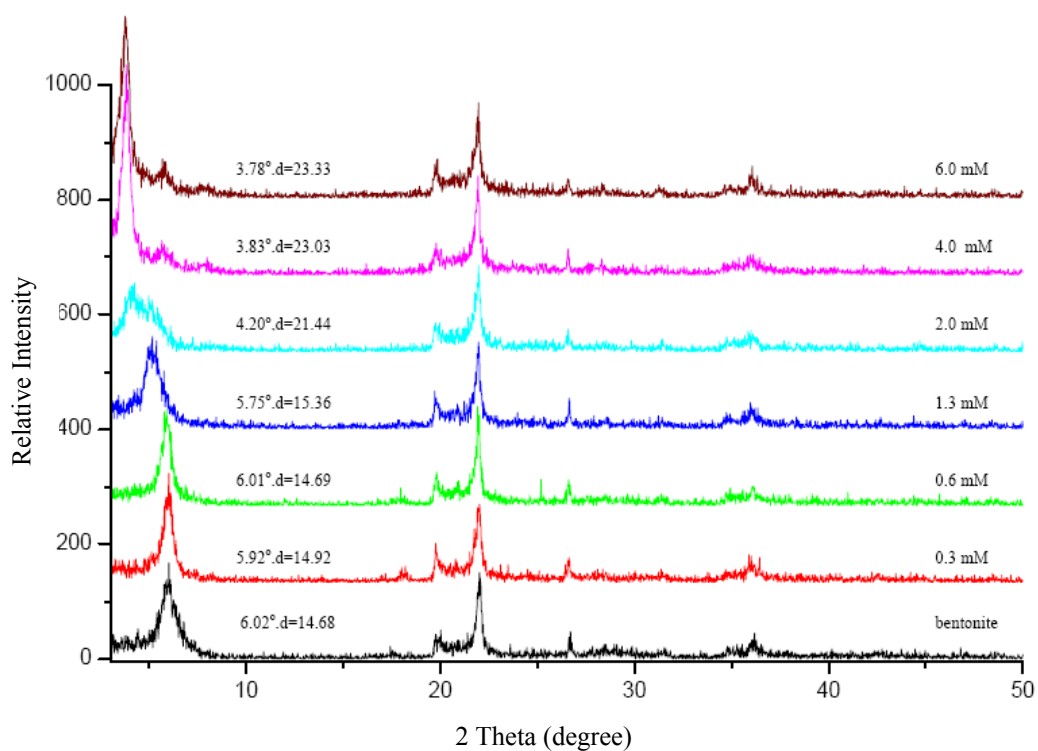
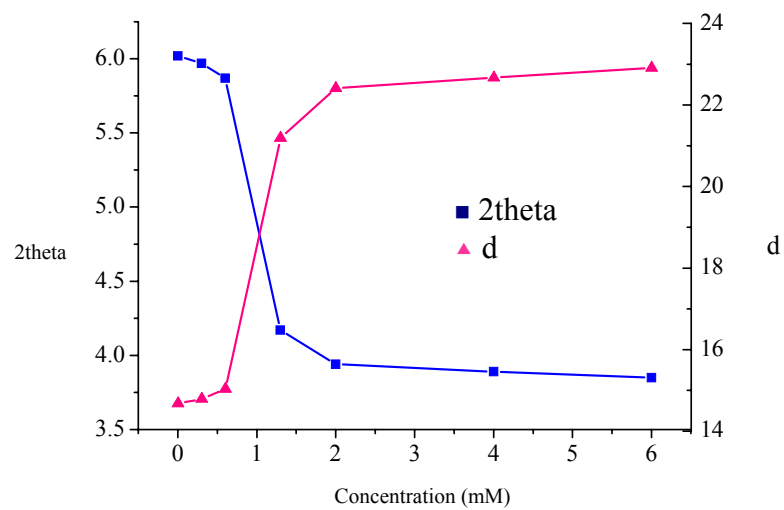


Figure 4.15 The XRD patterns of the organobentonite with various concentrations of HDTMA prepared by microwave method

The correlation between 2θ and d-spacing value depending on concentration of HDTMA of both preparation methods for organobentonite was shown in Figure 4.16. It indicated that the expansion of interlayer spacing with both methods trended to be similar. However, at low concentration (0.3 - 1.3 mM HDTMA) d_{001} of COB is slightly larger than that of MOB, but at concentration of 4.0 mM and 6.0 mM HDTMA, the interlayer spacing of MOB was larger than that of COB. It showed that preparation of organobentonite with microwave was able to increase interlayer spacing slightly more than that with convention at high concentration of HDTMA.

(a)



(b)

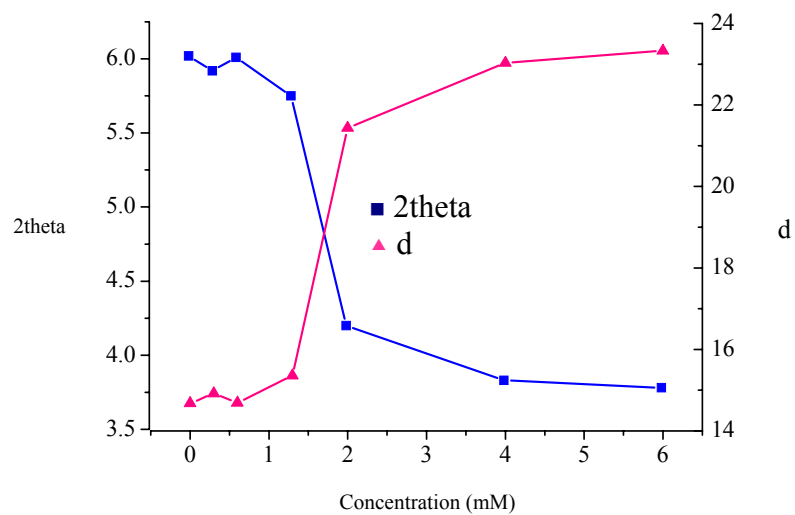


Figure 4.16 2 theta plotted against d spacing of the organobentonite with various concentrations of HDTMA (a) prepared by convention method (b) prepared by microwave method

The XRD (see Figure 4.17-4.18) of natural kaolin and halloysite showed the reflection peaks at about $2\theta = 12.33$ and 12.06° which correspond to a basal spacing 7.17 and 7.33 Å, respectively. After modification of kaolin its interlayer spacing was changed very slightly from 7.17 to 7.29 Å with 6.0 mM HDTMA, while in the case of halloysite it seemed to be constant.

The results from XRD indicated that HDTMA was mostly adsorbed on the interlayer spacing in bentonite whereas in kaolin and halloysite it was mostly adsorbed on external surface which corresponded to their swelling properties of clay minerals.

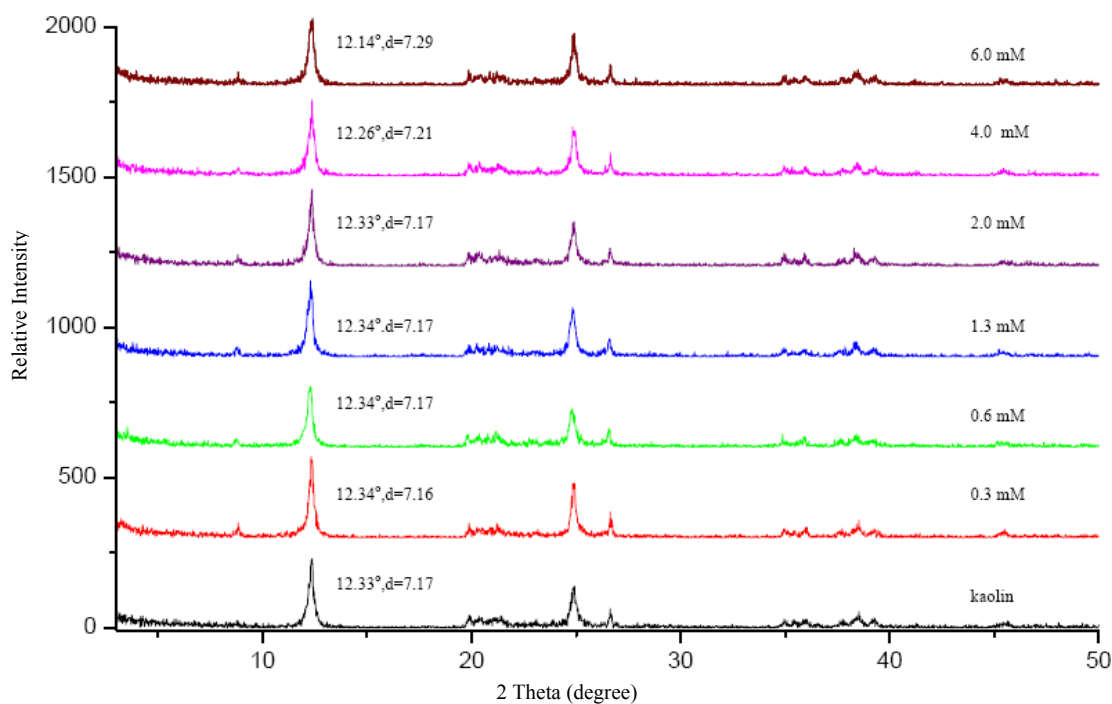


Figure 4.17 The XRD patterns of the organokaolin with various concentrations of HDTMA prepared by convention method

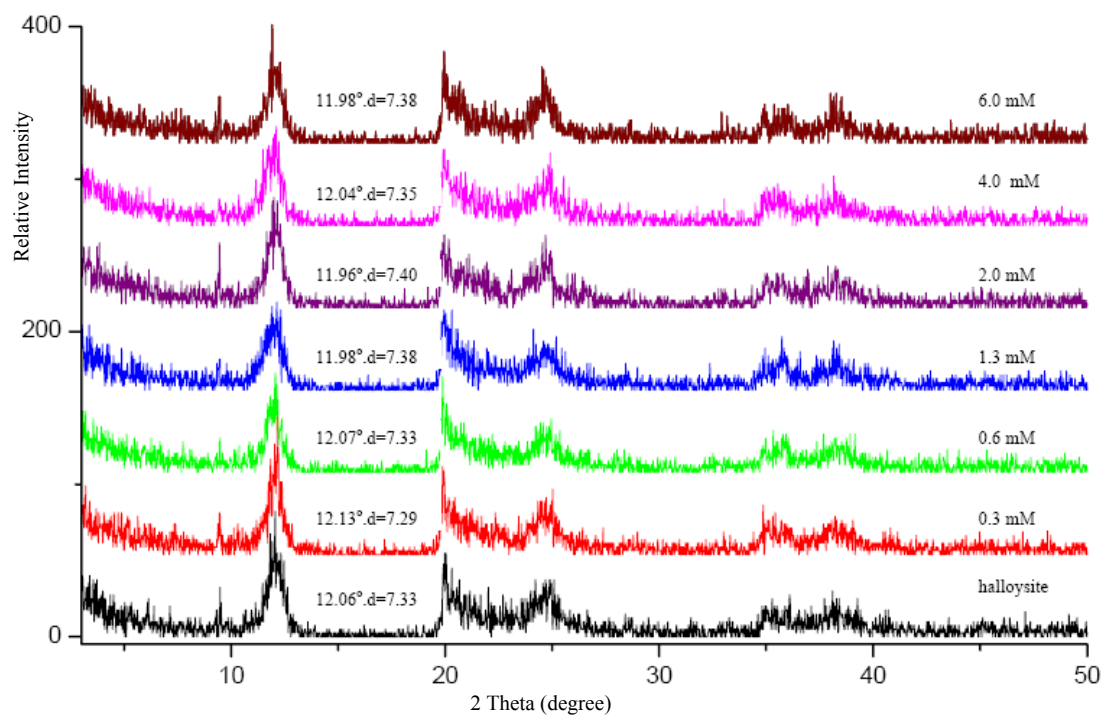


Figure 4.18 The XRD patterns of the organohalloysite with various concentrations of HDTMA prepared by convention method

The XRD of zeolite NaX and organozeolite NaX were shown in Figure 4.19. The interlayer spacing of zeolite NaX and organozeolite NaX were very slightly change from 14.36 Å to 14.48 Å even with concentration of 6.0 mM HDTMA. It indicated that HDTMA was only adsorbed on external surface of zeolite NaX. It could not insert into the cavities of zeolite due to the size of cavity and the head group of HDTMA.

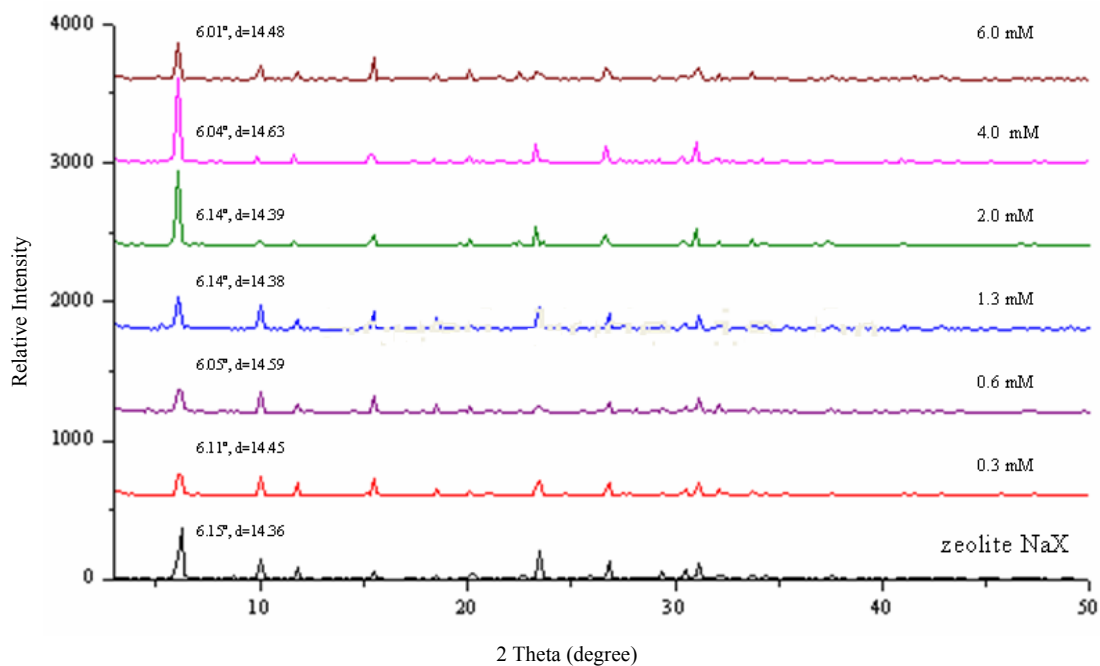


Figure 4.19 The XRD patterns of the organozeolite NaX with various concentrations of HDTMA prepared by convention method

4.4.4 Thermal analysis of organoclays and organozeolite NaX

DTA curves of organobentonite, organokaolin, organohalloysite and organozeolite NaX were shown in Figure 4.20-4.23. DTA curve of organobentonite with 0.6 mM HDTMA showed the broad band with maximum peak at about 361°C when concentration increased to 2.0 mM it appeared the endothermic band consisting of three overlapping peaks at 290, 320 and 360°C (confirmed with derivative of DTA, DDTA, in Figure 4.24). With 6.0 mM HDTMA it showed the additional band at 235°C. It implied that with concentration of 2.0 mM HDTMA there are three different arrangements of HDTMA adsorbed on bentonite when with the concentration of 6.0 mM HDTMA the new band occurred at 235°C maybe due to the arrangement of HDTMA which was mainly adsorbed on external surface of bentonite. The results of DTA agreed with that of XRD. In XRD results the interlayer spacing of bentonite was

increased from 14.68 Å to 22.41 Å with 2.0 mM HDTMA. When the concentration was increased to 6.0 mM HDTMA, the interlayer spacing changed slightly and increased to 22.91 Å. It indicated that in the concentration range of 0.3-2.0 mM HDTMA most of HDTMA was adsorbed between the layer. Therefore, the interlayer spacing was significantly expanded. With the concentration more than 2.0 mM most of HDTMA adsorbed on external surface of bentonite because of d-spacing somewhat constant.

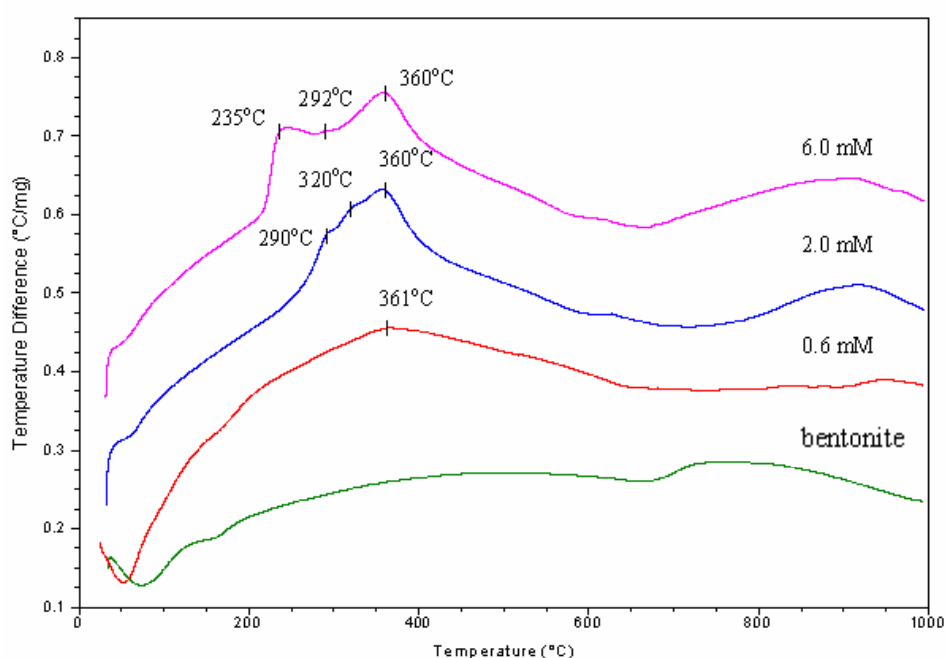
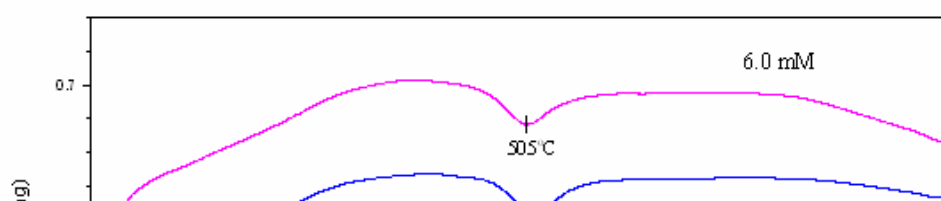


Figure 4.20 DTA profile of the organobentonite with various concentrations of HDTMA prepared by convention method



2.0 mM
0.6 mM
kaolin

Figure 4.21 DTA profile of the organokaolin with various concentrations of HDTMA prepared by convention method

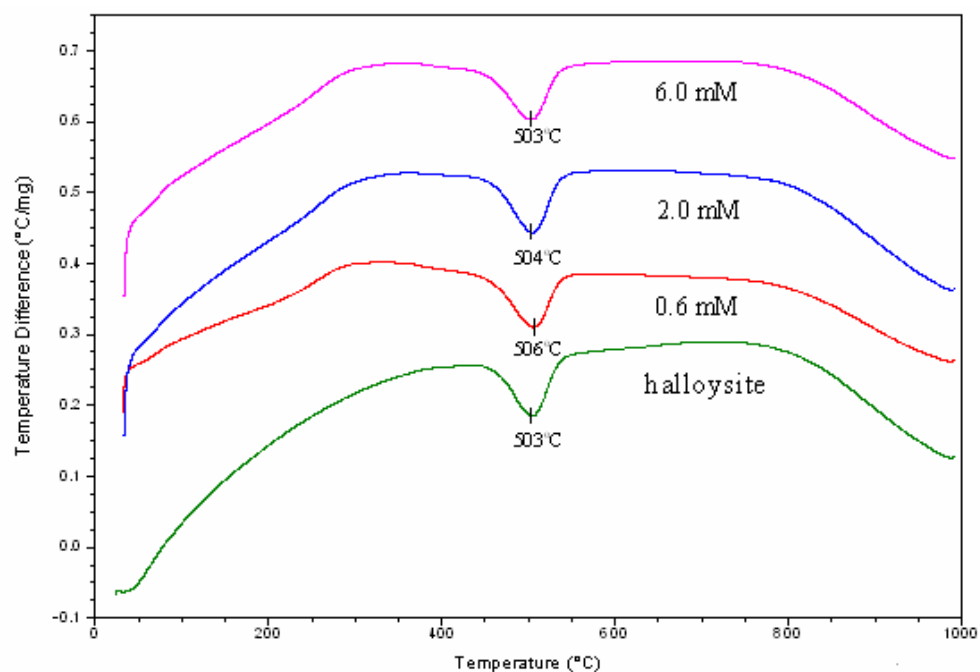
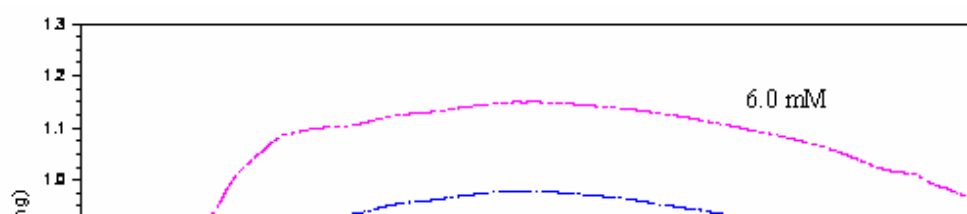


Figure 4.22 DTA profile of the organohalloysite with various concentrations of HDTMA prepared by convention method



2.0 mM

0.6 mM

Figure 4.23 DTA profile of the organozeolite NaX with various concentrations of HDTMA prepared by convention method

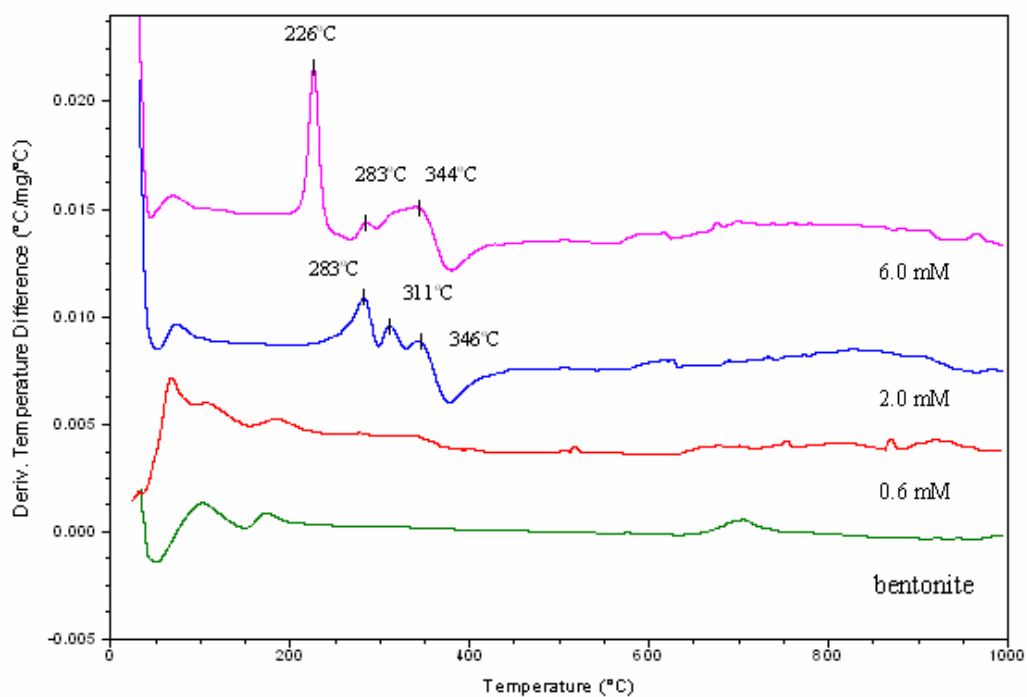


Figure 4.24 DDTA profile of the organobentonite with various concentrations of HDTMA prepared by convention method

In Figure 4.23 DTA of kaolin showed an exothermic peak at 504°C which related to the transformation of kaolin into metakaolin. In the case of organokaolins

with various concentration of HDTMA it appeared an exothermic peak transformation of kaolin into metakaolin at 512°C (with 0.6 mM), 515°C (with 2.0 mM) and 505°C (with 6.0 mM). For DTA of halloysite it appeared as the same profile of kaolin (see Figure 4.22).

The derivative of DTA (DDTA) for kaolin and halloysite were shown in Figure 4.25-4.26. It found that in the rang of 200-400°C DDTA curves of organokaolin and organohalloysite at all the of concentration of HDTMA were similar and they were very broad with the maximum around 246°C for organokaolin and 262°C for organohalloysite. It indicated the loss of HDTMA, while it was very difficult to indicate the loss of HDTMA with DTA profile.

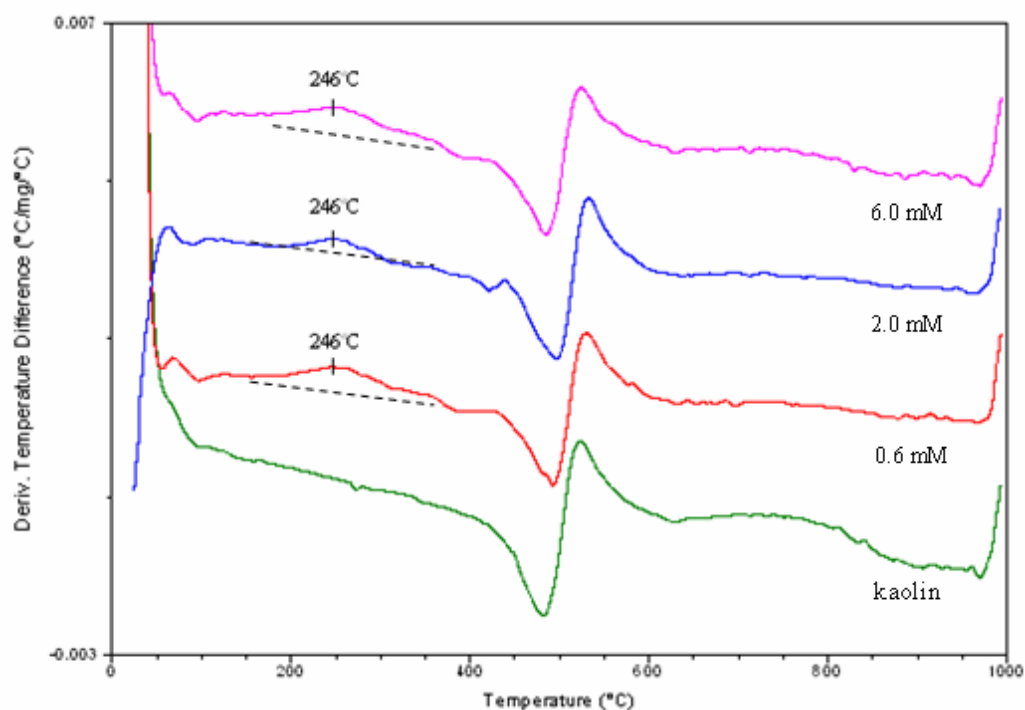
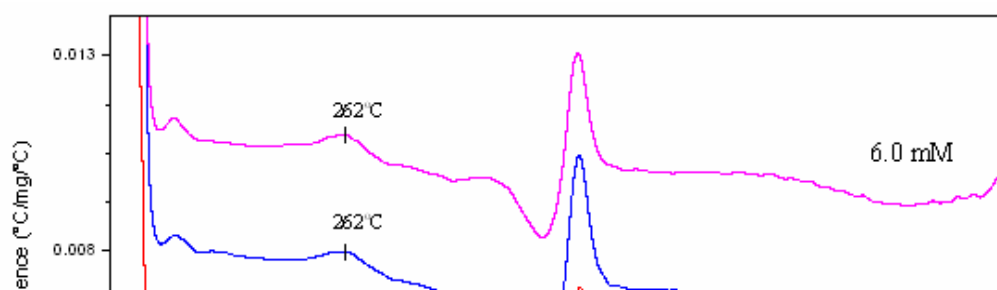


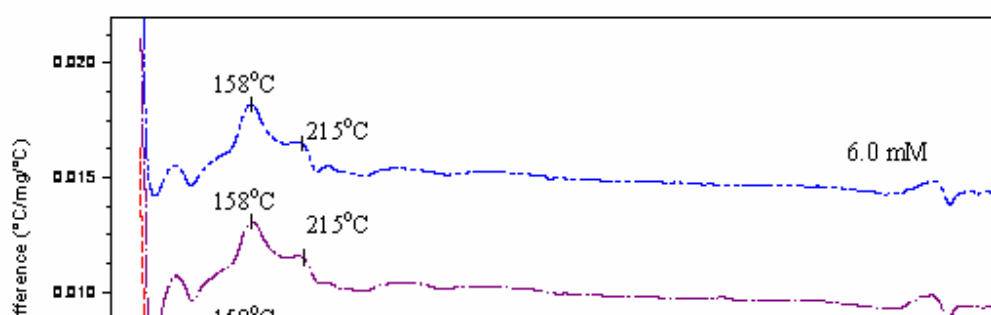
Figure 4.25 DDTA profile of the organokaolin with various concentrations of HDTMA prepared by convention method



2.0 mM
0.6 mM
halloysite

Figure 4.26 DDTA profile of the organohalloysite with various concentrations of HDTMA prepared by convention method

Figure 4.23 showed the DTA curve of organozeolite NaX with different concentrations of HDTMA. The DTA profile were similar at all the concentrations and very broad. However, from DDTA curve of zeolite NaX in Figure 4.27 it showed another peak at 215°C when compared to unmodified zeolite NaX and the peak at 167 °C for zeolite NaX shifted to 158°C for organozeolite NaX. It implied that at all the concentrations of HDTMA there was quite similar arrangements of HDTMA which corresponded to the result of XRD which showed the basal spacing of unmodified and modified zeolite NaX quite constant (14.36 Å for zeolite NaX and 14.48 Å for organozeolite NaX).



2.0 mM
0.6 mM
zeolite NaX

Figure 4.27 DDTA profile of the organozeolite NaX with various concentrations of HDTMA prepared by convention method

From thermogravimetric analysis the results of percent mass loss of HDTMA were shown in Table 4.4. The determination of percent mass loss was done in the different ranges of temperature. In the range of 0-200°C which related to the mass loss of water it showed that the mass loss of water in zeolite NaX was very high compared to all clay minerals and mass loss of water in bentonite was higher than that in kaolin and halloysite. In the range of 200-400°C it found that the change of the mass loss of HDTMA in organobentonite was significant with increasing HDTMA concentration. It indicated that in this temperature range most of adsorbed HDTMA was eliminated which is consistent with the result of DTA. For organokaolin, organohalloysite and organozeolite NaX the mass loss was rather constant with increasing HDTMA concentration. In the temperature range of 400-550°C the percent mass loss of natural

kaolin and halloysite was very high compared to bentonite and zeolite NaX. This implied that the mass loss was the result of dehydroxylation in the process of transformation of kaolin into metakaolin and halloysite to metahalloysite.

Table 4.4 Summary of the percent mass loss of the clay minerals, zeolite NaX, organoclays and organozeolite NaX with various concentrations of HDTMA determined in different ranges of temperature

| | Range of temperature (°C) | | | | Range of temperature (°C) | | |
|-----------|---------------------------|---------|---------|--------|---------------------------|---------|---------|
| | 0-200 | 200-400 | 400-550 | | 0-200 | 200-400 | 400-550 |
| Bentonite | 4.97 | 0.88 | 0.69 | Kaolin | 1.15 | 1.04 | 10.97 |
| 0.6 mM | 9.04 | 2.13 | 1.09 | 0.6 mM | 0.88 | 1.87 | 9.53 |
| 2.0 mM | 3.47 | 8.15 | 2.54 | 2.0 mM | 0.78 | 2.12 | 9.90 |
| 6.0 mM | 4.23 | 11.78 | 2.81 | 6.0 mM | 0.97 | 2.45 | 10.09 |

| | Range of temperature (°C) | | | | Range of temperature (°C) | | |
|------------|---------------------------|---------|---------|-------------|---------------------------|---------|---------|
| | 0-200 | 200-400 | 400-550 | | 0-200 | 200-400 | 400-550 |
| Halloysite | 1.86 | 1.33 | 11.40 | Zeolite NaX | 20.20 | 3.60 | 0.50 |
| 0.6 mM | 1.26 | 2.45 | 11.61 | 0.6 mM | 20.26 | 4.74 | 0.88 |
| 2.0 mM | 1.19 | 2.61 | 11.89 | 2.0 mM | 20.74 | 4.91 | 0.83 |
| 6.0 mM | 1.55 | 2.59 | 11.96 | 6.0 mM | 20.53 | 4.68 | 0.78 |

4.5 Study of adsorption of AFB₁

The adsorption of AFB₁ was carried out under various effects, such as effect of adsorption time, amount of adsorbate as well as amount of adsorbents and pH of solution. The amount of AFB₁ was determined by HPLC. The chromatogram of pure AFB₁ solution at different concentrations (see Figure 4.28) showed only one peak of AFB₁ with retention time at 7 min.

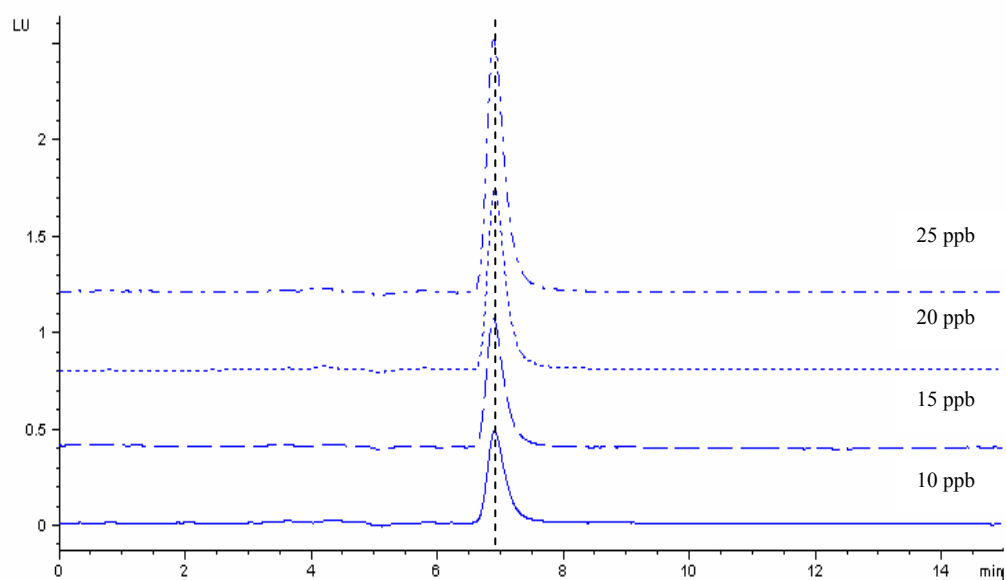


Figure 4.28 The chromatogram of pure AFB₁ solution at different Concentrations

For adsorption of AFB₁ with all the adsorbents in this study, it was found that the chromatograms showed not only the peak at 7 min but also the other peak at about 4 min which supposed to be complex of AFB₁ which produced by adsorbents (see Figure 4.29). Therefore, it is very difficult to examine AFB₁ concentration remaining in the solution by standard curve. However, in the adsorption study the amounts of AFB₁ remaining in solution were related to the peak area at 7 min and at about 4 min.

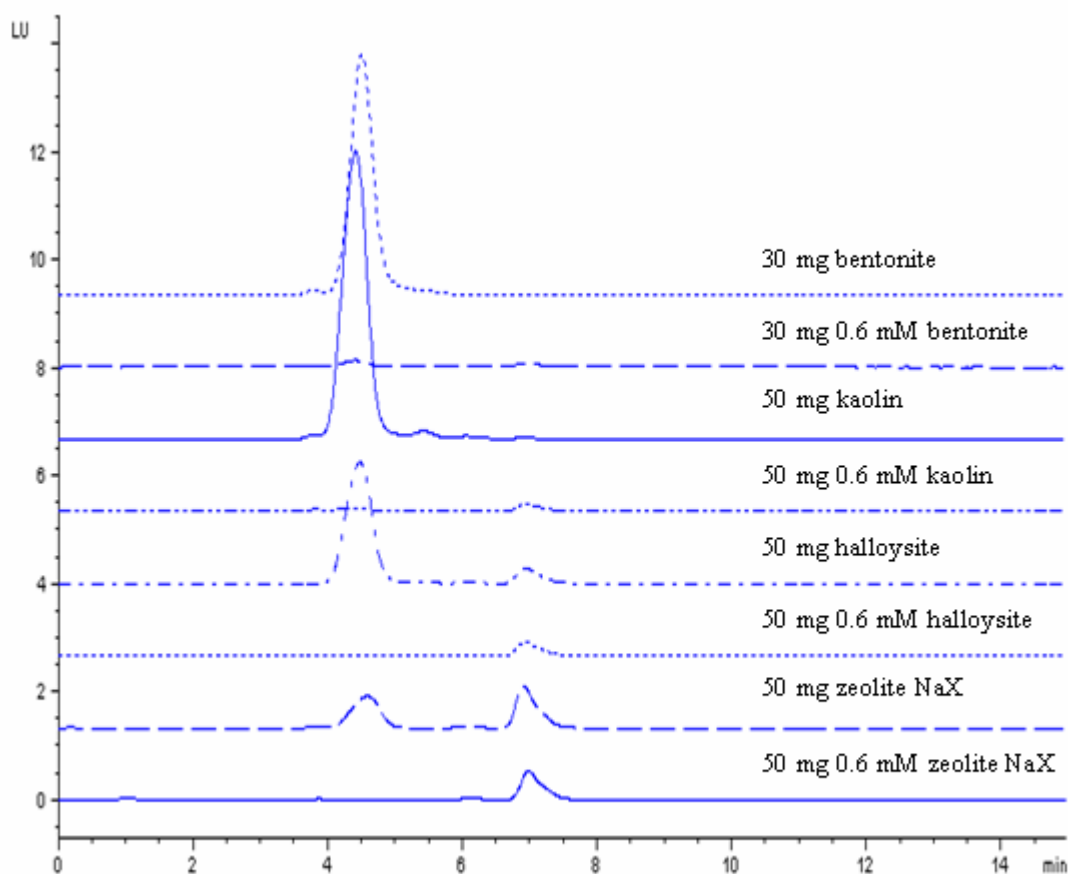


Figure 4.29 The chromatogram of adsorption AFB₁ solution at 100 ppb with adsorbent

The peak area at 7 min and at about 4 min in the study of AFB₁ adsorption time with bentonite was shown in Figure 4.30. Before mixing AFB₁ solution at 60 ppb with bentonite it gave one peak area at 7 min without that at about 4 min, after mixing with 10 mg of bentonite for 12 h the peak area at about 4 min was increased but the peak area at 7 min was decreased. For 24 and 48 h the peak at 7 min disappeared, while the peak area at about 4 min reached maximum and constancy. Therefore, the adsorption time at 24 h were chosen for further study.

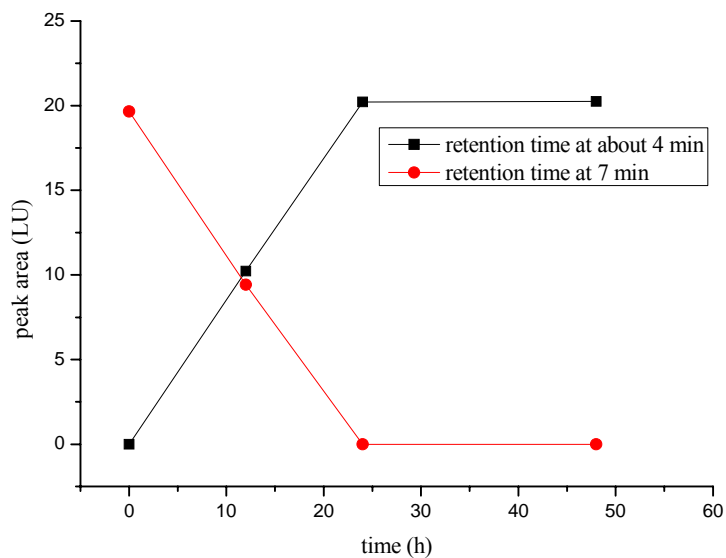


Figure 4.30 Adsorption of AFB₁ with different time

In the AFB₁ adsorption depending on the amount of bentonite, the solution of AFB₁ at 100 ppb was mixed with 5, 10, 15, 20, 30, 50 and 80 mg of bentonite. The results are shown in Figure 4.31. The peak at 7 min disappeared when the use of only 10 mg, while the peak at about 4 min had a maximum area. It indicated that the complex of AFB₁ occurred considerably. With increasing amount of bentonite the peak area at about 4 min decreased continuously. It implied that bentonite could adsorb both AFB₁ and AFB₁ complex.

The study of AFB₁ adsorption with organobentonite was performed with the AFB₁ concentration of 100 ppb and 30 mg of organobentonites which were modified with 0.3, 0.6, 1.3, 2.0, 4.0 and 6.0 mM HDTMA. The result are shown in Figure 4.32. It was found that 30 mg of the organobentonite with 0.3, 0.6 and 1.3 mM could not absolutely eliminate the both forms of AFB₁, whereas organobentonite with 2.0, 4.0 and 6.0 mM could completely eliminate them. Again, the AFB₁ adsorption was done with the AFB₁ concentration of 200 ppb. The result showed that the both forms of

AFB₁ were still minute by organobentonite with 2.0 and disappeared by organobentonite with 6.0 mM (see Figure 4.33).

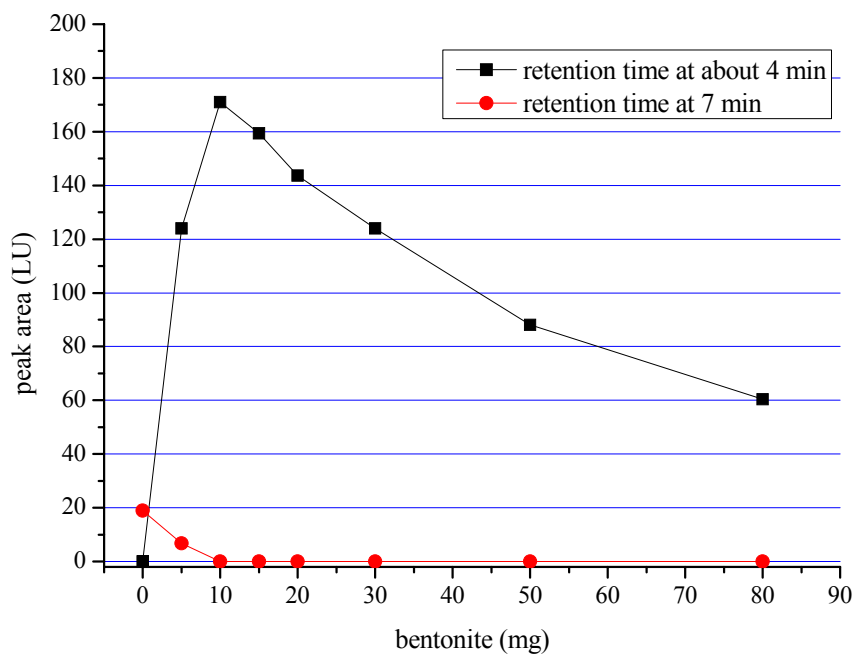


Figure 4.31 Adsorption of 100 ppb AFB₁ with 5, 10, 15, 20, 30, 50 and 80 mg of bentonite

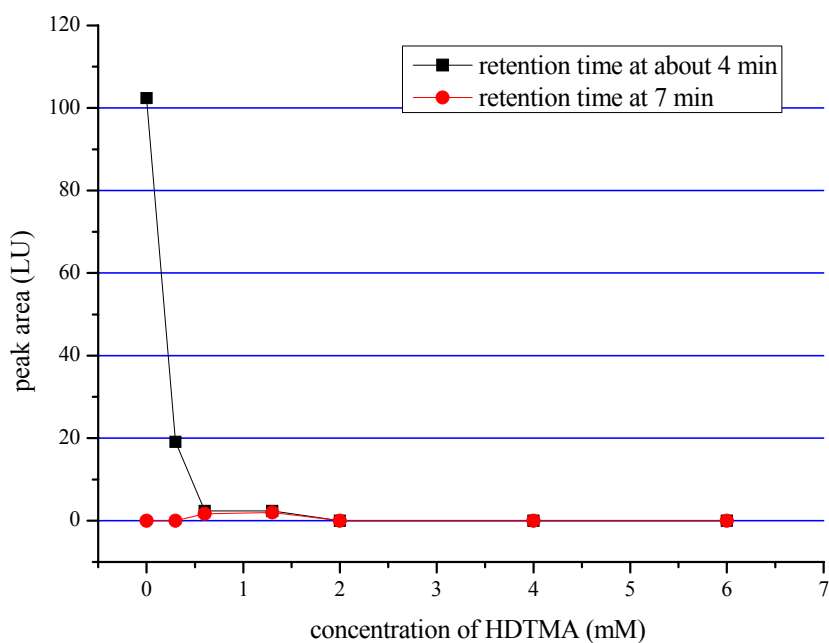


Figure 4.32 Adsorption of 100 ppb AFB₁ on bentonite and modified bentonite with 0.3, 0.6, 1.3, 2.0, 4.0 and 6.0 mM HDTMA.

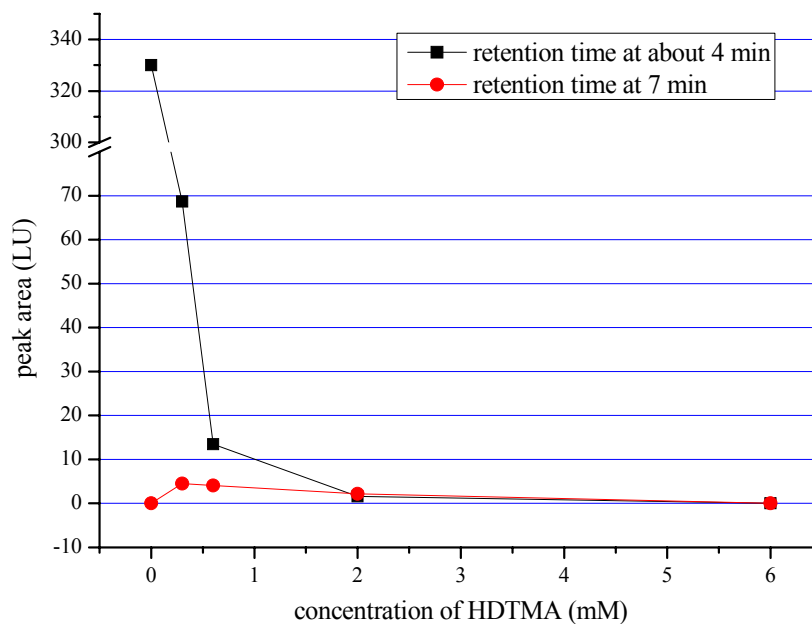


Figure 4.33 Adsorption of 200 ppb AFB₁ on bentonite and organobentonite with 0.3, 0.6, 2.0 and 6.0 mM HDTMA

In case of the AFB₁ adsorption by kaolin, halloysite, zeolite NaX and organosamples, the experiment was carried at under the condition with using 50 mg of adsorbents and 150 ppb AFB₁. The results showed that the peak at about 4 min disappeared after adsorption by all organosamples, but the peak at 7 min still remained (see Figure 4.34-4.36). When the concentration of AFB₁ was decreased to 100 ppb, the results gave the same trend, but the peak area at 7 min was lower compared to the experiment with 150 ppb AFB₁ (see in Figure 4.37-4.39).

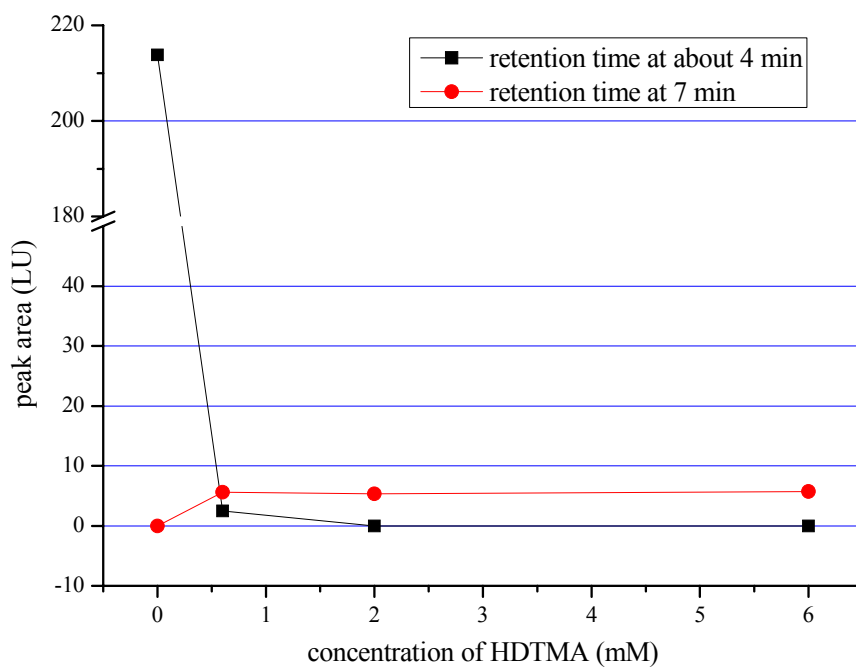


Figure 4.34 Adsorption of 150 ppb AFB₁ on kaolin and organokaolin with 0.6, 2.0 and 6.0 mM HDTMA

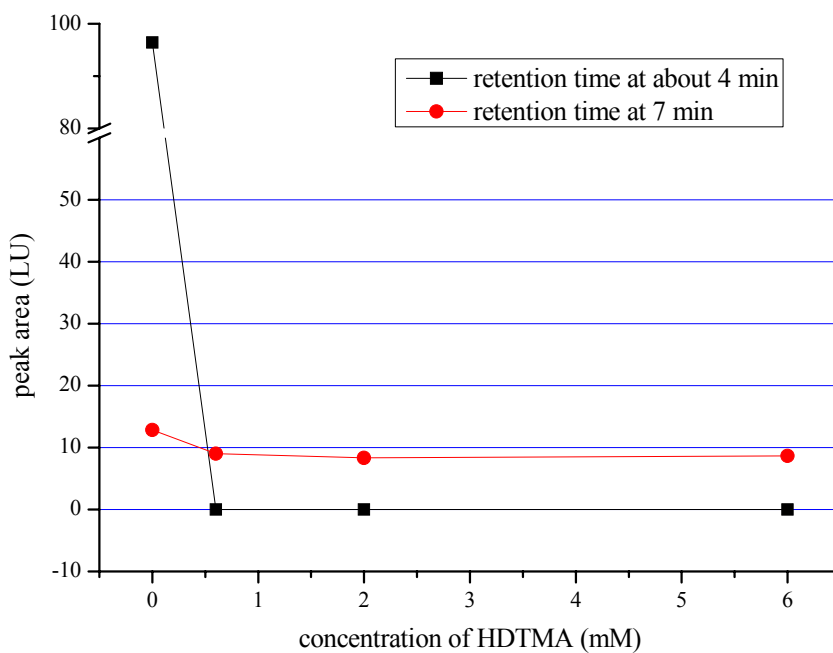


Figure 4.35 Adsorption of 150 ppb AFB₁ on halloysite and organohalloysite with 0.6, 2.0 and 6.0 mM HDTMA

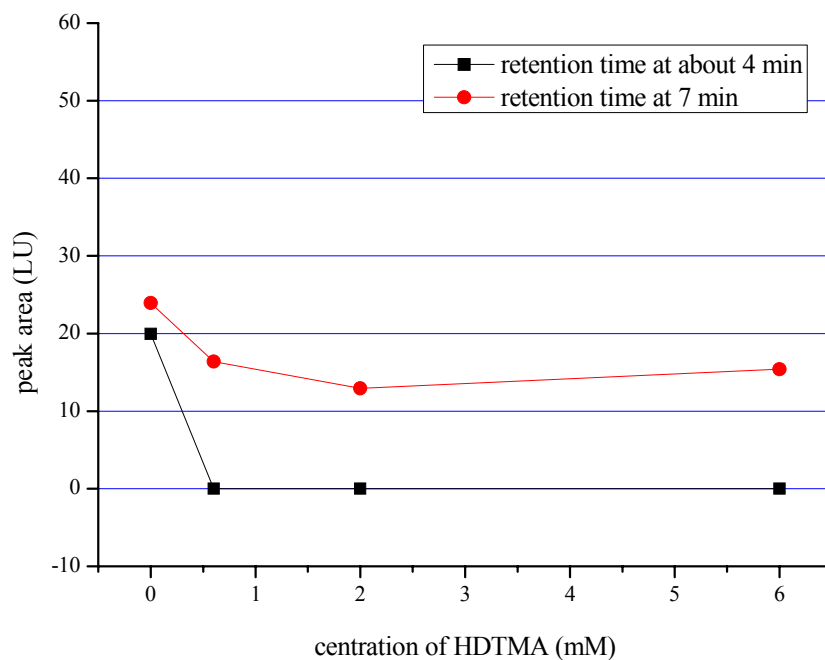


Figure 4.36 Adsorption of 150 ppb AFB₁ on zeolite NaX and modified zeolite NaX with 0.6, 2.0 and 6.0 mM HDTMA

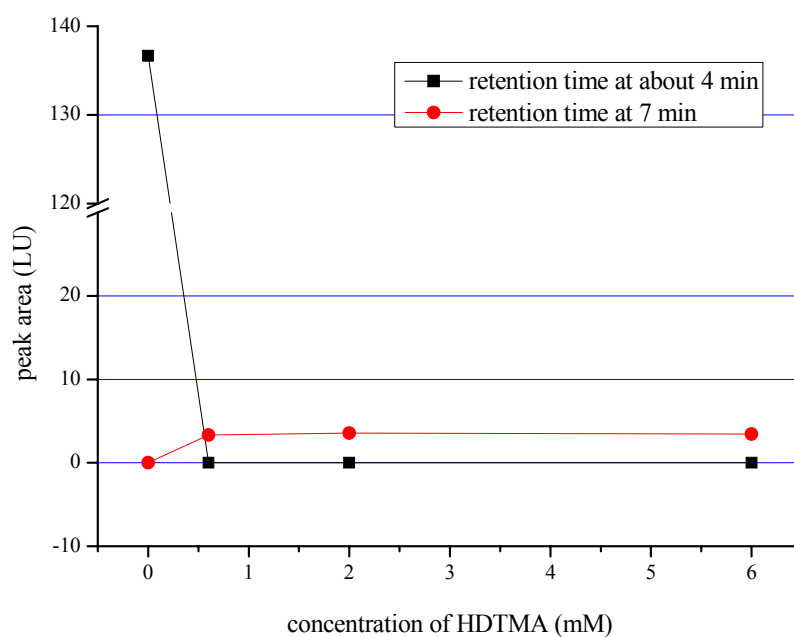


Figure 4.37 Adsorption of 100 ppb AFB₁ on kaolin and modified kaolin with 0.6, 2.0 and 6.0 mM HDTMA

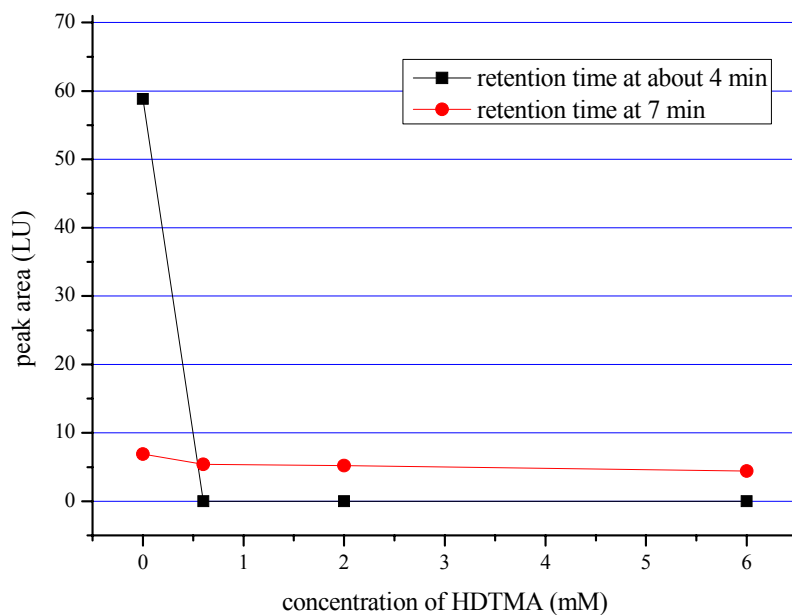


Figure 4.38 Adsorption of 100 ppb AFB₁ on halloysite and modified halloysite with 0.6, 2.0 and 6.0 mM HDTMA

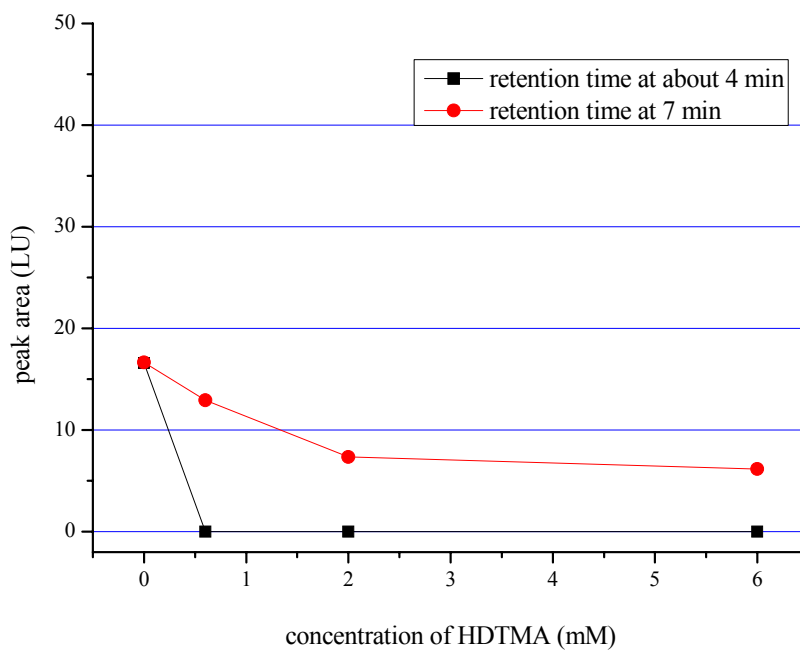


Figure 4.39 Adsorption of 100 ppb AFB₁ on zeolite NaX and modified zeolite NaX with 0.6, 2.0 and 6.0 mM HDTMA

The effect of pH solution on the AFB₁ adsorption was also investigated. In order to examine the effect of pH on AFB₁, the experiment was performed without adsorbent and the solutions of AFB₁ at pH 1.82, 2.12, 2.38, 2.99 and 5.75 (the pH at 5.75 being the solution of AFB₁ solution without acidic adjustment) were used. The results showed that the peak area at about 4 min was significantly increased with decreasing pH, but peak area at 7 min was slightly decreased (see Figure 4.40). It implied that at very low pH, AFB₁ at 7 min was changed well to be its complex form at about 4 min.

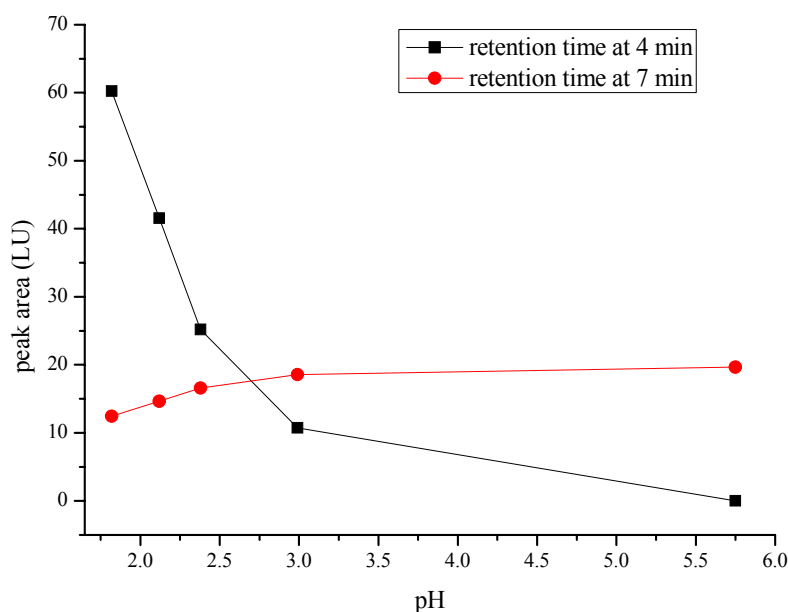


Figure 4.40 Peak area of 100 ppb AFB₁ at pH 1.52, 1.80, 2.16 and 5.75

In case with adsorbents the results showed that for all unmodified adsorbents the solution contained both AFB₁ and its complex form except kaolin having only peak at about 4 min (see Figure 4.41).

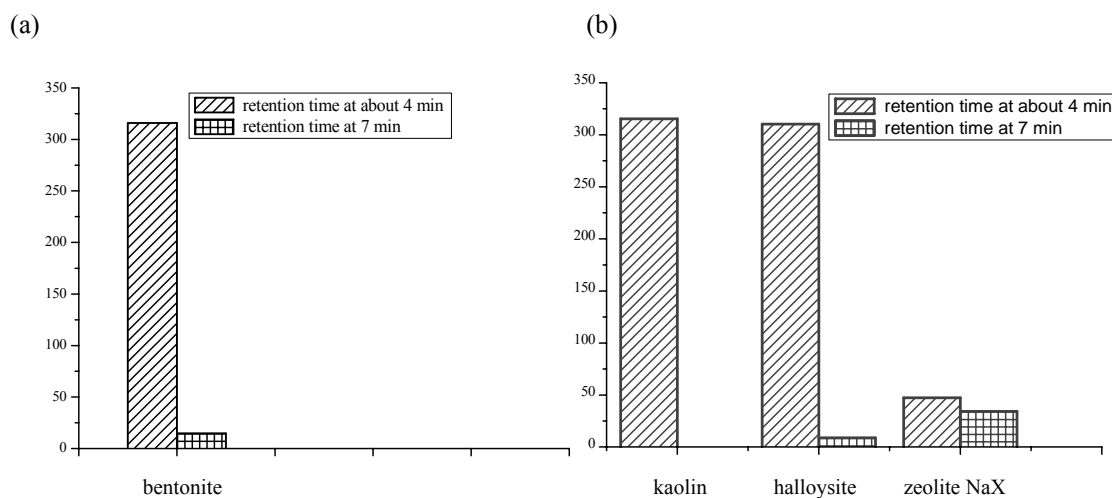


Figure 4.41 Peak area of (a) bentonite with 200 ppb AFB₁ (b) kaolin, halloysite and zeolite NaX with 150 ppb

For organosamples the results showed that two peaks were still remained except organozeolite NaX which showed only one peak at 7 min. Compared to unmodified samples the peak area at about 4 min was dramatically decreased (see Figure 4.42-4.45).

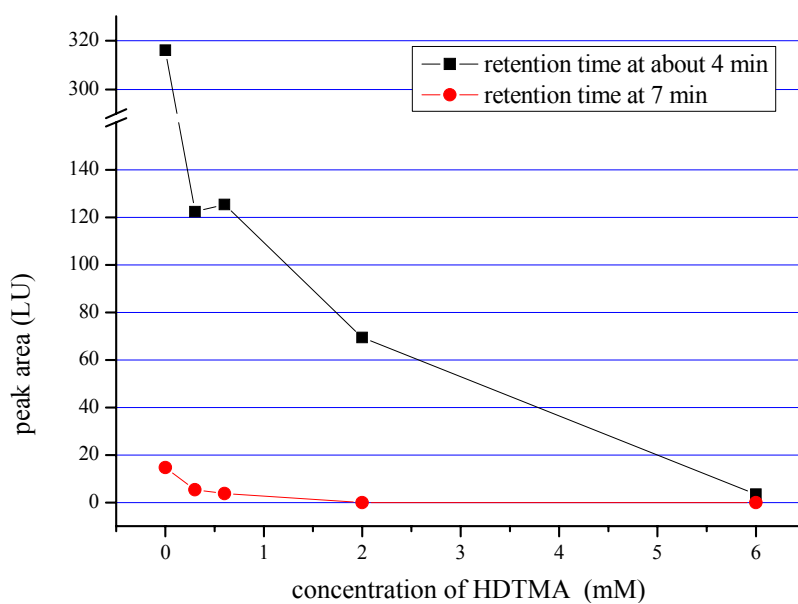


Figure 4.42 Adsorption of 200 ppb AFB₁ on bentonite and modified bentonite with concentration at 0.3, 0.6, 2.0 and 6.0 mM HDTMA at pH 3

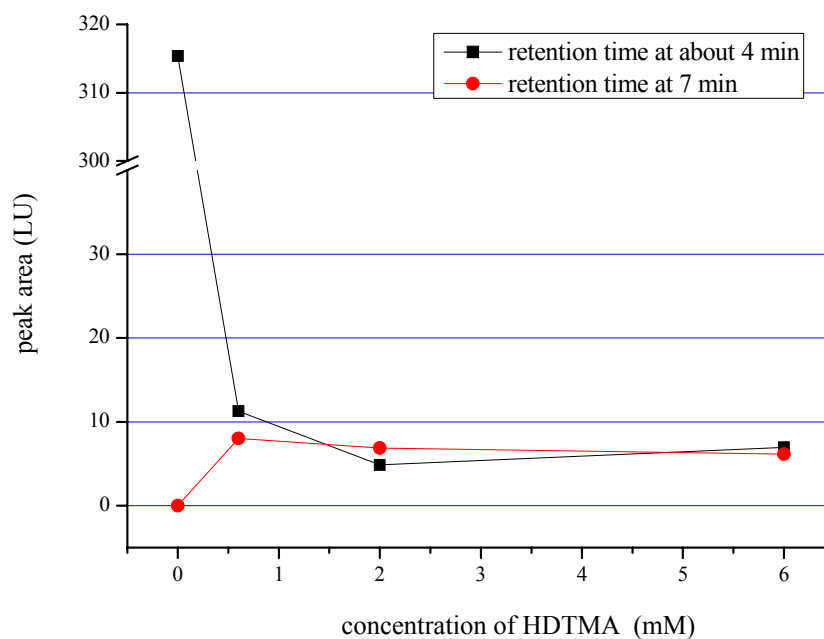


Figure 4.43 Adsorption of 150 ppb AFB₁ on kaolin and modified kaolin with concentration at 0.6, 2.0 and 6.0 mM HDTMA at pH 3

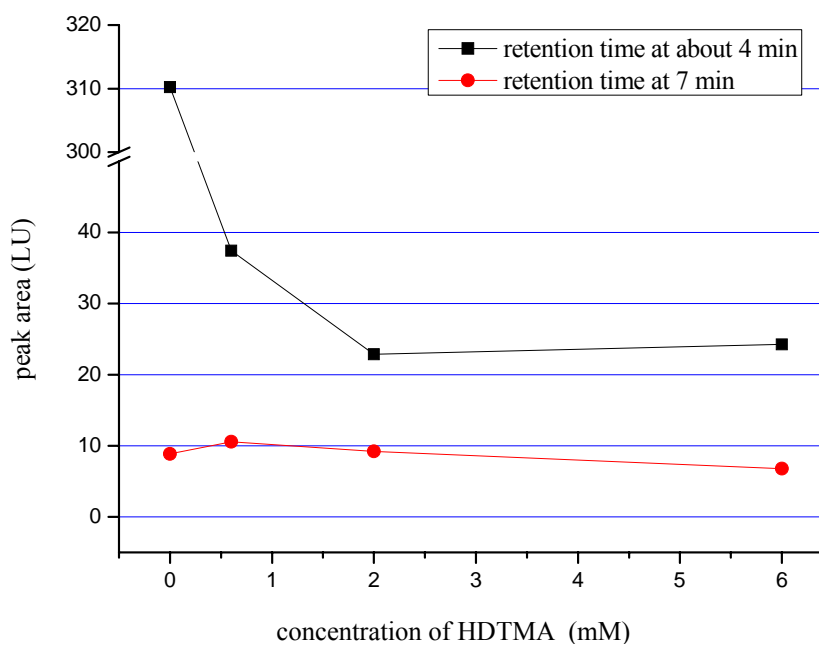


Figure 4.44 Adsorption of 150 ppb AFB₁ on halloysite and modified halloysite with concentration at 0.6, 2.0 and 6.0 mM HDTMA at pH 3

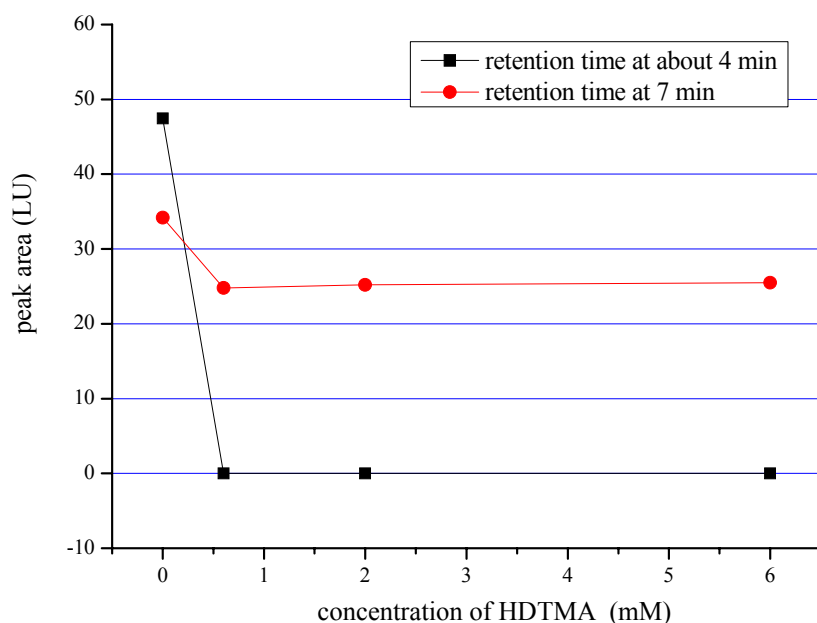


Figure 4.45 Adsorption of 150 ppb AFB₁ on zeolite NaX and modified zeolite NaX with concentration at 0.6, 2.0 and 6.0 mM HDTMA at pH 3

Finally, The values of peak area at about 4 min and 7 min in the adsorption study were summarized in Table 4.5. In our adsorption study the additional peak appeared in chromatogram when existence of adsorbents or addition of acid and it was assigned to be complex form of AFB₁. It might be produced from the β -dicarbonyl system of AFB₁ through the chelation of metal ions at the surface and within the interlayers of clay or through reaction with H⁺ in the case of acidic addition, that giving the yield as in Figure 4.46.

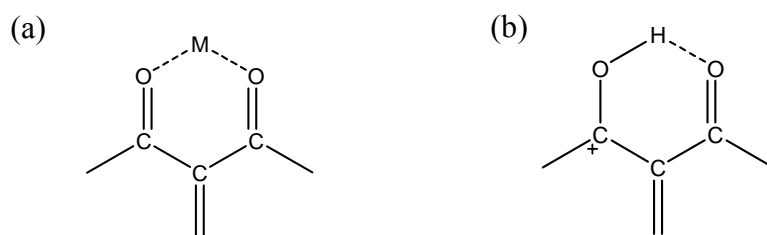


Figure 4.46 Proposed β -dicarbonyl system (a) chelation of metal ion (b) reaction with H⁺

Table 4.5 Summary of the peak area value of adsorption AFB₁ with (a) kaolin/organokaolin, halloysite/organohalloysite and zeolite NaX/organozeolite NaX, (b) bentonite/organobentonite

(a)

| | | Peak area at retention time at about 4 min | | | Peak area at retention time at 7 min | | |
|-------------------|--------|--|-------------------------|-------------------------|--------------------------------------|-------------------------|-------------------------|
| | | Normal condition | | pH 3 | Normal condition | | pH 3 |
| | | 100ppb AFB ₁ | 150ppb AFB ₁ | 150ppb AFB ₁ | 100ppb AFB ₁ | 150ppb AFB ₁ | 150ppb AFB ₁ |
| | | 0 | 0 | 4.2 | 27.8 | 37.3 | 37.1 |
| kaolin | | 136.7 | 213.8 | 315.4 | 0 | 0 | 0 |
| organokaolin | 0.6 mM | 0 | 2.5 | 11.3 | 3.3 | 5.6 | 8.0 |
| | 2.0 mM | 0 | 0 | 4.9 | 3.6 | 5.3 | 6.9 |
| | 6.0 mM | 0 | 0 | 6.9 | 3.4 | 5.7 | 6.2 |
| halloysite | | 58.8 | 96.5 | 310.2 | 6.9 | 12.9 | 8.9 |
| organohalloysite | 0.6 mM | 0 | 0 | 37.5 | 5.4 | 9.0 | 11.0 |
| | 2.0 mM | 0 | 0 | 22.9 | 5.2 | 8.3 | 9.2 |
| | 6.0 mM | 0 | 0 | 24.2 | 4.4 | 8.7 | 7.0 |
| Zeolite NaX | | 16.6 | 20.0 | 47.4 | 16.7 | 23.9 | 34.2 |
| organozeolite NaX | 0.6 mM | 0 | 0 | 0 | 10.0 | 16.4 | 24.8 |
| | 2.0 mM | 0 | 0 | 0 | 7.4 | 12.9 | 25.2 |
| | 6.0 mM | 0 | 0 | 0 | 6.2 | 15.3 | 25.5 |

Table 4.5 Summary of the peak area value of adsorption AFB₁ with (a) kaolin/organokaolin, halloysite/organohalloysite and zeolite NaX/organozeolite NaX, (b) bentonite/organobentonite (continued)

(b)

| | Peak area at retention time 4 min | | | Peak area at retention time 7 min | | | |
|-----------------|-----------------------------------|-------------------------|-------------------------|-----------------------------------|-------------------------|-------------------------|-----|
| | Normal condition | | pH 3 | Normal condition | | pH 3 | |
| | 100ppb AFB ₁ | 200ppb AFB ₁ | 200ppb AFB ₁ | 100ppb AFB ₁ | 200ppb AFB ₁ | 200ppb AFB ₁ | |
| | 0 | 0 | 18.1 | 27.8 | 51.4 | 45.6 | |
| bentonite | 102.4 | 330.0 | 316.0 | 0 | 0 | 14.7 | |
| organobentonite | 0.3 mM | 19.1 | 68.7 | 122.4 | 0 | 4.5 | 5.4 |
| | 0.6 mM | 2.3 | 13.5 | 125.1 | 1.98 | 4.1 | 3.7 |
| | 1.3 mM | 2.2 | - | - | 1.64 | - | - |
| | 2.0 mM | 0 | 1.6 | 69.4 | 0 | 2.2 | 0 |
| | 4.0 mM | 0 | - | - | 0 | - | - |
| | 6.0 mM | 0 | 0 | 3.5 | 0 | 0 | 0 |

CHAPTER V

CONCLUSION

Modification of adsorbents like clay minerals or zeolite with surfactants have been interesting. It provides the adsorbents with high hydrophobic property which enhances their capabilities to adsorb organic compounds. Therefore, this work focused on preparations of organoclays (bentonite, kaolin and halloysite) and organozeolite NaX using hexadecyltrimethyl ammonium chloride (HDTMA) including their applications for adsorption of aflatoxin B₁ (AFB₁).

The experimental investigations on the surface modification with HDTMA of organoclays and organozeolite NaX can be prepared by microwave and convention method. It was found that the preparation reaction time for organoclay was decreased from 24 h by convention to only 10 min by microwave, which confirms that microwave method is very effectively for preparing organosamples, but these two methods gave the similar results of their characterizations. In the characterization based on the results of TGA and XRD it indicated that the amount of adsorbed HDTMA was very high in the case of bentonite compared to that of the other and HDTMA could be adsorbed not only on the surface but also within the interlayer. The d_{001} was expanded from 14.68 to 22.33 Å when HDTMA concentration of 6.0 mM. For kaolin, halloysite and zeolite NaX, HDTMA was mainly adsorbed on external surface, because the d-spacing was quite constant although HDTMA concentration was increased. According to DTA profile it indicated that there were at least three

different arrangements of adsorbed

HDTMA on bentonite at the highest HDTMA concentration. From the result of FT-IR asymmetric and symmetric stretching vibration of methyl group C-CH₂ shifted to lower wavenumber with increasing concentration of HDTMA. It implied that the arrangement of HDTMA on the bentonite interlayer was changed from disorder to ordered form with increasing concentration of HDTMA.

The adsorption of AFB₁ with the unmodified samples and the organosamples were considered under various influences. It found the new peak with retention time at 4 min besides standard peak AFB₁ with retention time at 7 min. The additional peak might be produced from the β -dicarbonyl system of AFB₁ chelating to metal ions at the surface and within the interlayers of clay or reacting with H⁺ in acidic addition. In all cases of the adsorption study it found that the organosamples with all the concentration of HDTMA could adsorb AFB₁ and the complex form much more than the unmodified samples. When compared their adsorption capabilities, it found that the capability of organobentonite with 6.0 mM is the highest. All the organosamples enabled to adsorb the both forms of AFB₁ and complex form not only at the normal condition but also at the acidic condition. However, at acidic condition they could adsorb lower amount of AFB₁.

REFERENCES

REFERENCES

- Abdel-Wahhab, M. A., Hasan, A. M., Aly, S. E., and Mahrous, K. F. (2005). Adsorption of sterigmatocystin by montmorillonite and inhibition of its genotoxicity in the Nile tilapia fish (*Oreochromis niloticus*). **Mutation Research/Genetic Toxicology and Environmental Mutagenesis**. 582: 20-27.
- Abdel-Wahhab, M. A., Nada, S. A., and Khalil, F. A. (2002). Physiological and toxicological responses in rats fed aflatoxin-contaminated diet with or without sorbent materials. **Animal Feed Science and Technology**. 97: 209-219.
- Adamo, P., Violante, P., and Wilson, M. J. (2001). Tubular and spheroidal halloysite in pyroclastic deposits in the area of the Roccamonfina volcano (Southern Italy). **Geoderma**. 99: 295-316.
- Akiyama, H., Goda, Y., Tanaka, T., and Toyoda, M. (2001). Determination of aflatoxins B1, B2, G1 and G2 in spices using a multifunctional column clean-up. **Journal of Chromatography A**. 932: 153-157.
- Aljundi, I. H., Belovich, J. M., and Talu, O. (2005). Adsorption of lactic acid from fermentation broth and aqueous solutions on Zeolite molecular sieves. **Chemical Engineering Science**. 60: 5004-5009.
- Andrejkovičová, S., Janotka, I., and Komadel, P. (2008). Evaluation of geotechnical properties of bentonite from Lieskovec deposit, Slovakia. **Applied Clay Science**. 38: 297-303.
- Breck, D.W. (1974). Zeolite molecular sieve: structure chemistry and use. John Wiley and sons. New York.

- Breen, C., Illés, J., Yarwood, J., and Skuse, D. R. (2007). Variable temperature diffuse reflectance infrared Fourier transform spectroscopic investigation of the effect of ball milling on the water sorbed to kaolin. **Vibrational Spectroscopy**. 43: 366-379.
- Brain, C., and Smith, B. C. (1996). Fundamentals of Fourier transform infrared spectroscopy. **Boca Raton** : CRC Press.
- Carrizosa, M. J., Koskinen, W. C., Hermosin, M. C., and Cornejo, J. (2001). Dicamba adsorption-desorption on organoclays. **Applied Clay Science**. 18: 223-231.
- Coker, E. N., and Rees, L. V. C. (2005). Kinetics of ion exchange in quasi-crystalline aluminosilicate zeolite precursors. **Microporous and Mesoporous Materials**. 84: 171-178.
- Daković, A., Matijasevic, S. A., Rottinghaus, G. E., Ledoux, D. R., Butkeraitis, P., and Sekulic, Z. (2008). Aflatoxin B1 adsorption by natural and copper modified montmorillonite. **Colloids and Surfaces B: Biointerfaces**. 66:20-25.
- Daković, A., Tomasević-Čanović, M., Dondur, V., Rottinghaus, G. E., Medaković, V., and Zarić, S. (2005). Adsorption of mycotoxins by organozeolites. **Colloids and Surfaces B: Biointerfaces**. 46: 20-25.
- Daković, A., Tomasević-Čanović, M., Rottinghaus, G., Dondur, V., and Mašić, Z. (2003). Adsorption of ochratoxin A on octadecyldimethyl benzyl ammonium exchanged-clinoptilolite-heulandite tuff. **Colloids and Surfaces B: Biointerfaces**. 30: 157-165.
- Dultz, S., and Bors, J. (2000). Organophilic bentonites as adsorbents for radionuclides: II. Chemical and mineralogical properties of HDPy-montmorillonite. **Applied Clay Science**. 16: 15-29.

- Dyer, A. (1988). **An Introduction to Zeolite Molecular Sieves**. John Wiley and Sons. New York.
- Eren, E., and Afsin, B. (2008). An investigation of Cu(II) adsorption by raw and acid-activated bentonite: A combined potentiometric, thermodynamic, XRD, IR, DTA study. **Journal of Hazardous Materials**. 151: 682-691.
- Farmer, V. C. (2000). Transverse and longitudinal crystal modes associated with OH stretching vibrations in single crystals of kaolinite and dickite. **Spectrochimica Acta Part A: Molecular and Biomolecular Spectroscopy**. 56: 927-930.
- Felhi, M., Tlili, A., Gaied, M. E., and Montacer, M. (2008). Mineralogical study of kaolinitic clays from Sidi El Bader in the far north of Tunisia. **Applied Clay Science**. 39: 208-217.
- Frost, R. L., Makó, É., Kristóf, J., and Klopogge, J. T. (2002). Modification of kaolinite surfaces through mechanochemical treatment--a mid-IR and near-IR spectroscopic study. **Spectrochimica Acta Part A: Molecular and Biomolecular Spectroscopy**. 58: 2849-2859.
- Gilbert, J. C., Rubinsky, B., Wong, S. T. S., Brennan, K. M., Pease, G. R., and Leung, P. P. (1997). Temperature determination in the frozen region during cryosurgery of rabbit liver using MR image analysis. **Magnetic Resonance Imaging**. 15: 657-667.
- Hajian, R., and Ensafi, A. A. (2009). Determination of aflatoxins B1 and B2 by adsorptive cathodic stripping voltammetry in groundnut. **Food Chemistry**. 115: 1034-1037.
- He, H., Zhou, Q., Frost, R. L., Wood, B. J., Duong, L. V., and Klopogge, J. T. (2007). A X-ray photoelectron spectroscopy study of HDTMAB distribution

- within organoclays. **Spectrochimica Acta Part A: Molecular and Biomolecular Spectroscopy**. 66: 1180-1188.
- Hummel, D. O. (2000). Handbook of surfactant analysis: chemical, physico-chemical and physical methods. Chichester. New York.
- Hiemenz, P. C., and Rajagopalan, R. (1997). **Principles of Colloid and Surface Chemistry**. RCR Press.
- Ip, K. H., Stuart, B. H., Ray, A. S., and Thomas, P. S. (2008). A spectroscopic investigation of the weathering of a heritage Sydney sandstone. **Spectrochimica Acta Part A: Molecular and Biomolecular Spectroscopy**. 71: 1032-1035.
- Joussein, E., Petit, S., and Delvaux, B. (2007). Behavior of halloysite clay under formamide treatment. **Applied Clay Science**. 35: 17-24.
- Karapanagioti, H. K., Sabatini, D. A., and Bowman, R. S. (2005). Partitioning of hydrophobic organic chemicals (HOC) into anionic and cationic surfactant-modified sorbents. **Water Research**. 39: 699-709.
- Lee, H. J., Kim, Y. M., Kweon, O. S., and Kim, I. J. (2007). Structural and morphological transformation of NaX zeolite crystals at high temperature. **Journal of the European Ceramic Society**. 27: 561-564.
- Lee, S. Y., Kim, S. J., Chung, S. Y., and Jeong, C. H. (2004). Sorption of hydrophobic organic compounds onto organoclays. **Chemosphere**. 55: 781-785.
- Li, J., Zhu, L., and Cai, W. (2006). Characteristics of organobentonite prepared by microwave as a sorbent to organic contaminants in water. **Colloids and Surfaces A: Physicochemical and Engineering Aspects**. 281: 177-183.

- Li, Z., and Bowman, R. S. (2001). Retention of inorganic oxyanions by organo-kaolinite. **Water Research**. 35: 3771-3776.
- Li, Z., and Gallus, L. (2005). Surface configuration of sorbed hexadecyltrimethylammonium on kaolinite as indicated by surfactant and counterion sorption, cation desorption, and FTIR. **Colloids and Surfaces A: Physicochemical and Engineering Aspects**. 264: 61-67.
- Lee, R. E. (1993). Scanning electron microscopy and X-ray microanalysis. Englewood Cliffs, N.Y. : Prentice Hall
- Lange, K. R. (1999). Surfactants: A Practical Handbook.
- Machado, G. S., de Freitas Castro, K. A. D., Wypych, F., and Nakagaki, S. (2008). Immobilization of metalloporphyrins into nanotubes of natural halloysite toward selective catalysts for oxidation reactions. **Journal of Molecular Catalysis A: Chemical**. 283: 99-107.
- Majdan, M., Maryuk, O., Pikus, S., Olszewska, E., Kwiatkowski, R., and Skrzypek, H. (2005). Equilibrium, FTIR, scanning electron microscopy and small wide angle X-ray scattering studies of chromates adsorption on modified bentonite. **Journal of Molecular Structure**. 740: 203-211.
- Majdan, M., Pikus, S., Rzaczyńska, Z., Iwan, M., Maryuk, O., Kwiatkowski, R., *et al.* (2006). Characteristics of chabazite modified by hexadecyltrimethylammonium bromide and of its affinity toward chromates. **Journal of Molecular Structure**. 791: 53-60.
- Makó, É., Senkár, Z., Kristóf, J., and Vágvolgyi, V. (2006). Surface modification of mechanochemically activated kaolinites by selective leaching. **Journal of Colloid and Interface Science**. 294: 362-370.

- Maria, C. (1997). Environmental sampling and analysis lab manual. Lewis publishers. New York. P.313.
- McKean, C., Tang, L., Tang, M., Billam, M., Wang, Z., Theodorakis, C. W., *et al.* (2006). Comparative acute and combinative toxicity of aflatoxin B1 and fumonisin B1 in animals and human cells. **Food and Chemical Toxicology**. 44: 868-876.
- Otta, K. H., Papp, E., and Bagócsi, B. (2000). Determination of aflatoxins in food by overpressured-layer chromatography. **Journal of Chromatography A**. 882: 11-16.
- Papp, E., H-Otta, K., Záray, G., and Mincsovcics, E. (2002). Liquid chromatographic determination of aflatoxins. **Microchemical Journal**. 73: 39-46.
- Pecharsky, V. K., and Zavalij, P. Y. (2003). Fundamentals of powder Diffraction and Structure Characterization of Material.
- Qi, L., Liao, W., and Bi, Z. (2007). Adsorption of conventional and gemini cationic surfactants in nonswelling and swelling layer silicate. **Colloids and Surfaces A: Physicochemical and Engineering Aspects**. 302: 568-572.
- Ramos, A. J., and Hernández, E. (1997). Prevention of aflatoxicosis in farm animals by Means of hydrated sodium calcium aluminosilicate addition to feedstuffs: a review. **Animal Feed Science and Technology**. 65: 197-206.
- Richards, S., and Bouazza, A. (2007). Phenol adsorption in organo-modified basaltic clay and bentonite. **Applied Clay Science**. 37: 133-142.
- Sanchez-Martin, M. J., Rodriguez-Cruz, M. S., Andrades, M. S., and Sanchez-Camazano, M. (2006). Efficiency of different clay minerals modified with a cationic surfactant in the adsorption of pesticides: Influence of clay type and

- pesticide hydrophobicity. **Applied Clay Science**. 31: 216-228.
- Sullivan, E. J., Carey, J. W., and Bowman, R. S. (1998). Thermodynamics of Cationic Surfactant Sorption onto Natural Clinoptilolite. **Journal of Colloid and Interface Science**. 206: 369-380.
- Tavcar-Kalcher, G., Vrtac, K., Pestevsek, U., and Vengust, A. (2007). Validation of the procedure for the determination of aflatoxin B1 in animal liver using immunoaffinity columns and liquid chromatography with postcolumn derivatisation and fluorescence detection. **Food Control**. 18: 333-337.
- Treacy, M. M. J., Treacy, J., Higgins, J. B., and Ballmoss, R. V. (1996). **COLLECTION OF SIMULATED XRD POWER PATTERNS FOR ZEOLITES**.
- Tomašević-Čanović, M., Daković, A., Rottinghaus, G., Matijašević, S., and Đuričić, M. (2003). Surfactant modified zeolites new efficient adsorbents for mycotoxins. **Microporous and Mesoporous Materials**. 61: 173-180.
- Upton, R. T., and Burns, S. E. (2006). Sorption of nitroaromatic compounds to synthesized organoclays. **Journal of Colloid and Interface Science**. 297: 70-76.
- Wingenfelder, U., Furrer, G., and Schulin, R. (2006). Sorption of antimonate by HDTMA-modified zeolite. **Microporous and Mesoporous Materials**. 95: 265-271.
- Xi, Y., Ding, Z., He, H., and Frost, R. L. (2004). Structure of organoclays an X-ray diffraction and thermogravimetric analysis study. **Journal of Colloid and Interface Science**. 277: 116-120.
- Yapar, S., Özbudak, V., Dias, A., and Lopes, A. (2005). Effect of adsorbent concentration to the adsorption of phenol on hexadecyl trimethyl ammonium-

bentonite. **Journal of Hazardous Materials**. 121: 135-139.

Yildiz, N., Gönülşen, R. Y., Koyuncu, H. I., and Çalimli, A. (2005). Adsorption of benzoic acid and hydroquinone by organically modified bentonites. **Colloids and Surfaces A: Physicochemical and Engineering Aspects**. 260: 87-94.

Breck, D. W. (1974). **Zeolite molecular sieve: structure chemistry and use**. John Wiley and sons. New York.

APPENDICS

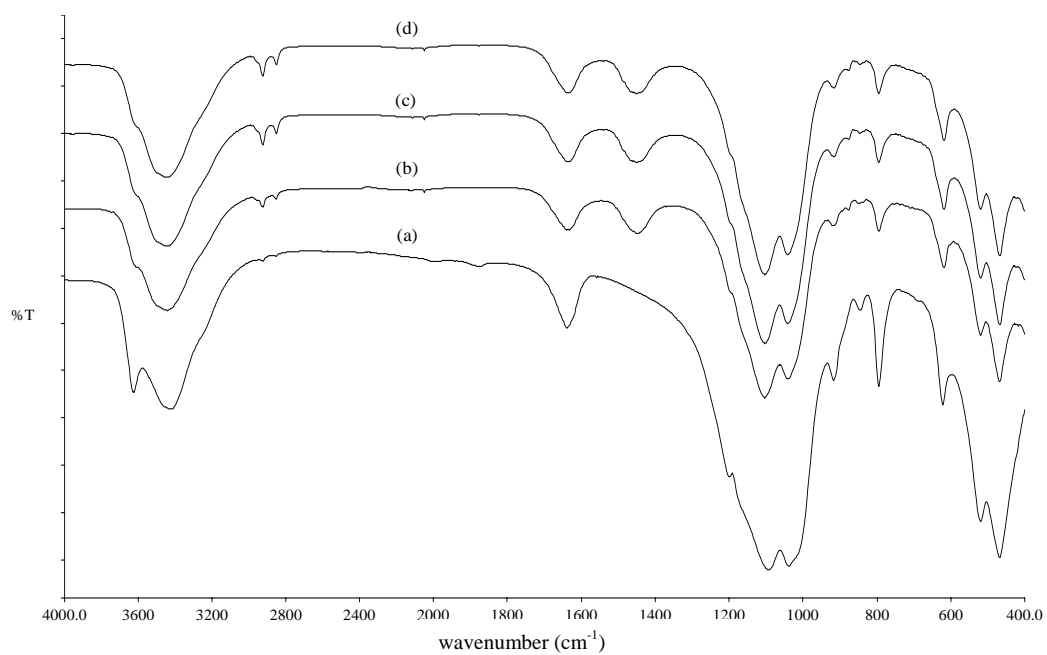


Figure 1 IR spectra of bentonite (a) before and (b-d) after modification with 2.0 mM HDTMA by microwave method at 5, 10 and 15 h, respectively

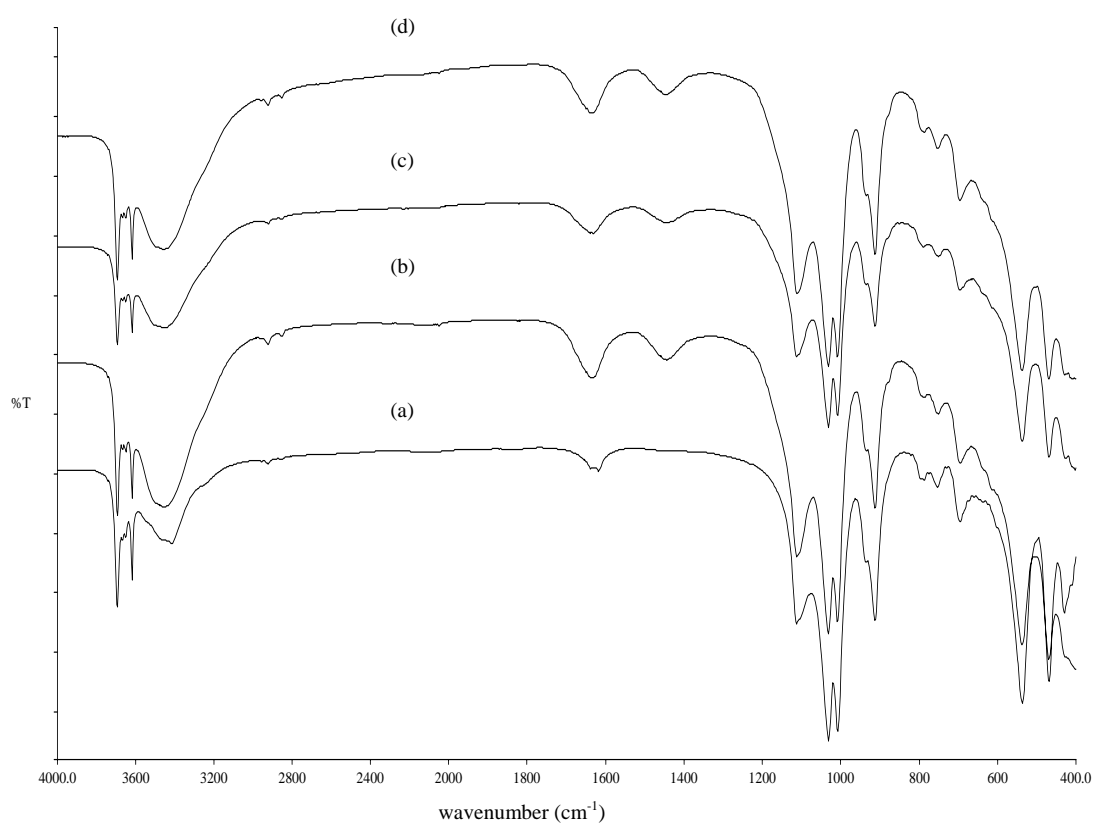


Figure 2 IR spectra of kaolin (a) before and (b-d) after modification with 2.0 mM HDTMA by microwave method at 5, 10 and 15 h, respectively

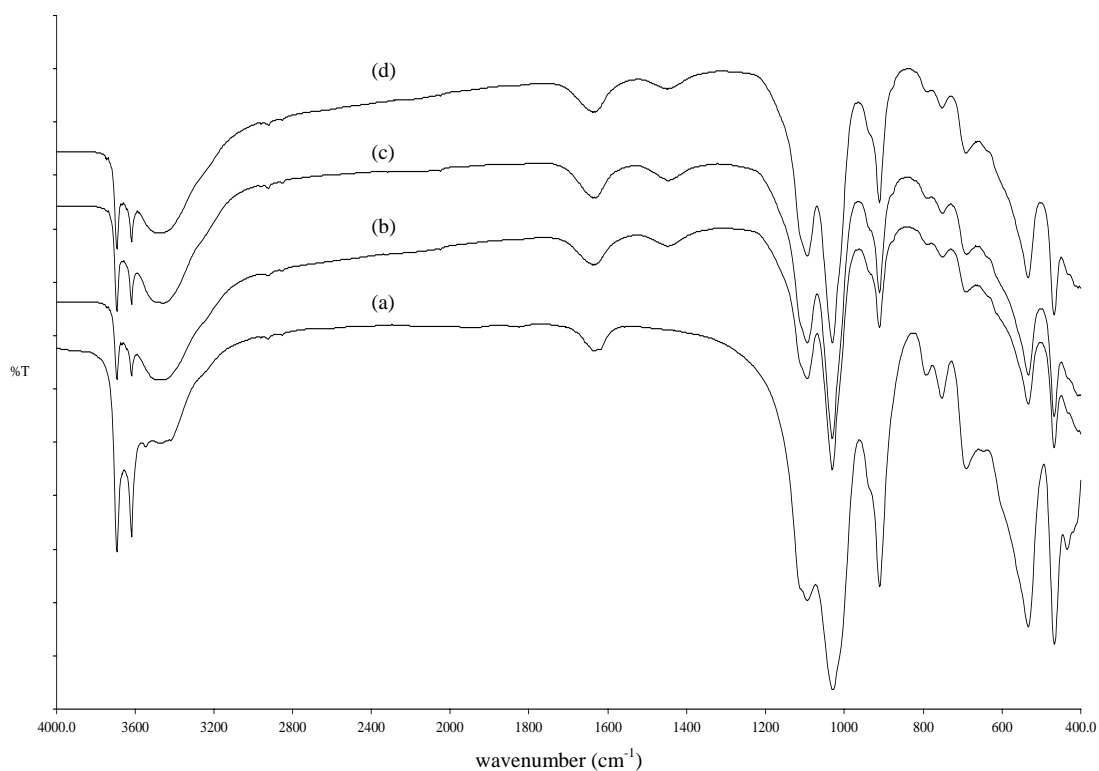


Figure 3 IR spectra of halloysite (a) before and (b-d) after modification with 2.0 mM HDTMA by microwave method at 5, 10 and 15 h, respectively

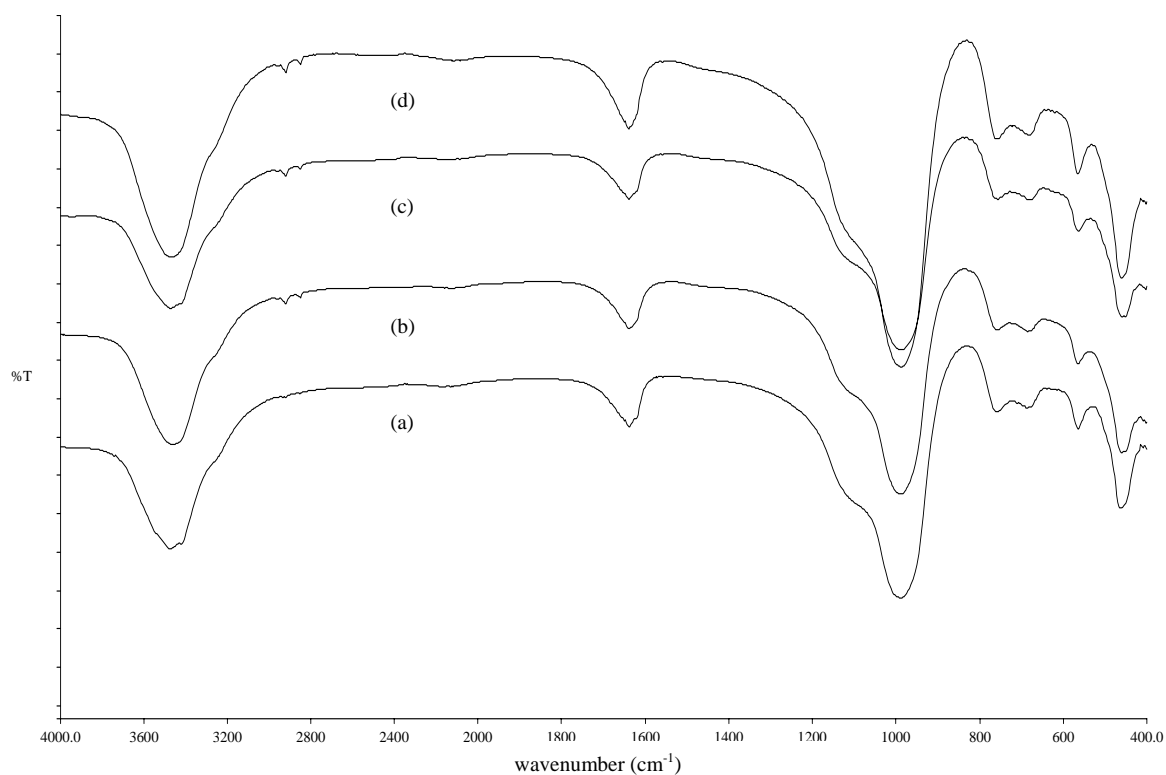


Figure 4 IR spectra of zeolite NaX (a) before and (b-d) after modification with 2.0 mM HDTMA by microwave method at 5, 10 and 15 h, respectively

CURRICULUM VITAE

NAME: Miss Thapanee Khambudda **DATE OF BIRTH:** May 31,1981

PLACE OF BIRTH: Buriram, Thailand **CITIZENSHIP:** Thailand

EDUCATIONAL BACKGROUND:

2004 Bachelor of Science (Chemistry), B.Ed. (Chemistry)
Nakhon Ratchasima Rajabhat University, Nakhon Ratchasima,
Thailand

WORK EXPERIENCE:

2005-2006 Technician, Center of Scientific, Nakhon Ratchasima Rajabhat
University,
Nakhon Ratchasima, Thailand

2006-2009 Teaching A sistance, School of Chemistry, Institute of Science,
Suranaree University of Technology, Nakhon Ratchasima.

PRESENTATION:

2006 1. Poster presentation “Characteristics of organobentonite modified
With hexadecyltrimethylammonium chloride prepared by microwave
and convention” 1st NSC Faculty of Science Naresuan University,
Phitsanulok, Thailand.

2008 2. Poster presentation “Characteristics of organoclays modified with
hexa-decyltrimethylammonium chloride prepared by convention and
micro-wave” The 9th National Grad Research Conference. March 14-
15, 2008, Burapha University, Bangsaen Chonburi, Thailand.